



*Università degli Studi di Firenze*

**DOTTORATO DI RICERCA IN  
SCIENZE CHIMICHE**  
CICLO XXV

COORDINATORE Prof. Andrea Goti

Synthetic peptide probes mimicking aberrant modifications of  
protein antigens involved in autoimmunity

Settore Scientifico Disciplinare CHIM/06

**Dottoranda**  
Dott. Margherita Di Pisa

**Tutore**  
Prof. Anna Maria Papini

Anni 2010/2012

*Questa tesi la dedico a te, Nonna,  
che te ne sei andata con le nuvole  
lasciandomi molto più di una voglia di pioggia.*

<b>1. INTRODUCTION.....</b>	<b>6</b>
<b>1.1 Introduction to the immune system.....</b>	<b>7</b>
<b>1.2 Antigen-Antibody interaction .....</b>	<b>9</b>
1.2.1 <i>Classes and functions of antibodies .....</i>	11
1.2.2 <i>Epitopes in antibodies .....</i>	12
<b>1.3 Molecular mechanisms of autoimmunity .....</b>	<b>13</b>
<b>1.4 The Autoimmune Diseases .....</b>	<b>15</b>
1.4.1 <i>Aberrant PTMs triggering autoimmunity .....</i>	16
<b>1.5 The role of glycosylation in autoimmune diseases .....</b>	<b>17</b>
1.5.1 <i>Protein glycosylation .....</i>	18
1.5.2 <i>Bacteria transferring sugar moieties in host proteins .....</i>	19
1.5.3 <i>N-linked protein glycosylation.....</i>	19
<b>1.6 Serologic Biomarkers for autoimmune diseases diagnostics.....</b>	<b>20</b>
1.6.1 <i>The “Chemical Reverse Approach” and autoimmune diseases.....</i>	21
1.6.2 <i>ELISA for diagnostics .....</i>	23
1.6.3 <i>Peptide-based ELISA .....</i>	24
<b><u>PART A: DESIGN AND SYNTHESIS OF MODIFIED PEPTIDE PROBES TO STUDY</u></b>	
<b><u>COELIAC DISEASE .....</u></b>	<b><u>26</u></b>
<b><u>2. COELIAC DISEASE: AN OVERVIEW .....</u></b>	<b><u>26</u></b>
<b>2.1 Tissue Transglutaminase, structural insights for antibody recognition .....</b>	<b>31</b>
<b>2.2 Epitope mapping of antigenic proteins .....</b>	<b>37</b>
2.2.1 <i>Epitope mapping of tTG(1-230).....</i>	40
2.2.2 <i>Synthesis of the linear peptides.....</i>	42
<b>2.3 Immunoassays: SP- and Inhibition- ELISA.....</b>	<b>44</b>
2.3.1 <i>Inhibition experiments using Eu-tTG Aeskulisa.....</i>	44
2.3.2 <i>SP ELISA experiments: screening of peptides I-XXIII .....</i>	46
2.3.3 <i>Results and discussion .....</i>	48
<b>2.4 Cross-linked peptide probes for the development of an <i>in vitro</i> diagnostics for Coeliac Disease .....</b>	<b>52</b>
2.4.1 <i>Tissue Transglutaminase’ fragments selection .....</i>	54
2.4.2 <i>Identification of the possible antigenic gliadin epitopes .....</i>	57
<b>2.5 Peptide-based cross-linked antigens design and synthesis.....</b>	<b>59</b>

## SUMMARY

2.5.1 Automatic synthesis of linear gliadin peptides: DQ2(I), DQ2(II), DQ2(III)	61
2.5.2 Manual synthesis of peptide tTGI, a case study	63
2.5.3 Manual synthesis of linear peptides tTGII and tTGIII	72
2.5.4 Synthesis of the nine cross-linked tTG-Gliadin peptides: tTGI-DQ2(I), tTGI-DQ2(II), tTGI-DQ2(III), tTGII-DQ2(I), tTGII-DQ2(II), tTGII-DQ2(III), tTGIII-DQ2(I), tTGIII-DQ2(II), and tTGIII-DQ2(III)	73
<b>2.6 SP-ELISA using the nine cross-linked peptides as synthetic antigens</b>	<b>75</b>
2.6.1 Investigation of the nature of the antigen-antibody recognition of tTGI-DQ2(I) by SP-ELISA	79
2.6.2 Results and discussion	80
<b><u>PART B: GLYCOPEPTIDOMIMETIC-BASED IMMUNOASSAYS FOR MULTIPLE SCLEROSIS</u></b>	<b>82</b>
<b><u>3. MULTIPLE SCLEROSIS: AN OVERVIEW</u></b>	<b>82</b>
3.1 The N-Glycosylated peptide CSF114(Glc) for the diagnosis of MS	89
3.2 Glycopeptidomimetic-based diagnostics in MS	92
3.2.1 Multivalent interactions in antigen-antibody recognition system	92
3.2.2 Synthesis of Multiple Epitope peptides	94
3.3 Immunochemical assays with MEPs	96
3.3.1 Results and discussion	99
3.4 Type I' beta turn CSF114(Glc) cyclic analogues	99
3.4.1 Synthesis of MDP-I : Ac-c[Cys-Arg-Asn-Gly-His-Cys]-NH <sub>2</sub>	101
3.4.2 Synthesis of MDP-II: Ac-c[Cys-Arg-Asn(Glc)-Gly-His-Cys]-NH <sub>2</sub>	103
3.5 Immunochemical assays with cyclic glycopeptides	104
3.5.1 Results and discussion	106
3.6 Side chain to side chain cyclic peptides by Glaser-coupling	106
3.6.1 On resin Glaser cyclization of peptides	111
3.6.2 Optimization of the Glaser-type reaction to synthesize Ac-c[Pra-Arg-Asn-Gly-His-Pra]-NH <sub>2</sub>	113
3.6.3 Optimization of the Glaser-type reaction to synthesize Ac-c[NPra-Arg-Asn-Gly-His-NPra]-NH <sub>2</sub>	117
3.6.4 Results and discussion	121
<b><u>4. CONCLUSIONS</u></b>	<b>122</b>
<b><u>5. EXPERIMENTAL PART A</u></b>	<b>124</b>
5.1 Materials and Methods	124
5.2 Solid Phase Peptide Synthesis	125

5.3 Immunoassays .....	133
<b><u>6. EXPERIMENTAL PART B.....</u></b>	<b><u>135</u></b>
6.1 Materials and Methods.....	135
6.2 Synthesis of building blocks for SPPS.....	136
6.3 Solid Phase Peptide Synthesis .....	142
6.4 Immunochemical assays.....	148
<b><u>7. ABBREVIATIONS .....</u></b>	<b><u>150</u></b>

### **1. Introduction**

The rationale of the research performed during this PhD project was to apply the peptide-based approach defined "Chemical Reverse Approach" previously developed at the Interdepartmental Laboratory of Peptide & Protein Chemistry & Biology of the University of Florence (Department of Chemistry "Ugo Schiff", Department of Pharmaceutical Sciences, and Department of Neurology) for the identification and characterization of antigen-antibody interaction in order to dissect the molecular mechanisms of autoimmune responses in disease conditions.

In particular final aim of this PhD was the design, synthesis, and set-up of specific immunoassays, i.e., SP-ELISA, as new peptide-based diagnostic tools for particular disease phases of Coeliac Disease and Multiple Sclerosis.

### 1.1. Introduction to the immune system

The human immune system has evolved over millions of years from both invertebrate and vertebrate organisms to develop sophisticated defense mechanisms to protect the hosts from microbes and their virulence factors. From invertebrates, humans have inherited the innate immune system, an efficient defense system that uses germ line-encoded proteins to recognize pathogens. Upon contact with pathogens, macrophages and natural killer (NK) cells may kill pathogens directly or may activate a series of events that both slow the infection and recruits the more recently evolved arm of the human immune system, the adaptive immune system.

The adaptive immune system consists of dual limbs of cellular (T-lymphocytes) and humoral (B-lymphocytes) immunity. B-lymphocytes produces antibodies (Abs) that are able to bind, neutralize and kill foreign, dangerous molecules, termed antigens (Ags). In infected cells, the Antigen Presenting Cell (APC) exposes peptide fragments, derived from hydrolysis of all the proteins present into the cell, to the T-lymphocytes attack by a special class of cell-surface glycoproteins, e.g. the Major Histocompatibility Complex (MHC) molecules<sup>1</sup>, as shown in *Figure 1.1*.

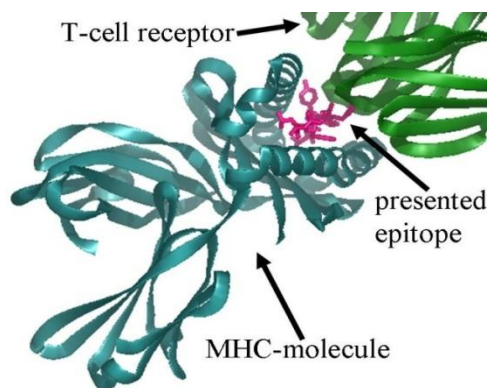


**Figure 1.1** MHC-I bound antigen is scanned by T-cell receptor.

---

<sup>1</sup> Rose, N.; Mackay, I., *The Autoimmune Diseases*, Elsevier Academic Press, 4<sup>th</sup> Edition., Elsevier Academic Press, 4<sup>th</sup> edition, 2006.

## INTRODUCTION

Depending on the antigen presented and the type of MHC molecule, several types of immune cells can be activated. Both B and T lymphocytes derive from a common stem cell and the proportion and distribution of these immunocompetent cells in various tissues reflect cell traffic, homing patterns and functional capabilities. Cytokines are the soluble proteins that direct, focus and regulate specific B- versus T- lymphocyte immune response, thus triggering humoral or cell mediated pathways, as summarized in *Figure 1.2*.

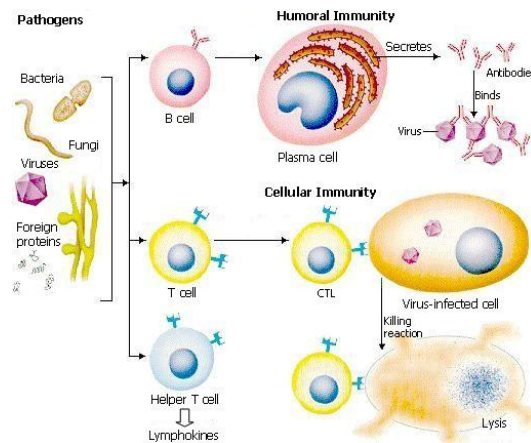


*Figure 1.2. Mechanism of the immune response.*

Coupled with finely tuned specific recognition mechanisms that maintain tolerance (non reactivity) to self antigens, T- and B- lymphocytes bring both *specificity* and *immune memory* to vertebrate host defenses. One of the classically accepted features of the immune system is the capacity to distinguish *self* from *non self*. Most animals do not mount immune responses to self antigens under ordinary circumstances and thus are tolerant to *self*. Whereas *self* recognition plays an important role in shaping both the T cell and B cell repertoires of immune receptors and in recognition of nominal antigen

by T cells, the development of potentially harmful immune response to *self* antigens is, in general, precluded<sup>2</sup>.

### 1.2 Antigen-Antibody interaction

The modern definition of **antigen** encompasses all substances that can be recognized by the adaptive immune system thus acting as an immunogen. An antigen is generally a protein molecule that often protrudes from the cell surface eliciting an immune response leading to the production of specific antibodies. **Antibodies** are host proteins found in plasma and extracellular fluids that serve as the first response to pathogens. Also referred to as Immunoglobulins (Igs), because they contain a common structural domain found in many proteins, antibodies are composed of four polypeptides. Two identical copies of both a heavy (~55 kD) and light (~25 kD) chain are held together by disulfide bonds as well as noncovalent interactions, and the resulting molecule is often represented by a schematic Y-shaped molecule of ~150 kD (*Figure 1.3*).

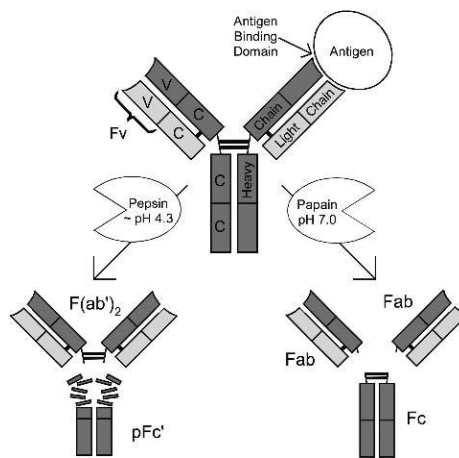


**Figure 1.3.** The basic structural molecule of an antibody.

<sup>2</sup>Kasper, D.L. ; Braunwald, E.; Fauci, A.S.; Hauser, S.L.; Longo, D.L.; Jameson J.L., *Principles of internal Medicine*, Mcgraw Hill Medical, 16<sup>th</sup> Edition, **2005**.

## INTRODUCTION

Antibodies perform two essential roles:

1. Epitope or antigen binding with the arms of the Y. Each arm or monovalent antibody fragment (fragment antigen-binding, Fab1) domain contains a binding site.
2. The fragment crystallizable (Fc) domain of the Y imparts to the antibody the biological effector functions such as natural killer cell activation, activation of the classical complement pathway, and phagocytosis.

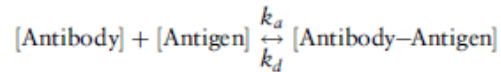
Antibodies can bind to different targets, allowing the immune system to recognize an equally wide diversity of antigens. Ag-Ab interaction is central to the antibodies' natural biological function and this property is used both for a research or therapeutic aim. Antibodies bind only a determinant or an **epitope** region of a macromolecule, which can also contain multiple determinants. The part of the antibody that binds to the antigenic determinant is termed the "antigen combining site", e.g. the **paratope**. Small molecules cannot induce an adaptive immune response by themselves. In fact, molecules with molecular weight below 5000Da are usually non-effective immunogens. However, many of these small non-immunogenic molecules, when covalently linked to a large molecule, i.e. a protein, can stimulate an immune response. These molecules, which are non-immunogenic by itself, are termed **haptens**, and the large molecules to which can be covalently attached, generally proteins, are termed **carriers**. Once the hapten-carrier complex is formed, a specific antibody response can occur. This is the case of human gastrin where conventional gastrin/carrier protein conjugates prepared via classical crosslinking reactions generally lead to strong anti-gastrin responses in terms of antisera titers<sup>3</sup>.

For simplicity, the binding of antibody with a simple hapten, which has only one antigenic determinant site, is used to illustrate the antigen-antibody

---

<sup>3</sup>Moroder, L.; Kocher, K.; Papini, A.M.; and Dufresne, M., *Chemistry of peptides and proteins*, **1993**, 783-791.

interaction. As shown in *Equation 1*, the interaction depends on the equilibrium or affinity constant ( $K = k_a/k_d$ ), which is the ratio of the association ( $k_a$ ) and dissociation rate constant ( $k_d$ ), and the concentrations of the reactants, i.e. [antibody] and [antigen].



*Equation 1. Equation of Antigen-Antibody interaction.*

In general, the  $K$  values for antibody-antigen interaction are in the range of  $10^6$ – $10^9$   $\text{L}\cdot\text{mol}^{-1}$ , but they may vary from  $10^3$  to  $10^{14}$  ( $\text{L}\cdot\text{mol}^{-1}$ ).

### **1.2.1 Classes and functions of antibodies**

In mammals there are five classes of antibodies, each characterized by a different function, **IgG**, **IgA**, **IgM**, **IgD**, and **IgE**.

**IgG** antibodies are the most common and the most important. They circulate in blood and other body fluids, defending against invading bacteria and viruses. IgGs move easily across cell membranes and in humans this mobility allows the IgGs in a pregnant woman to pass through the placenta to her fetus, providing a temporary defense to the unborn child.

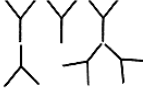
**IgA** antibodies are present in tears, saliva, and mucus, as well as in secretions of the respiratory, reproductive, digestive, and urinary tracts. IgA function is to neutralize bacteria and viruses and prevent them from entering the body or reaching the internal organs.

**IgMs** are present in blood and are the largest antibody form, combining five Y-shaped units. Their function is similar to IgGs in defending against antigens but cannot cross membranes because of the size. IgMs are produced in an initial attack by a specific bacterial or viral antigen, while IgGs are usually produced in later infections caused by the same agent.

## INTRODUCTION

**IgDs** may play a role in eliminating B-lymphocytes generating self-reactive autoantibodies.

**IgE** antibodies trigger the body to respond against foreign matter like pollen, spores, pet dander and fungus. They are present in lungs, skin and mucous membranes. IgE levels are typically high in people with allergies. They may also be present where there are allergic reactions to drugs and food, i.e. milk.

Characteristics	IgG	IgM	IgA	IgE	IgD
Heavy Chain	$\gamma$	$\mu$	$\alpha$	$\epsilon$	$\delta$
Light Chain	$\kappa$ or $\lambda$	$\kappa$ or $\lambda$	$\kappa$ or $\lambda$	$\kappa$ or $\lambda$	$\kappa$ or $\lambda$
Molecular Formula	$\gamma_2\kappa_2$ or $\gamma_2\lambda_2$	$(\mu_2\kappa_2)_5$ or $(\mu_2\lambda_2)_5$	$(\alpha_2\kappa_2)_n$ * or $(\alpha_2\lambda_2)_n$	$\epsilon_2\kappa_2$ or $\epsilon_2\lambda_2$	$\delta_2\kappa_2$ or $\delta_2\lambda_2$
Y Structure					
Valency	2	10	2, 4, or 6	2	2
Concentration in Serum	8–16 mg/ml	0.5–2 mg/ml	1–4 mg/ml	10–400 ng/ml	0–0.4 mg/ml
Function	Secondary response	Primary response	Protects mucous membranes	Protects against parasites (?)	?

\*n = 1, 2, or 3.

*Figure 1.4. Classes of antibodies.*

### 1.2.2 Epitopes in antibodies

The specificity of the antibody response refers to its ability to recognize a specific epitope in the presence of other epitopes. The binding site of an antibody can usually lodge an antigenic epitope of approximately 6 amino acids. The epitopes composed by linear (continuous) amino acid sequences are termed **linear epitopes**. Linear epitopes can be accessible to antibodies if they are exposed on the external surface of the antigen or in a conformationally extended regions of the folded protein antigen. Differently, in **conformational epitopes**, the antibody interacts with amino acids not sequentially linked but spatially close one to each other, because of the protein folding. Antigen-

antibody binding is reversible, and follows the basic thermodynamic principles of any reversible bimolecular interaction<sup>4</sup>.

The binding energy between an antibody molecule and the antigen determinant is termed **affinity**. Thus, antibodies with paratopes recognizing epitopes perfectly, will have higher affinity for the antigen in question. On the contrary antibodies for which the antigen fit is less perfect, will have fewer non-covalent bonds established into the complex, and the binding strength will be lower. **Avidity** can be regarded as the sum of all different affinities. Mathematically, affinity and avidity are expressed as an association constant (K, L/mol) calculated under equilibrium conditions<sup>5</sup>.

### 1.3 Molecular mechanisms of autoimmunity

Autoimmunity represents the end result of the breakdown of one or more of the basic mechanisms regulating immune tolerance. Since Paul Ehrlich (who was the first to postulate the existence of mechanisms preventing the generation of self-reactivity), several ideas concerning the nature of this inhibition have developed in parallel with the progressive increase in understanding the immune system. Currently, three general pathways are thought to be involved in the maintenance of selective unresponsiveness to autoantigens: sequestration of self-antigens, rendering them inaccessible to the immune system; specific unresponsiveness (**tolerance** or **anergy**) of relevant T or B cells; and limitation of potential reactivity by regulatory mechanisms. Derangements of these normal processes might predispose to the development of autoimmunity. Microbial superantigens, such as staphylococcal protein A and staphylococcal enterotoxins, are substances that can stimulate a broad range of T and/or B cells based upon specific interactions with selected

---

<sup>4</sup>Harlow, E.; and Lane, D., "Using Antibodies, a laboratory manual", Cold Spring Harbor Laboratory Press, NY, **1999**.

<sup>5</sup>Crowther, J.R., "ELISA Theory and Practice Methods in Molecular Biology" Vol.42, Editor John M. Walker, HUMANA PRESS, **1995**.

## INTRODUCTION

families of immune receptors irrespective of their antigen specificity. If autoantigen-reactive T and/or B cells express these receptors, autoimmunity might develop. Alternatively, **molecularmimicry** or cross reactivity between a self antigen and a microbial molecule with a very similar structure and/or conformation to mammalian surface glycoproteins and/or glycolipids, might lead to activation of autoreactive lymphocytes. Molecular mimicry has been reported in type I diabetes mellitus, rheumatoid arthritis, and multiple sclerosis<sup>6</sup>. The most commonly identified triggering agents are pathogens having carbohydrate sequences (considered the antigens) in common with the peripheral nervous tissue.

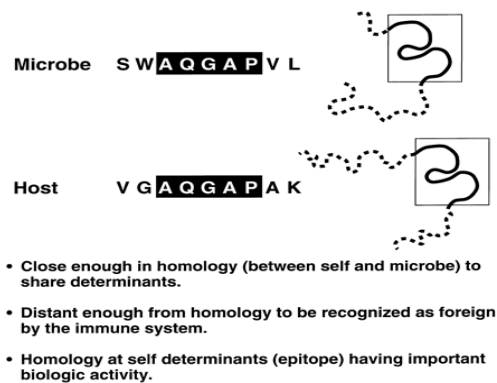


*Figure 1.5. Molecular mimicry<sup>7</sup>.*

The human stomach pathogen *Helicobacter pylori* exposes lipopolysaccharide (LPS) containing Lewis antigens mimicking human glycan structures interacting with human dendritic cells: these are thought to induce a suppression of the immune response thus facilitating a chronic *H. Pylori* infection. Moreover, LPS biosynthetic pathway can be considered evolutionarily connected to bacterial protein N-glycosylation<sup>8</sup>.

<sup>6</sup> Oldstone, M. B. A., *Cell*, **1987**, *50*, 819-820.

<sup>7</sup> Oldstone, M.B.A., *The FASEB J.*, **1998**, *12*, 1255-1265.

<sup>8</sup> Hug, I.; and Feldman, M.F., *PLoS Pathogens*, **2010**, *6*(3), e1000829.

### 1.4 The Autoimmune Diseases

Autoimmune diseases are syndromes caused by the activation of T and/or B cells, with no evidence of other causes such as infections or malignancies. The essential feature of an autoimmune disease is that tissue injury is caused by the immunologic reaction of the organism with its own tissues. In some autoimmune disorders a pathologic immune response is localised to specific antigens confined to a particular organ system. Alternatively, systemic autoimmune diseases are characterized by an immune response to ubiquitous intracellular antigens in which the relationship between immune specificity and disease manifestations may not be obvious. Multiple factors can contribute to the genesis of clinical autoimmune disease syndromes including genetic susceptibility, environmental immune stimulants such as drugs, infectious agent triggers, and loss of T regulatory cells, as shown in *Figure 1.6*.

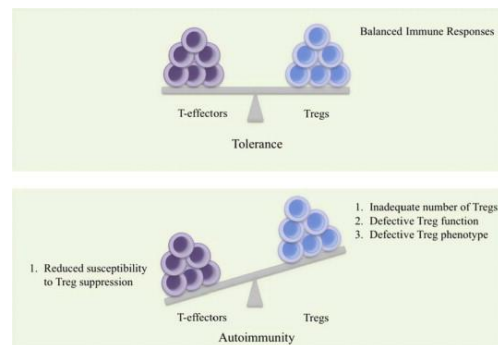


**Figure 1.6.** Possible causes of immune regulation failure in Systemic lupus erythematosus and rheumatoid arthritis autoimmune diseases<sup>9</sup>.

Genetic evaluation has shown that the occurrence in type 1 diabetes, rheumatoid arthritis, multiple sclerosis, and systemic lupus erythematosus is approximately 15 to 30% of pairs of monozygotic twins, whereas in the case of coeliac disease is 60%. Autoimmune diseases affect approximately 8% of

<sup>9</sup>Chavele, K.M.; and Ehrenstein, M.R., *FEBS Lett.*, **2011**, 585(23), 3603–3610.

## INTRODUCTION

the population, 78% of whom are women. They often cause chronic debilitating illnesses thus having a high social impact<sup>10</sup>.

### 1.4.1 Aberrant PTMs triggering autoimmunity

Alterations in antigen presentation may also contribute to autoimmunity. This may occur by epitope spreading, in which protein determinants (*epitopes*) not routinely seen by lymphocytes (*cryptic epitopes*) are recognized as a result of immunologic reactivity to associated molecules. Growing evidences indicate that post-translational modifications (PTMs), either native or aberrant, may play a fundamental role for specific autoantibody recognition in autoimmune diseases<sup>11</sup>. In autoimmune diseases in which the antigens have not yet been characterised, several molecules (not only carbohydrates) could modify by a covalent bond a self-protein antigen, which will become a *non-self* one triggering an abnormal antibody response<sup>12</sup>. Aberrant glycosylation of self-antigens (proteins), deamidation, biotinylation and lipoylation, as well as transamidation and other modifications can be responsible of influencing the level of epitope production, and the generation of neoepitopes, leading to autoimmune responses.

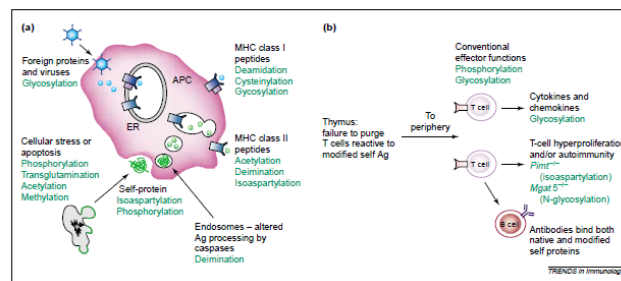


**Figure 1.7.** Examples of common PTMs triggering autoimmune mechanisms.

<sup>10</sup>Lipman, N.S.; Jackson, L.R.; Trudel, L.J.; and Weis-Garcia, F., *ILAR J.*, **2005**,46(3), 258-268.

<sup>11</sup>Doyle, H.A.; and Mamula, M.J., *Trends. Immunol.* **2001**, 22, 443-449.

<sup>12</sup>S. Mouritsen, M. Meldal, I. Christiansen-Brands, H. Elsner, O. Werdelin, *Eur. J. Immunol.*, **1994**, 24, 1066-1072.

The modified regions are termed neo-antigenic epitopes and can be recognized by different specific antibodies. Therefore, glycopeptides with simple sugars or synthetic peptides reproducing other modifications can be suitable tools to investigate the antigen fine specificity of specific T cells.

### 1.5 The role of glycosylation in autoimmune diseases

Interest in glycobiology has dramatically increased amongst immunologists during the last few years due to the fact that oligosaccharides also play a central role in adhesion and homing events during inflammatory processes, comprise powerful xenotransplantation antigens, and may provide targets for tumor immunotherapy. Additionally, alterations in glycosylation are now known to occur in a number of autoimmune diseases<sup>13</sup>.

Interestingly, for the first time Lolli *et al.* in 2005<sup>14</sup>, Schwarz *et al.* in 2006<sup>15</sup>, and more recently Brettschneider *et al.* in 2009<sup>16</sup>, demonstrated that glucosylation could be one of the PTMs responsible of triggering autoAbs in a relapsing-remitting form of multiple sclerosis (MS). Almost all of the key molecules involved in the innate and adaptive immune response are glycoproteins and in the cellular immune system, specific glycoforms have been reported to be involved in folding, quality control, and assembly of peptide-loaded MHC antigens and the T cell receptor complex. Oligosaccharide structures play also a key role in antigenicity of a number of clinically relevant antigens such as blood group determinants. Moreover, oligosaccharides attached to glycoproteins in the junction between T cells and APCs help to orient binding faces, providing protease protection, and

<sup>13</sup> a) Delves, P.J., *Autoimmunity*, **1998**, 27(4), 239-53; b) Rudd, P.M.; Elliott, T.; Cresswell, P.; Wilson, I.A.; Dwek, R.A., *Science*, **2001**, 291(5512), 2370-2376.

<sup>14</sup> Lolli, F.; Mulinacci, B.; Carotenuto, A.; Bonetti, B.; Sabatino, G.; Mazzanti, B.; D'Ursi, A. M.; Novellino, E.; Pazzagli, M.; Lovato, L.; Alcaro, M. C.; Peroni, E.; Pozo-Carrero, M. C.; Nuti, F.; Battistini, L.; Borsellino, G.; Chelli, M.; Rovero, P.; Papini, A.M. *Proc. Natl. Acad. Sci., U.S.A.* **2005**, 102(29), 10273-10278.

<sup>15</sup> Schwarz, M.; Spector, L.; Gortler, M; *et al.*, *J. Neurol. Sci.*, **2006**, 244, 59-68.

<sup>16</sup> Brettschneider, J., Jaskowski, T.D.; Tumani, H., *J. Neuroimmunol.*, **2009**, 217, 95-101.

## INTRODUCTION

restricting nonspecific lateral protein-protein interactions. Last but not least, in the humoral immune system, all of the immunoglobulins and most of the complement components are glycosylated.

### **1.5.1 Protein glycosylation**

Protein glycosylation is a phenomenon shared by all domains of life. Over 70% of the eukaryotic proteome is thought to be glycosylated. Protein modification by enzymatic glycosylation, is an event that reaches beyond the genome and is controlled by factors greatly differing among cell types and species. Gangliosides, glycosphingolipids, and glycoproteins found on the surface of oligosaccharides provide cells with distinguishing surface markers that can serve in cellular recognition and cell-to-cell communication. The defining event in the biogenesis of peptide-linked oligosaccharides is clearly the formation of sugar-amino acid bond. This, in most instances, determines the nature of the carbohydrate units that will subsequently be formed by the cellular enzymatic machinery, which in turn influences specific protein's biological activity.

Protein glycosylation is structurally divided into O- and N-linked glycosylation. In the former, the first sugar of the oligosaccharide is attached to the hydroxyl group of Ser, Thr, Hyl, or Hyp residues, whereas in the latter it is attached to the terminal amide group of Asn residues. Although more and more bacterial and archaeal N-glycosylation systems are becoming known, the best characterized system is the N-glycosylation pathway of eukaryotes and especially of *Saccharomyces cerevisiae*<sup>17</sup>. Mechanisms for glycan attachment to proteins and further studies will shed more light on the variety of glycosylation pathways.

---

<sup>17</sup>Dwek, R.A., *Chem. Rev.*, **1996**, 96, 683–720.

### **1.5.2 Bacteria transferring sugar moieties in host proteins**

We now know that carbohydrates are involved in a wide range of biological processes, including host-pathogen interactions and the immune response and that glycoproteins are a common feature in all domains of life. Bacteria surfaces are decorated with glycans. Today, many pathways by which prokaryotes can promote glycosylation mechanisms have been reported. Considering the huge diversity of prokaryotic glycoproteins discovered in recent years it is clear that glycosylation in these organisms is the normal rather than the exception. In this sense, the discovery of a general N-glycosylation system in *Campylobacter jejuni* represents the starting point a great deal of progress in understanding prokaryotic glycosylation<sup>18</sup>.

### **1.5.3. N-linked protein glycosylation**

Asn N-linked glycosylation of proteins is a fundamental and extensive co-translational modification that results in the covalent attachment of the first sugar of an oligosaccharide onto Asn residue of polypeptide chains. The biosynthetic machinery responsible for this elaborate protein modification follows a similar overall progression, whereby an oligosaccharide is assembled in a stepwise fashion on a polyisoprenyl-pyrophosphate carrier and then ultimately transferred to proteins. Glycosylated proteins in both eukaryotes and prokaryotes contain the Asn-Xaa-Ser/Thr sequon. In both systems, glycosylation is abolished when the Xaa amino acid is Pro, suggesting that local conformation plays an important role in the glycosylation reaction, catalyzed by oligosaccharil transferase (OT).

---

<sup>18</sup>Szymanski, C.M.; Wren, B.W., *Nat Rev Microbiol.*, **2005**, 3, 225-37.

## INTRODUCTION

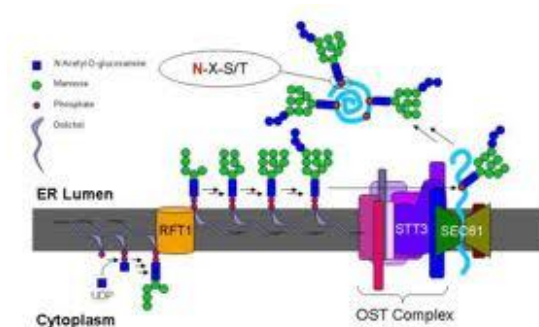


**Figure 1.8.** *N-Glycosylation in Eukaryotes.*

There is evidence that the local secondary structure around the site of glycosylation in eukaryotes may be a vital determinant in this enzymatic process where glycosylation induces conformational switch from an Asn-turn to a  $\beta$ -turn structure. Bacteria utilize a wide variety of amino- and deoxy-sugars that are not found in eukaryotic systems, for example *C. jejuni* heptasaccharide is structurally very different from the tetrasaccharide in eukaryotic N-linked glycosylation<sup>19</sup>. These modified proteins might have important roles in pathogenic pathways, as well as aberrant glycosylation of self-antigens promoted by bacteria could be the first event of tolerance loss to develop an autoimmune disorder.

### **1.6 Serologic Biomarkers for autoimmune diseases diagnostics**

A biomarker is an anatomical, physiological, and/or biochemical parameter, which should be easily determined and used as indicator of normal physiological or pathogenic processes. Molecules present in tissues and biological fluids can be identified as biomarkers and used to set up diagnostic/prognostic tools, as well as for monitoring the efficacy of a therapeutic treatment<sup>20,21</sup>. In particular, autoantibody detection is extremely valuable to follow up patients when disease exacerbations or remissions

<sup>19</sup>Weerapana, E.; and Imperiali, B., *Glycobiol.*, **2006**, 16(6), 91R-101R.

<sup>20</sup>Roland, P.; Atkinson, J.A.; and Lesko, L., *J. Clin. Pharm. Ther.*, **2003**, 73, 284-291.

<sup>21</sup>Baker, M., *Nature Biotech.*, **2005**, 23, 297-304.

correlates with antibody titer. As a consequence, antibodies present in patients' serum can be used as disease biomarkers<sup>22,23</sup> as a non-invasive alternative diagnostics. Unfortunately, in autoimmune diseases only very low specific antibodies were demonstrated to be detectable in serum, possibly because proteins used in the assays cannot reproduce the real autoantigen. Moreover, an entire protein should contain more than one epitope specific for different autoantibodies. These observations account, at least in part, for the limited success got in the discovery of biomarkers for autoimmune diseases using proteomic analysis and/or protein microarrays.

### **1.6.1 The "Chemical Reverse Approach" and autoimmune diseases**

In autoimmune diseases diagnostics, specific identification of autoantibodies by protein antigens isolated from biological material or reproduced by recombinant technologies has sometimes failed. Native protein antigens (particularly if underexpressed) can be difficult to be fully sequenced or cannot often be successfully reproduced using recombinant techniques. In any case protein folding and exposition of the epitope can be also a difficult task. Moreover, proteins may be difficult to isolate with correct co- or post-translational modifications. Synthetic peptides derived from native protein sequences and reproducing specific epitopes, or mimicking immunogenic modifications could be even more effective and specific than native proteins in antibody detection.

To identify and optimise synthetic peptides as antigenic probes for fishing out autoantibodies circulating in biological fluids as biomarkers, an innovative "Chemical Reverse Approach" has been developed for the first time in the Laboratory of Peptide and Protein Chemistry and Biology of the University of

---

<sup>22</sup> Leslie, D.; Lipsky, P.; and Notkins, A.L., *J. Clin. Invest.*, **2001**, 108, 1417-1422.

<sup>23</sup> Alcaro, M.C.; Lolli, F.; Migliorini, P.; Chelli, M.; Rovero, P.; and Papini, A.M., *Chem. Today*, **2007**, 25 (5), 14-16.

## INTRODUCTION

Florence, (PeptLab). This approach was defined “Reverse” because the screening of the synthetic antigenic probe is guided by autoantibodies circulating in autoimmune disease patients’ blood. “Chemical” because autoantibody recognition drives selection and optimisation of the “chemical” structure from defined peptide libraries<sup>24</sup>. Autoantibodies circulating in patients’ biological fluids drive the selection of synthetic post-translationally modified peptides mimicking new epitopes in antigens. Peptide epitopes identified by this approach, if selectively and specifically recognizing autoantibodies in a statistical significant number of patients, can be used as antigenic probes in immunoenzymatic assays to detect disease biomarkers in an efficient way. Therefore, screening of focused libraries of unique modified peptide molecules can be a valuable strategy to develop optimised peptide antigens containing the minimal epitope with the correct modification to detect at the best autoantibodies specific of the autoimmune disease under investigation<sup>25</sup>. As a proof-of-concept this approach has been successfully applied for the identification of autoantibodies as biomarkers of an autoimmune mediated form of MS (the most difficult disease since protein antigens are localized in the central nervous system), Rheumatoid Arthritis (RA), and more recently Rett Syndrome (RS) using simple peptide-based Enzyme Linked Immunosorbent Assays (ELISA). In the case of RA, a key step in setting up the commercially available ELISA was represented by identification of deiminated sequences of filaggrin that are recognized in a high percentage of RA sera<sup>26,27</sup>. Sensitivity of the assay was increased modifying the peptide structure to optimally expose the citrulline moiety. In fact a cyclic citrullinated peptide allows detection of antibodies with high

---

<sup>24</sup>Papini, A.M. *J. Pept. Sci.* (2009), 15, 621-628.

<sup>25</sup>Lolli, F.; Rovero, P.; Chelli, M.; and Papini, A.M. *Expert Rev. Neurotherapeutics.*, 2006, 6 (5), 781-794.

<sup>26</sup>Sebbag, M.; Simon, M.; Vincent, C.; Masson-Bessiere, C.; Girbal, E.; Durieux, J.J.; and Serre, G.; *J. Clin. Invest.*, 1995, 95, 2672-2679.

<sup>27</sup>Serre, G., *Joint Bone Spine*, 2001, 68, 103-105.

specificity in RA patients<sup>28,29</sup>. These ELISAs are now considered a gold standard for RA diagnosis and follow up.

### **1.6.2. ELISA for diagnostics**

In the field of autoimmune diseases, a number of autoantibody detection techniques have been developed. Over the past years, autoimmunity diagnosis has gone through a very dynamic period, associated with the introduction of new tests deriving from the identification of new families of autoantibodies and the demonstration of their usefulness into the clinic. The Radio-ImmunoAssay (RIA) has been traditionally used in autoantibody detection and it is based on labelled targets providing a radioactive signal. Today RIA is largely supplanted by ELISA, because in ELISA the antigen-antibody reaction is measured using a colorimetric signal instead of a radioactive signal thus avoiding requirements for special radioactivity instrumentation and precautions. ELISA is a versatile tool that is used for diagnosis of different kind of diseases, from viral infections to immune mediated diseases and it can be used to detect and quantify any antigen or antibody that one may desire to look for. It stands for “Enzyme Linked Immunosorbent Assay” and that means a test which uses an immunosorbent (a substance that either is or reacts with an immune compound to bind to it) linked to an enzyme. Depending on whether one is looking for antigens or antibodies, antibodies or antigens, respectively, are chemically bound to the surface of wells of the ELISA plates. The design of different types of immune assays is possible. The employ of a wide range of methods to detect and quantitate antigens or antibodies makes the ELISA one of the most powerful of all the immunochemical techniques. The main three classes of immunoassays that can be performed are: the

---

<sup>28</sup> Schellekens, G.A.; de Jong, B.A.; van den Hoogen, F.H.; van de Putte, L.B.; and van Venrooij, W.J., *J. Clin. Invest.* **1998**,101, 273-281.

<sup>29</sup>Method for the diagnosis of rheumatoid arthritis". Inventors: Alcaro M.C.; Pratesi F.; Paolini I.; Chelli M.; Lolli F.; Papini A.M.; Rovero P.; and Migliorini P., Applicant Toscana Biomarkers Srl. Patent application number EP11167420.6. (**2011**).

## INTRODUCTION

antibody capture assays and the antigen capture assays and the antibody sandwich assays. Moreover, any immunoassay can be performed with four variations; the assay can be done in antibody excess, in antigen excess, as an antibody competition, or as an antigen competition<sup>30</sup>.

### **1.6.3 Peptide-based ELISA**

Many small chemicals, such as peptides, can be used in ELISA helping to dissect and elucidate the properties of an antibody response. Peptides are particularly useful when the epitope sequence has been discovered inside the total protein. To this end, epitope mapping and Ala-scan are valid strategies to define the minimal epitopes recognised by the immune system. Moreover, peptide antigens can display enhanced recognition specificity eliminating or minimizing potential cross-reactivity between structurally homologous protein epitopes. Peptides have several advantages: they are relatively easy to produce and may retain chemical stability over time. Finally, reproduction of co- or post-translational modifications in peptides is a quite easy task to be achieved by a synthetic point of view, if compared to recombinant techniques<sup>31</sup>.

The most frequently asked question concerning synthetic peptides is what sequence should be reproduced. The presence of Pro residues in synthetic peptides originally was suggested because  $\beta$ -turns often form portions of known epitopes, moreover in several papers it is reported that carboxy-terminal sequences are often exposed and can be targeted by anti-peptide sequences. Similarly, many amino terminal regions are exposed, and these may also make good targets. Another potentially useful parameter for selecting peptide sequences is their “mobility”, i.e. regions that are more flexible are more likely to be epitopes respect to the more static ones.

---

<sup>30</sup>Harlow, E.; and Lane, D., *Antibodies: A laboratory manual*, CSH Ed. Cold Spring Harbor Laboratory Press, NY, **1999**

<sup>31</sup>Papini, A.M. “Peptide-based Immunoassays for Biomarkers Detection: a Challenge for Translational Research” *Zervas Award Lecture 30<sup>th</sup> European Peptide Symposium*, August 31-September 5 **2008**, Helsinki, Finland.

## INTRODUCTION

Theoretical ability to understand the immune response with defined peptide epitopes coupled to the correct set up of the ELISA experiments can have important advantages not only for diagnostic purposes but even to dissect the pathological pathways leading to the development of a disease.

## **PART A: Design and synthesis of modified peptide probes to study Coeliac Disease**

### **2. Coeliac Disease: an overview**

Coeliac disease (CD), also called gluten-sensitive enteropathy, as the other immune mediated diseases, has a complex and multifactorial aetiology and occurs in genetically susceptible individuals in association with environmental factors (gluten), leading to a chronic inflammatory condition and villous atrophy shown in *Figure 2.1*.

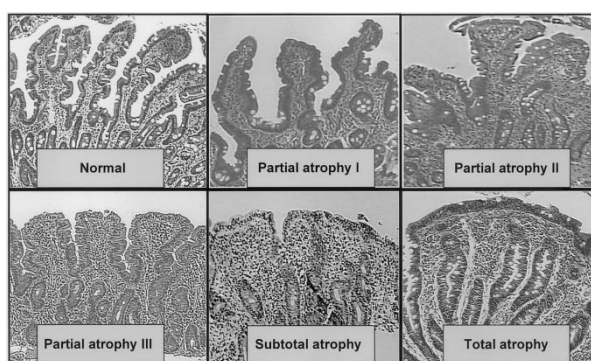


**Figure 2.1** Marsh classification of intestinal coeliac lesions<sup>32</sup>.

CD may present in early childhood soon after the introduction of gluten-containing food. It is triggered by the gliadin fraction of wheat gluten and similar alcohol soluble proteins called prolamines<sup>33</sup>. The massive penetration of gliadin fractions across the intestine lumen has been observed in association with the dysregulation of a human intestinal protein, zonulin. Zonulin regulates the intestinal permeability acting on the tight junctions and, during the acute phase of CD the lumen permeability dramatically increases. This discovery

<sup>32</sup>Fasano, A.; and. Catassi, C., *Gastroenterol.*, **2001**, 120, 636-651.

<sup>33</sup>Schuppan, D., *Nutr. Clin. Care*, **2005**, 8(2), 54-69.

suggests that increased levels of zonulin are a contributing factor for the development of the disease<sup>34</sup>. CD is classically characterized by gastrointestinal symptoms, but also atypical or silent forms are known (dermatitis, iron deficiency *anaemia*, osteoporosis, and many others), and sometimes is associated with other autoimmune disorders<sup>35</sup>. If a genetic predisposition is present the gluten intake leads to a complex immune response, both a cell-mediated form involving T cells and humoral form leading to the secretion of autoantibodies, mainly to gliadin and tissue transglutaminase, tTG<sup>36</sup>.

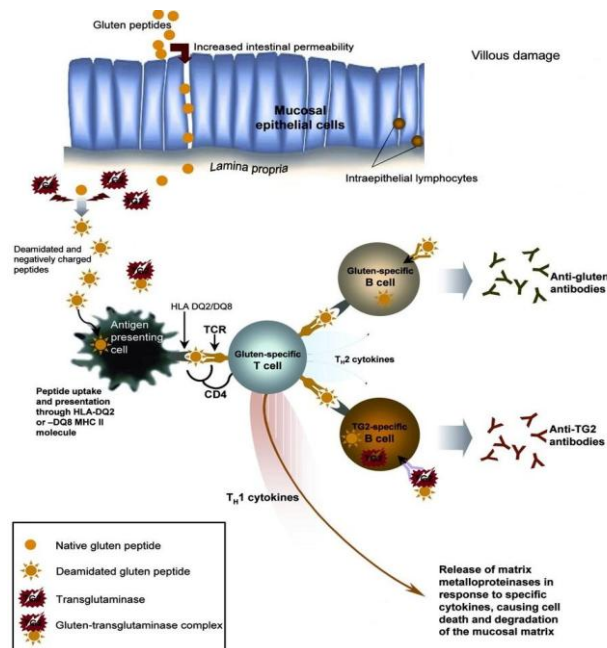


**Figure 2.2.** Postulated mechanism for the pathogenesis of CD.

In the pathway shown in *Figure 2.2*, HLA-DQ2 and DQ8 molecules bound to deamidated gliadin peptides are able to present gluten to T cells leading to the

<sup>34</sup>Fasano, A.; and Not, T. *Lancet*, **2000**, 358, 1518-1519.

<sup>35</sup>Schuppan, D.; and Cicciocioppo, R., *Dig Liver Dis*, **2002**, 34, 13–15.

<sup>36</sup>Murray, J.A., *Am. J. Clin. Nutr.*, **1999**, 69, 354-365

## PART A

activation of gluten-specific CD4<sup>+</sup> T-helper 1 (Th1) cells in the *lamina propria*, as shown in *Figure 2.3*.

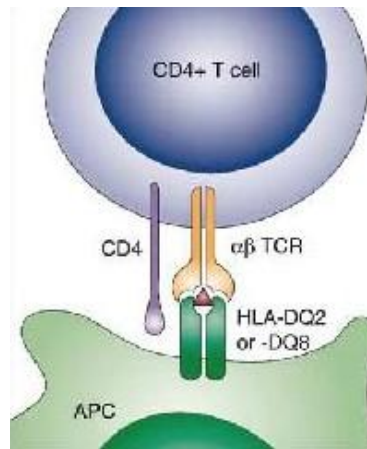


**Figure 2.3.** CD4<sup>+</sup> T-cells recognize modified gliadin peptides presented by HLA-DQ2 or -DQ8 on the surface of APCs.

The activated T-cells are able to secrete Th1 cytokines such as IFN- $\gamma$  and TNF $\alpha$ , inducing the release and activation of Matrix Metalloproteinases (MMPs) by myofibroblasts, finally resulting in mucosal remodelling and villous atrophy. Additionally, Th2 cytokines driving the production of autoantibodies to deamidated gliadin peptides, tTG, and gliadin-tTG complexes are produced. Catalytically inactive extracellular tTG is transiently activated in response to innate immune signals such as exposure to a potent ligand of the toll-like receptor TLR-3<sup>37</sup>. Other cytokines, such as IL-18, IFN- $\alpha$ , or IL-21 seem to play a role in polarizing and maintaining the Th1 response. Furthermore, IL-15 links the adaptive immune system to innate immune responses<sup>38</sup>. These are central effector cells of the intestinal inflammation resulting in crypt hyperplasia and villous atrophy<sup>39</sup>.

<sup>37</sup>Siegel, M.; Strnad, P.; Watts, R.E.; Choi, K.; Jabri, B.; Bishr Omary, M.; and Khosla, C., *PLoS One*, **2008**, 3(3), e1861. doi:10.1371/journal.pone.0001861

<sup>38</sup>Schuppan, D.; Junker, Y.; and Barisani, D., *Gastroenterol*, **2009**, 137, 1912–1933.

<sup>39</sup>Halstensen, T.S.; Scott, H.; Fausa, O.; and Brandtzaeg, P., *Scand. J. Immunol.*, **1993**, 38, 581–590.

*Autoantibodies in CD*

Untreated CD patients (on a wheat-containing diet) usually have increased levels of antibodies against gluten-derived peptides, several other food antigens, and autoantigens present in the mucosa. The autoantibodies in CD are primarily directed against the  $\text{Ca}^{2+}$ -activated (extracellular) form of the enzyme tTG<sup>40</sup>. The autoantibodies to tTG are both of the IgA and IgG isotypes, but the IgA antibodies which are primarily produced in the intestinal mucosa demonstrate the highest disease specificity.

The mechanism underlying the formation of the autoantibodies in CD is not completely understood. The production of anti-tTG IgA antibodies is likely to be dependent on cognate T-cell help to facilitate isotype switching of autoreactive B cells. Autoreactive T cells specific for tTG could provide the necessary help for B-cell production of anti-tTG IgA, but since tTG is expressed in the thymus such cells are unlikely to survive thymic selection. An alternative explanation could be that the complexes of gluten derived peptides and tTG allows the gluten-reactive T-cells to provide help to the tTG-specific B cells by a possible mechanism of intramolecular help. This model could explain why the serum anti-tTG antibodies in CD patients disappear when patients are following a gluten free diet<sup>41</sup>.

*HLA genes confer genetic susceptibility*

The high prevalence of CD (around 10%) among first-degree relatives indicates that the susceptibility to this disease is strongly influenced by inherited factors. The strong genetic influence in coeliac disease is supported

---

<sup>40</sup> Dieterich, W.; Ehnis, T.; Bauer, M.; Donner, P.; Volta, U.; Riecken, E.O.; et al., *Nat. Med.*, **1997**, 3, 797-801.

<sup>41</sup> Sollid, L.M., *Nat. Rev. Immunol.*, **2002**, 2, 647–655.

## PART A

by a very high concordance rate (around 75%) in monozygotic twins<sup>42</sup>. The genetic predisposition is mainly associated with HLA class II genes, 90% of celiac patients have HLA-DQ2 and HLA-DQ8 for a minority of patients is present<sup>43</sup>. The HLA-DQ2 and DQ8 molecules confer the genetic susceptibility to coeliac disease by presenting disease-related peptides to T cells in the small intestine thanks to the peculiarity of the amino acid residues in their binding site<sup>44</sup>, or by shaping the T-cell repertoire during T-cell development in the thymus<sup>45</sup>.

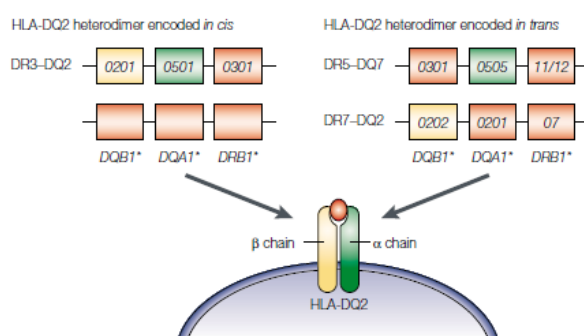


**Figure 2.4.** HLA association in coeliac disease.

### *Environmental features*

Gluten dietary intake is associated with alterations of small intestinal mucosa classified according to the criteria introduced by Marsh<sup>46</sup>. Gluten can be defined

<sup>42</sup>Greco, L.; Corazza, G.; Babron, M.C.; Clot, F.; Fulchignoni-Lataud, M.C.; Percopo, S.; Zavattari, P.; Bouguerra, F.; Dib, C.; Tosi, R.; Troncone, R.; Ventura, A.; Mantavoni, W.; Magazzù, G.; Gatti, R.; Lazzari, R.; Giunta, A.; Perri, F.; Iacono, G.; Cardi, E.; de Virgiliis, S.; Cataldo, F.; De Angelis, G.; Musumeci, S.; and Clerget-Darpoux, F., *Am. J. Hum. Genet.*, **1998**, 62, 669–675.

<sup>43</sup> a) Shaoul, R.; and Lerner, A. *Autoimmun. Rev.*, **2007**, 6(8), 559–565; b) Sollid, L. M.; et al. *J. Exp. Med.*, **1989**, 169, 345–350; c) Lundin, K. E. A.; Scott, H.; Hansen, T.; Paulsen, G.; Halstensen, T.S.; Fausa, O. Thorsby, E.; and Sollid, L. M., *J. Exp. Med.*, **1993**, 178, 187–196.

<sup>44</sup>Kim, C.Y.; Quarsten, H.; Bergseng, E.; Khosla, C.; and Sollid, L.M. *PNAS*, **2004**, 101(12), 4175–4179.

<sup>45</sup>Schuppan, D. *Gastroenterol.*, **2000**, 119, 234–242.

as the rubbery mass that remains when wheat dough is washed to remove starch granules and water-soluble constituents. Depending on the thoroughness of washing, the dry solid contain 75–85% protein and 5–10% lipids, most of the remainder is starch and non starch carbohydrates. Gluten is an extreme complex mixture of diverse proteins, gluten proteins can be divided into two main fractions according to their solubility in aqueous alcohols: the soluble gliadins and the insoluble glutenins. Due to their high content of Pro and Gln residues, the proteins of wheat gluten are collectively referred to as prolamines. The high content of Pro residues makes these prolamines particularly resistant to gastrointestinal digestion. This has important implications for their immunogenicity since gluten-derived peptides fulfil length requirements to be recognised by T cells. In particular, the gliadin fraction is referred to as the more toxic for CD patients. Gliadins are usually classified into  $\alpha$ -,  $\beta$ -, and  $\omega$ -gliadins whereas glutenins are classified according to their high and low molecular weight (HMW and LMW)<sup>47</sup>.

Type	MW $\times 10^{-3}$	Proportions <sup>a</sup> (%)	Partial amino acid composition (%)				
			Gln	Pro	Phe	Tyr	Gly
$\omega$ S-Gliadins	49-55	3-6	56	20	9	1	1
$\omega$ L,2-Gliadins	39-44	4-7	44	26	8	1	1
$\alpha/\beta$ -Gliadins	28-35	28-33	37	16	4	3	2
$\gamma$ -Gliadins	31-35	23-31	35	17	5	1	3
$\alpha$ -HMW-GS	83-88	4-9	37	13	0	6	19
$\beta$ -HMW-GS	67-74	3-4	36	11	0	5	18
LMW-GS	32-39	19-25	38	13	4	1	3

<sup>a</sup>According to total gluten proteins.

**Figure 2.5.** Characterization of gluten protein types.

## 2.1 Tissue Transglutaminase, structural insights for antibody recognition

The 76kDa enzyme tissue Transglutaminase belongs to a family of ubiquitous enzymes that are included in many pathways such as GTP hydrolysis in signal

<sup>46</sup> Marsh, M.N., *Gastroenterol.*, **1992**, 102, 330-354.

<sup>47</sup> Wieser, H. *Food Microbiol.*, **2007**, 24(2),115-119.

PART A

transducing<sup>48</sup>, cellular, and tissutal homeostasis, cellular cycle regulation, proliferation<sup>49</sup>, differentiation and apoptosis<sup>50</sup>. In erythrocytes as well as in other cells, the enzyme is latent during normal cell lifespam and is subjected to fine regulation, involving GTP and calcium.

Activated tTG catalyzes PTMs of specific Gln residues within its substrate proteins. tTG catalyzes deamidation of Gln residues or protein cross linking through the formation of  $\epsilon$ -( $\gamma$ -glutamyl)-lysine isopeptide bonds between Lys exposed on its surface and Gln residues in gliadin-derived peptides<sup>51</sup>.

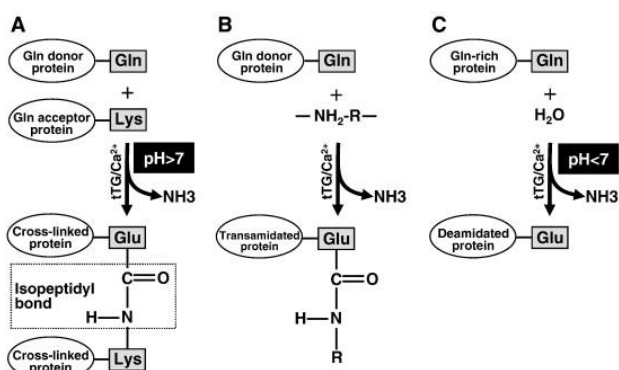


**Figure 2.6.** Reactions catalyzed by tissue Transglutaminase.

The increasing interest in transglutaminases because of their medical relevance led in the past few years to the production of numerous structural studies of the protein to clarify the basis of its regulation. The monomeric human tTG consists of four structural domains: the N-terminal  $\beta$ -sandwich; the core; and two C-terminal  $\beta$ -barrels. The structure of the human tTG was solved on the

<sup>48</sup> a) Iismaa, S.E.; Wu, M.J.; Nanda, N.; Church, W.B.; and Graham, R.M.; *J. Biol. Chem.*, **2000**, 275, 18259-18265; b) Nakaoka, H.; Perez, K.; Baek, D.M.; Das, T.; Husain, A.; Misono, K.; and Graham, R.M. *Science*, **1994**, 264, 1593-1596

<sup>49</sup> Haroon, Z.A.; Hettasch, J.M.; Lai, T.S.; Dewhirst, M.W.; and Greenberg, C.S., *FASEB J.*, **1999**, 13, 1787-1795.

<sup>50</sup> a) Melino, G.; Annicchiarico-Petruzzelli, M.; Piredda, L.; Candi, E.; Gentile, V.; Davies, P.J.; and Piacentini, M. *Mol. Cell. Biol.*, **1994**, 14, 6584-6596; b) Piacentini, M.; Rodolfo, C.; Farrace, M.G.; and Autuori, F., *Int J Dev Biol.*, **2000**, 44, 655-662.

<sup>51</sup> Qiao SW BE, Molberg O, Xia J, et al.. *J. Immunol.*, **2004**, 173, 1757-1762.

sequence of the human endothelial enzyme based on the alignment with the crystal structure of factor XIII. The ATP and GTP hydrolytic domain is localized in the N-terminus of tTG (amino acid residues 1-185). The predicted structure of this fragment contains a  $\beta$ -sandwich domain and part of the catalytic core region. The protein C-terminus also plays an important role in regulating the enzymatic activity. In the past years, since the first relevant findings published by Folk and Chung in 1973<sup>52</sup>, many research groups directed their efforts to characterize the tTG' structure associated with its enzymatic function<sup>53</sup>. As shown in several works and in the PDB deposited tTG-structure<sup>54</sup>, the protein active site is characterized by the presence of the so called "Catalytic triad" **Cys277**, **His335**, and **Asp358**.

Patent Application Publication Dec. 23, 2004 Sheet 4 of 575 US 2004/0259176 A1

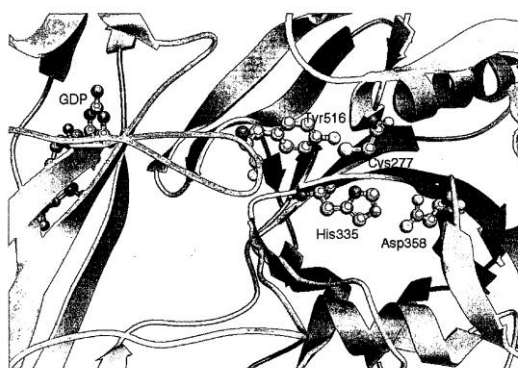


**Figure 2.7.** Tissue Transglutaminase' active site structure.

In the presence of GDP, tTG shows a closed conformation with the transamidating catalytic triad on the core domain in a hidden position. When the enzyme is functioning as a  $\text{Ca}^{2+}$ -dependent transglutaminase, the C-

<sup>52</sup>Folk, J.E.; and Chung, S.I., *Adv Enzymol Relat Areas Mol Biol.*, **1973**, 38, 109–191.

<sup>53</sup> a) Gentile, V.; Saydak, M.; Chiocca, E.A.; Akande, O.; Birckbichler, P.J.; Lee, K.N.; Stein, J.P.; and Davies, P.J., *J. Biol. Chem.*, **1991**, 266, 478-83; b) Lai, T.S.; Slaughter, T.F.; Koropchak, C.M.; Haroon, Z.A.; and Greenberg, C.S., *J. Biol. Chem.*, **1996**, 271, 31191-5.

<sup>54</sup> Liu, S.; Cerione, R. A.; and Clardy, J., *P.N.A.S.*, **2002**, 99, 2743–2747.

## PART A

terminal beta barrels are displaced of 120Å and the structure becomes open and extended, at least transiently<sup>55</sup>. Pinkas *et al.*<sup>56</sup> reported the tTG solved structure, at atomic resolution, in a complex with a molecule mimicking a natural substrate (i.e. gluten peptides deriving from proteolysis).

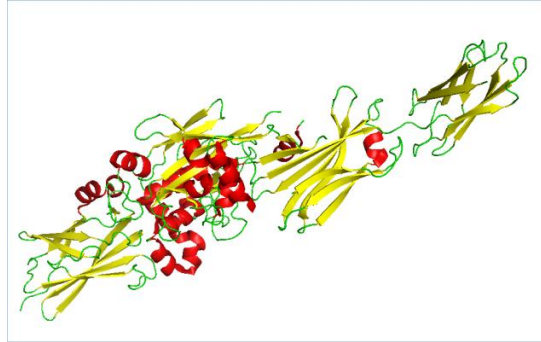


**Figure 2.8.** Activated tTG displays an open conformation.

The new structure exposes the active site undergoing to a very large conformational change with respect to previous tTG structures. Very few proteins have been observed to display this type of large-scale transformation. By the way this structural rearrangement could assume a significant role in the early stages of CD. Moreover, the open conformation described is likely to expose self-epitopes that are ordinarily inaccessible to the immune system. In this model, the catalytic Cys277 is located into a hydrophobic tunnel bridged by two Trp residues, i.e. Trp241 and Trp332. The other side of the tunnel is open and presumably serves as the binding site for a Lys residue or alternative nucleophilic substrates participating in the transamidation reaction. The enzyme displays selectivity for particular Gln residues. tTG identifies QxP and QxxF (where x can be Tyr, Trp, Met, Leu, Ile, Val) as consensus sequences,

<sup>55</sup> Casadio, R.; Polverini, E.; Mariani, P.; Spinozzi, F.; Carsughi, F.; Fontana, A.; Polverino De Laureto, P.; Matteucci, G.; Bergamini, C.M., *Eur. J. Biochem.*, **1999**, 262, 672-679.

<sup>56</sup> Pinkas, D.M.; Strop, P.; Brunger, A.T.; and Khosla, C.; *PLoS Biology*, **2007**, 5(12), 2788-2796.

whereas Gln followed directly by Pro will not be targeted. As shown in *Figure 2.9*, the modification introduced by tTG in peptide substrates in example  $\alpha 2$ -gliadin (57-89), allows the interaction between Glu residues, and the HLA-DQ2 binding site<sup>57,58</sup>.

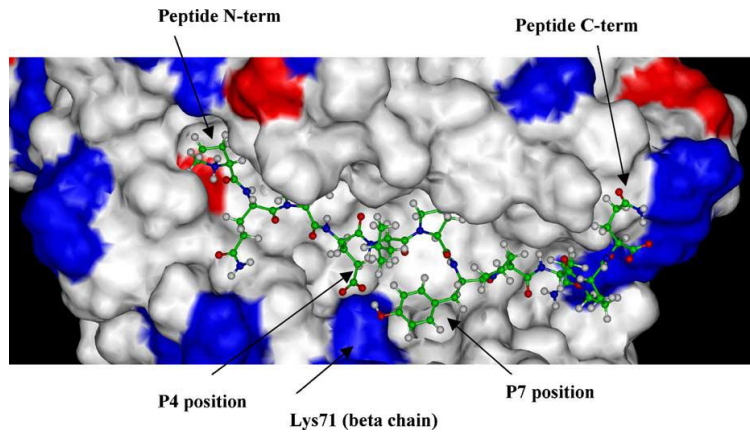


**Figure 2.9.** Interaction between deamidated gliadin peptides and Lys $\beta$ 71 residue in the DQ2 HLA pocket.

Deamidated gluten peptides are presented to the CD4+T-cells by HLA-DQ2 or -DQ8 molecules on the cell surface of antigen-presenting cells. This is thought to be the event triggering the T-cell autoimmune response in CD. It is evident that the role of tTG in the pathogenesis of coeliac disease, even if not completely understood, clearly encompasses more than simply being the target of the autoantibodies in the disease.

#### *Antigenic domains in tissue Transglutaminase*

The enzyme tTG is a highly sensitive and specific target of autoantibodies in CD. The characterization of tTG antigenic domains is a crucial step in understanding the autoimmune role and onset in the CD' pathogenesis, since

<sup>57</sup>Shan, L.; Molberg, O.; Parrot, I.; Hausch, F.; Filiz, F.; Gray, G.M.; Sollid, L.M.; Khosla, C., *Science*, **2002**, 297, 2275–2279.

<sup>58</sup>Costantini, S.; Rossi, M.; Colonna, G.; and Facchiano, A. M., *J. Mol. Graph. Model.*, **2005**, 23(5), 419-43.

## PART A

the pathogenic role and exact binding properties of these autoantibodies to tTG are still unclear. Sera from patients with CD at first diagnosis were demonstrated to have high levels of auto-antibodies recognising distinct functional domains of tTG. Analyzing the antigen-antibody recognition pattern in CD patients' sera it is possible to identify the presence of a complex and heterogeneous autoimmune response toward different tTG expressed constructs (both linear and related to the protein folding), mainly directed to conformation-dependent epitopes. This is a peculiarity of other autoimmune diseases having autoantibodies directed to multiple conformational epitopes of autoantigens such as GAD and IA-2 in diabetes mellitus and TPO antibodies in Hashimoto thyroiditis<sup>59</sup>.

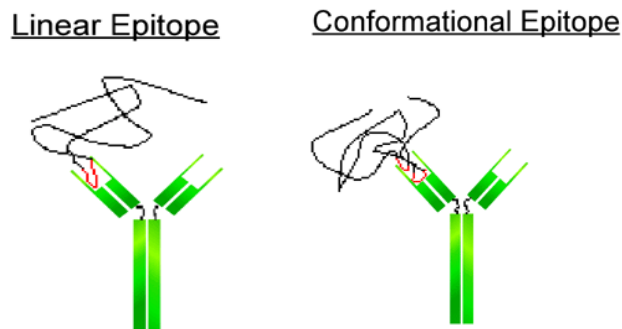


**Figure 2.10.** Linear and conformational epitopes.

Antibodies of different celiac patients can recognise parts of the same conformational epitopes constituted by amino acids located in different portions of the protein sequence. Simon-Vecsei *et al.* demonstrated that coeliac antibodies directly bind to the tTG surface in the following positions Arg19-

---

<sup>59</sup> a) R. Finke, P. Seto and B. Rapoport, *J. Clin. Endocrin. Metab.*, **1990**, 71, 53-59; b) K. Syren, L. Lindsay, B. Stoehrer, K. Jury, F. Luhder, S. Baekkeskov, W. Richter, *J. Immunol.*, **1996**, 157, 5208-5214; c) H. Xie, B. Zhang, Y. Matsumoto, Q. Li, A.L. Notkins, M.S. Lan, *J. Immunol.*, **1997**, 159, 3662-3667.

Glu153-Met659<sup>60</sup>. The identification of defined epitope boundaries suggests that these tTG regions may harbor amino-acid sequences of high immunogenicity, which could be crucially involved in the induction of autoimmunity in CD. Antibodies to tTG are able to recognize linear epitopes of the autoantigenic protein and these autoreactive domains are sex- and age-dependent<sup>61</sup>. The dominant epitopes are clustered in N- and C-terminal domains, one spanning from the N-terminus to the catalytic region and the other comprising the two C-terminal domains<sup>62,63</sup>.

## 2.2 Epitope mapping of antigenic proteins

Epitope mapping is an important tool in the selection and characterization of antibodies, particularly where epitope similarity or dissimilarity issues are involved. At their most elaborate epitope mapping techniques, e.g. X-ray crystallography, NMR, or electron microscopy, can provide detailed information on the amino acid residues in a protein antigen which is in direct contact with the antibody-binding site. “Functional” epitope mapping methods can be divided into four groups: (1) competition methods; (2) antigen modification methods; (3) fragmentation methods; and (4) the use of synthetic peptides or peptide libraries. Apart from its intrinsic value for understanding protein interactions, epitope mapping has also a practical value in generating antibody probes of defined specificity as research tools and in helping to define the immune response to pathogenic proteins and organisms. The term ‘epitope mapping’ has also been used to describe the attempt to determine all

---

<sup>60</sup>Simon-Vecsei, Z.; Király, R.; Bagossi, P.; Tóth, B.; Dahlbom, I.; Caja, S.; Csósz, É.; Lindfors, K.; Sblattero, D.; Nemes, É.; Mäki, M.; Fésüs, L.; and Korponay-Szabó, I.R., *Proc Natl Acad Sci U S A.*, **2012**,109(2),431-436.

<sup>61</sup>C. Tiberti, F. Bao, M. Bonamico, A. Verrienti, A. Picarelli, M. Di Tola, M. Ferri, E. Vecci, F. Dotta, G.S. Eisenbarth, and U. Di Mario, *Clin Immunol*, **2003**;109:318-324;

<sup>62</sup>Seissler, J.; Wohlrab, U.; Wuensche, C.; Scherbaum, W. A.; and Bohem, B.O., *Clin. Exp. Immunol.*, **2001**, 125, 216-221.

<sup>63</sup>Nakachi, K.; Powell, M.; Swift, G.; Amoroso, M.A.; Ananieva-Jordanova, R.; Arnold, C.; Sanders, J.; Furmaniak, J.; and Smith, B.R., *J. Autoimmunity*, **2004**; 22, 53-63.

## PART A

major sites on a protein surface that can elicit an antibody response in mice or humans. This information might be very useful, for example, to someone wishing to produce antiviral vaccines or diagnostic antigens<sup>64</sup>. Overlapping peptide libraries are ideal for T-cell epitope searching, because T-cell epitopes are by nature short linear peptides of the primary protein sequence. They are also appropriate for scanning the primary sequence of proteins for linear, or “continuous”, B-cell (antibody-defined) epitope characterisation.

Overlapping peptide libraries can be used for epitope mapping (linear and continuous epitopes), which can in turn be used to determine essential regions of a protein contributing to the bioactivity.

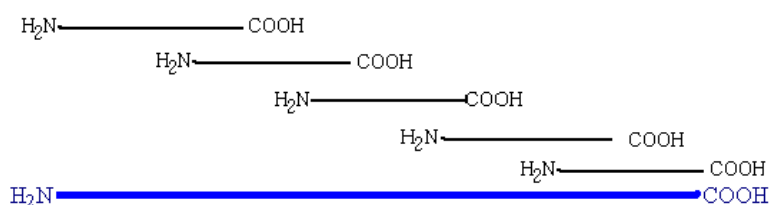


**Figure 2.11.** Proteins epitope mapping by overlapping peptides.

The library design is based on two parameters: peptide fragment length, and offset number. The peptide fragment length is the length of each peptide to be generated in the library, and it is typically between 10 and 25 amino acids in length. The offset number is the degree of overlap with regard to the following peptide fragment.

### *Selecting epitopes*

Any accessible part of a molecule may be considered to be a potential antigen. In fact, for antibody-binding to an antigen, the specific epitope must be

---

<sup>64</sup>Morris, G.E.; Epitope Mapping: B-cell Epitopes, *ENCYCLOPEDIA OF LIFE & SCIENCES*, 2007, John Wiley & Sons, doi: 10.1002/9780470015902.a0002624.pub2.

exposed on the molecular surface. There are a number of criteria that might affect the epitope position, such as:

- the mobility of the protein region;
- the nature of the primary sequence (in the case of protein antigens) where there is the possibility to form a loop or a turn, e.g. the presence of proline residues;
- the hydrophilicity.

With reference to the molecular mobility of an antigen, X-rays and NMR studies can allow the identification of the surface amino acid residues with higher mobility and areas on the molecule with the hydrophilic stretches found on the surface. Therefore highly hydrophilic sequences are likely to be on the surface of a molecular fold and thus are putative epitopes, particularly when used in conjunction with hydrophilicity parameters for each residue.

When investigating the nature of the putative epitopes on a protein, several enzymatic methods are available, e.g. digestion of the protein into smaller peptide fragments. Alternatively the use of synthetic probes is a valuable strategy. The purity of enzyme digestion requires consideration, that's why the use of synthetic antigens can have several advantages if compared to biotech approaches, in particular to overcome bias due to the low quality of expressed/extracted antigens. Analysis of overlapping peptides can produce precise data. In 1984, Geysen *et al.*<sup>65</sup> investigated possible ways of identifying epitopes on macromolecules like proteins and developed the Pepscan technique. Of course this method requires prior knowledge of the amino acid sequence for the protein of interest. Peptide libraries can be designed and synthesized overlapping the complete length of a protein (or the portion

---

<sup>65</sup>H M Geysen, R H Meloen, and S J Barteling, *PNAS*, **1984**, 81(13),3998-4002.

## PART A

considered of interest) to be used in solid phase ELISA (SP-ELISA) to screen panels of antibodies for distinguishing linear B-cell epitopes<sup>66</sup>.

### ***2.2.1 Epitope mapping of tTG(1-230)***

The characterization of tTG antigenic domains is a crucial step in understanding the autoimmune role and onset in the CD<sup>1</sup> pathogenesis, since the pathogenic role and exact binding properties of these autoantibodies to tTG are still unclear. Autoantigenic epitopes are formed, in the main part, into the N-terminal and C-terminal portion<sup>62,63</sup>.

We performed an epitope mapping study based on the “Chemical Reverse Approach”<sup>24</sup> previously set up in PeptLab to characterize linear putative autoantigenic epitopes present in the tTG N-terminal portion. A library of 23 overlapping peptide epitopes, listed in *Table 2.1*, was generated reproducing tTG(1-230) fragments.

---

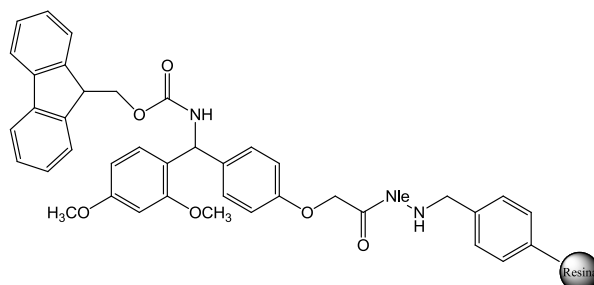
<sup>66</sup> a) Olwyn, M.; Westwood, R.; and Hay, F. C., *Epitope Mapping: A Practical Approach*, Oxford University Press, USA; **2001**; b) Carter, J.M.; and Loomis-Price, L., *Curr. Prot. Immunol.*, **2004**, DOI: 10.1002/0471142735.im0904s60.

Table 2.1 Overlapping peptides of the tTG N-terminal portion, i.e. tTG(1-230).

Peptide	tTG Protein Fragment	Protein Sequence
I	tTG(1-15)	MAEEL VLERC <b>DLELE</b>
II	tTG(11-25)	<b>DLELE</b> TNGRD <b>HHTAD</b>
III	tTG(21-35)	<b>HHTAD</b> LCREK <b>LVVRR</b>
IV	tTG(31-45)	<b>LVVRR</b> GQPFW <b>LTLHF</b>
V	tTG(41-55)	<b>LTLHF</b> EGRNY <b>EASVD</b>
VI	tTG(51-65)	<b>EASVD</b> SLTFS <b>VVTGP</b>
VII	tTG(61-75)	<b>VVTGP</b> APSQE <b>AGTKA</b>
VIII	tTG(71-85)	<b>AGTKA</b> RFPLR <b>DAVEE</b>
IX	tTG(81-95)	<b>DAVEE</b> GDWTA <b>TVVDQ</b>
X	tTG(91-105)	<b>TVVDQ</b> QDCTL <b>SLQLT</b>
XI	tTG(101-115)	<b>SLQLT</b> TPANA <b>PIGLY</b>
XII	tTG(111-125)	<b>PIGLY</b> RLSLE <b>ASTGY</b>
XIII	tTG(121-135)	<b>ASTGY</b> QGSSF <b>VLGHF</b>
XIV	tTG(131-145)	<b>VLGHF</b> ILLFN <b>AWCPA</b>
XV	tTG(141-155)	<b>AWCPA</b> DAVYL <b>DSEEE</b>
XVI	tTG(151-165)	<b>DSEEE</b> RQEYV <b>LTQQG</b>
XVII	tTG(161-175)	<b>LTQQG</b> FIYQG <b>SAKFI</b>
XVIII	tTG(171-185)	<b>SAKFI</b> KNIPW <b>NFGQF</b>
XIX	tTG(181-195)	<b>NFGQF</b> EDGIL <b>DICLI</b>
XX	tTG(191-205)	<b>DICLI</b> LLDVN <b>PKFLK</b>
XXI	tTG(201- 215)	<b>PKFLK</b> NAGRD <b>CSRRS</b>
XXII	tTG(211-225)	<b>CSRRS</b> <b>SPVYV</b> <b>GRVVS</b>
XXIII	tTG(216-230)	<b>SPVYV</b> <b>GRVVS</b> <b>GMVNC</b>

### 2.2.2 Synthesis of the linear peptides

Linear peptide fragments were synthesized using a Fmoc/*t*Bu strategy starting from Fmoc-*Rink Amide* resin.



**Figure 2.12.** Rink-linker structure.

Chemically synthesized peptides carry free amino and carboxy termini, being electrically charged in general. In order to remove this electric charge, peptide ends were often modified by <sup>α</sup>N-terminal acetylation and/or C-terminal amidation. Peptide ends are thus uncharged, compared to standard synthetic peptides, so they mimic natural peptides<sup>67</sup>. Moreover, permeability of cells increases, peptide ends are blocked against synthetase activities and acetylated peptides serve as optimized enzyme substrates. Moreover, amidation of peptides having acetylated <sup>α</sup>N-terminus enhances activity of peptide hormones. These modifications are indicated especially for peptides to be used in ELISA to minimize influences of charged C- or N-termini with ELISA binding characteristics.

The peptides reported in *Table 2.1* were synthesized using a Fmoc/*t*Bu protection scheme on the Advanced ChemTech Apex 396 synthesizer equipped with a 8-wells reaction block (0.16 scale), starting from Fmoc *Rink-Amide* resin (Iris Biotech GmbH), according to the General Procedure for the

<sup>67</sup>Lloyd-Williams,P.; Albericio,F.;and Giralt,E., “*Chemical approaches to the synthesis of peptides and proteins*”, CRC Press, **1997**.

automatic SPPS described in details in the Experimental Part and using commercially available Fmoc-protected amino acids and TBTU/DIPEA activation. <sup>15</sup>N-terminal acetylation was carried out as reported in the Experimental Part. Peptide cleavage from the resin and contemporary deprotection of the amino acids side chains was carried out for 3 h at room temperature with reagent K. The crude products were precipitated with diethyl ether, collected after centrifugation, dissolved in H<sub>2</sub>O and lyophilized.

The products were purified and characterized by RP-HPLC ESI-MS. Analytical data are reported in *Table 2.2*.

**Table 2.2. Analytical data of peptides I-XXIII.**

Peptide	tTG Fragment	Sequence	HPLC R <sub>t</sub> (min)	ESI-MS (m/z) [M+2H] <sup>2+</sup> Calc(found)
<b>I</b>	tTG(1-15)	Ac-MAEELVLERCDLELE-NH <sub>2</sub>	4.52 <sup>f</sup>	916.94 (917.77)
<b>II</b>	tTG(11-25)	Ac-DLELETNGRDHHTAD-NH <sub>2</sub>	3.67 <sup>a</sup>	882.40 (882.62)
<b>III</b>	tTG(21-35)	Ac-HHTADLCREKLVVRR-NH <sub>2</sub>	3.64 <sup>a</sup>	937.51 (937.84)
<b>IV</b>	tTG(31-45)	Ac-LVVRRGQPFWLTLHF-NH <sub>2</sub>	5.36 <sup>a</sup>	955.54 (956.29)
<b>V</b>	tTG(41-55)	Ac-LTLHFEGRNYEASVD-NH <sub>2</sub>	3.86 <sup>b</sup>	896.43 (897.15)
<b>VI</b>	tTG(51-65)	Ac-EASVDSLTFVVTGP-NH <sub>2</sub>	4.18 <sup>b</sup>	775.39 (776.02)
<b>VII</b>	tTG(61-75)	Ac-VVTGPAPSQEAGTKA-NH <sub>2</sub>	3.34 <sup>a</sup>	727.38 (727.52)
<b>VIII</b>	tTG(71-85)	Ac-AGTKARFPLRDAVEE-NH <sub>2</sub>	4.02 <sup>a</sup>	850.95 (851.05)
<b>IX</b>	tTG(81-95)	Ac-DAVEEGDWTATVVVDQ-NH <sub>2</sub>	4.36 <sup>a</sup>	838.37 (838.91)
<b>X</b>	tTG(91-105)	Ac-TVVDQQDCTLSLQLT-NH <sub>2</sub>	4.76 <sup>a</sup>	852.92 (853.38)
<b>XI</b>	tTG(101-115)	Ac-SLQLTTPANAPIGLY-NH <sub>2</sub>	4.97 <sup>a</sup>	800.44 (800.98)
<b>XII</b>	tTG(111-125)	Ac-PIGLYRLSLEASTGY-NH <sub>2</sub>	4.62 <sup>c</sup>	840.95 (841.68)
<b>XIII</b>	tTG(121-135)	Ac-ASTGYQGSSFVLGHF-NH <sub>2</sub>	3.58 <sup>e</sup>	799.88 (800.53)
<b>XIV</b>	tTG(131-145)	Ac-VLGHFILLFNAWCPA-NH <sub>2</sub>	2.51 <sup>g</sup>	871.46 (872.34)
<b>XV</b>	tTG(141-155)	Ac-AWCPADAVYLDSEEE-NH <sub>2</sub>	3.94 <sup>a</sup>	869.86 (870.69)
<b>XVI</b>	tTG(151-165)	Ac-DSEEEERQEYVLTQQG-NH <sub>2</sub>	3.6 <sup>a</sup>	926.42 (927.21)
<b>XVII</b>	tTG(161-175)	Ac-LTQQGFIYQGS AKFI-NH <sub>2</sub>	3.87 <sup>a</sup>	871.46 (872.27)
<b>XVIII</b>	tTG(171-185)	Ac-SAKFIKNIPWNFGQF-NH <sub>2</sub>	4.07 <sup>d</sup>	919.49 (920.46)
<b>XIX</b>	tTG(181-195)	Ac-NFGQFEDGILDICLI-NH <sub>2</sub>	4.8 <sup>f</sup>	869.42 (869.77)
<b>XX</b>	tTG(191-205)	Ac-DICLILLDVNPKFLK-NH <sub>2</sub>	4.76 <sup>c</sup>	893.02 (893.93)
<b>XXI</b>	tTG(201-215)	Ac-PKFLKNAGRDCSRRS-NH <sub>2</sub>	4.07 <sup>a</sup>	888.47 (889.21)
<b>XXII</b>	tTG(211-225)	Ac-CSRRSSPVYVGRVVS-NH <sub>2</sub>	4.01 <sup>a</sup>	846.95 (847.76)
<b>XXIII</b>	tTG(216-230)	Ac-SPVYVGRVVS GMVNC-NH <sub>2</sub>	4.26 <sup>c</sup>	804.40 (805.18)

Analytical HPLC gradients at 1 mL min<sup>-1</sup>, solvents system are A: 0.1% TFA in H<sub>2</sub>O, B: 0.1% TFA in CH<sub>3</sub>CN, <sup>a</sup>10-60% B in 5 min, <sup>b</sup>20-60% B in 5 min, <sup>c</sup> 10-90% B in 5 min, <sup>d</sup> 25-70% B in 5 min, <sup>e</sup> 20-70% B in 5 min, <sup>f</sup>20-90%B in 5 min, <sup>g</sup>30-80% B in 5 min.

### 2.3 Immunoassays: SP- and Inhibition- ELISA

The collection of the 23 pentadecapeptides, **I-XXIII**, corresponding to the tissue transglutaminase N-terminal portion, tTG(1-230), was screened on coeliac disease patients' sera, at the diagnosis to recognize and characterize the possible epitopes.

#### 2.3.1 Inhibition experiments using Eu-tTG Aeskulisa

We evaluated the ability of these **I-XXIII** peptides to try to inhibit the binding of anti-tTG(1-687) IgA antibodies present in CD patients' sera. This full length protein antigen is used in the commercial diagnostic ELISA kit (Eu-tTG IgA, Aeskulisa). We used two representative CD patients' sera, displaying high and medium titer (CD++ and CD+), and one Normal Blood Donor (NBD), as control, in Solid-Phase ELISA (SP-ELISA).

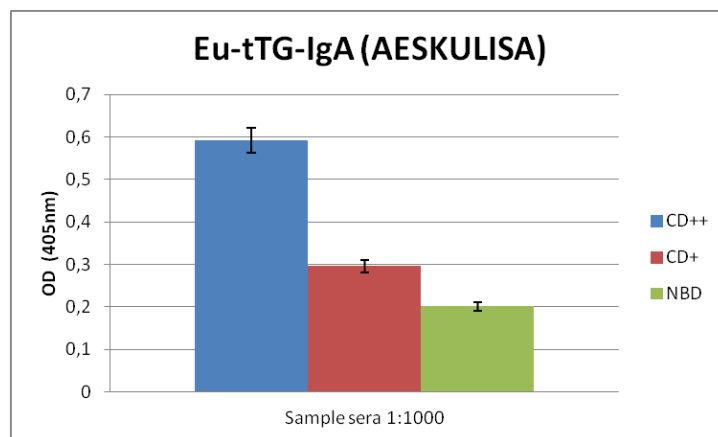


**Figure 2.13.** SP-ELISA performed with Eu-tTG IgA, Aeskulisa.

The two positive sera and the healthy control (NBD) were then preincubated with the 23 different synthetic overlapping peptides and added to the Eu-tTG IgA, in the Aeskulisa plate.

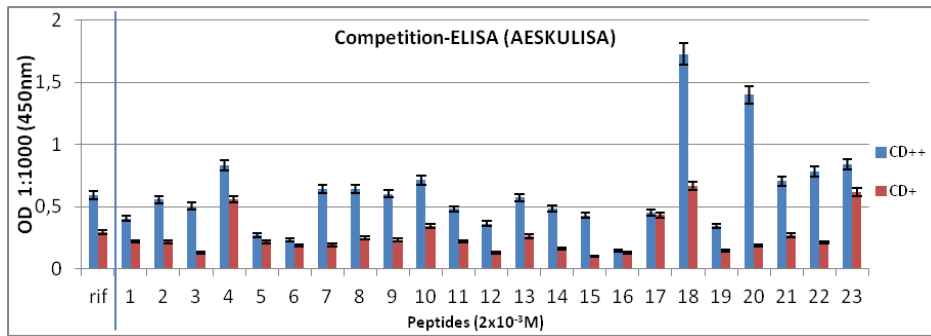


**Figure 2.14.** Competition-ELISA performed with the 2 CD patient's sera. On the left is reported the reference value of the sample sera measured in SP-ELISA performed with Eu-tTG IgA, Aeskulisa

We found that the peptides **I, V, VI, XII, XVI, and XIX** are able to inhibit the binding of the anti-tTG(1-687) IgA antibodies. Moreover, we found that these peptides do not cross-react if tested with the representative NBD serum.

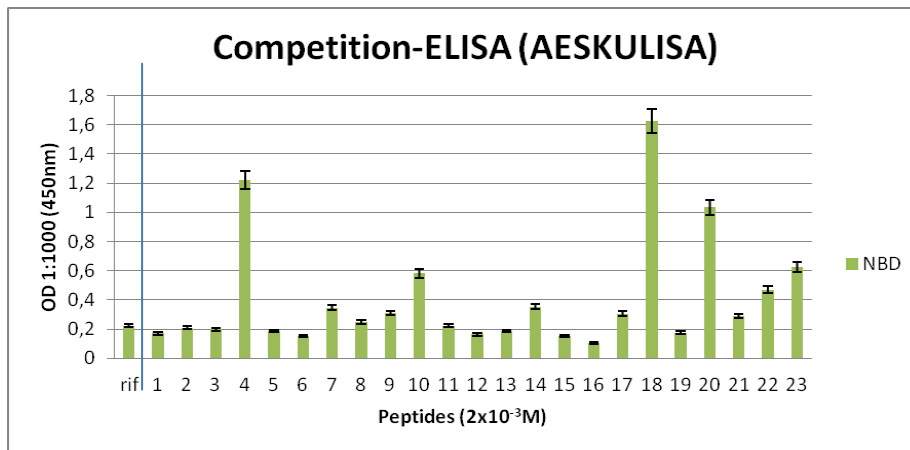


**Figure 2.15.** Competition-ELISA performed with NBD serum. On the left is reported the reference value of the sample serum measured in SP-ELISA performed with Eu-tTG IgA, Aeskulisa.

PART A

**2.3.2 Solid Phase-ELISA experiments: screening of peptides I-XXIII**

SP-ELISA reflects essentially the antibody affinity, which depends on the exposure of the minimal epitope in the solid-phase conditions of the assay. Therefore, we evaluated by SP-ELISA the possible IgA and IgG recognition by the peptides **I-XXIII** using the representative CD patient's serum (CD++) positive to Eu-tTG IgA, Aeskulisa and compared with the results obtained with the representative NBD. In a first instance IgA and IgG were tested using as secondary antibody anti-human IgA and anti-human IgG conjugated to Horseradish Peroxidase enzyme (HRP).

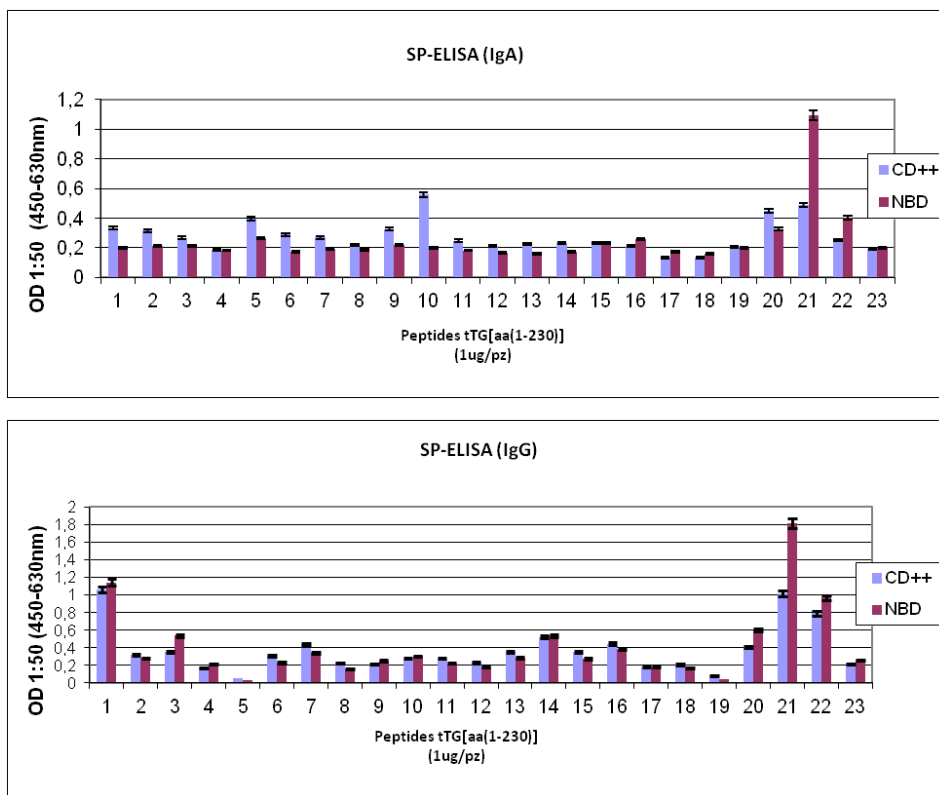


**Figure 2.16.** Screening of serum antibody recognition (IgA and IgG) using the peptides I-XXIII in SP-ELISA.

Data reported in the *Figure 2.16* show some interesting results of IgA. This is in line with what is reported in the literature concerning the higher specificity of anti-tTG IgA compared to anti-tTG IgG.

These preliminary data let us to select four peptides, i.e. **I**, **V**, **VI**, **XVI** that showed the better IgA antibody recognition both in inhibition- and SP-ELISA experiments. Therefore, we evaluated, by SP-ELISA, the possible antibody recognition with peptides **I**, **V**, **VI**, **XVI** in 8 CD patients' sera and 3 NBDs, as controls.

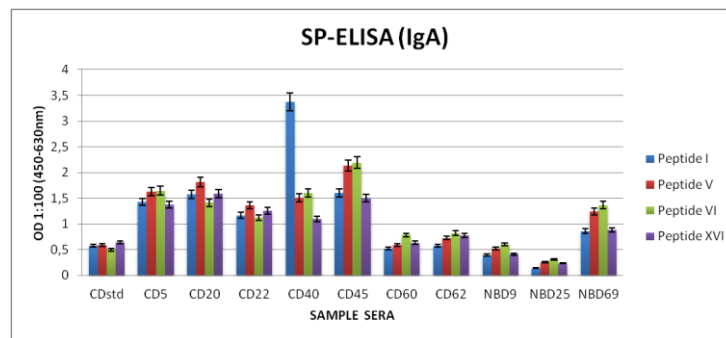


*Figure 2.17. SP-ELISA on a selected cohort of patients.*

Sera CD5, CD20, CD22, CD40, and CD45 are from patients with severe mucosal damages, classified according Marsh criteria<sup>46</sup> (3a-3c) and show high IgA values also with the commercial Aeskulisa. CD60 and CD62 sera are from patients with severe mucosal damages but display low titers even with the commercial Aeskulisa. CDstd is a pool of CD patients' sera and displays a low titer when tested with the commercial Aeskulisa. Each serum was also used to obtain dilution curves. In *Figure 2.18* we report as example the graph of the dilution curve obtained with CD20.

## PART A

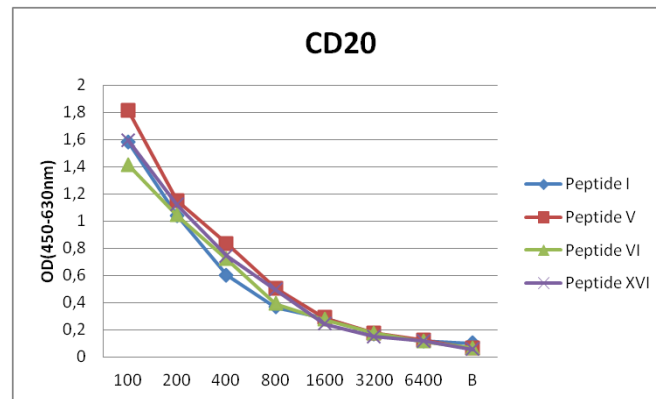


**Figure 2.18.** Dilution curve for serum CD20 measured with the peptides (I), (X), (VI), and (XVI).

As shown in *Figure 2.18*, the four peptides, **I**, **V**, **VI**, and **XVI** display more or less the same activity in detecting autoantibodies in SP-ELISA in coeliac patients' sera, at the diagnosis.

### **2.3.3 Results and discussion**

The results obtained with the 23 synthetic overlapping peptides confirm that autoantibodies in patients with coeliac disease recognize precise linear peptide epitopes (continuous) present in tTG(1-230)<sup>62,63</sup>.

**Peptide I**, ie tTG(1-15), includes the peptide epitope tTG(1-13). The most relevant N-terminal epitope requires the presence of the first 13 residues, and the truncation of the first 13 residues, completely abolishes antibody binding to all epitopes within the N-terminal part of the protein, as shown in *Figure 2.19*.

Deletion mutant	Fragment	Antibody reactivity
1-████████████████████-687	tTG full (aa 1-687)	49 (100%)
1-████████████████████-473	Frag. N1 (aa 1-473)	46 (93.4%)
1-████████████████████-347	Frag. N2 (aa 1-347)	40 (81.6%)
1-████████████████████-281	Frag. N3 (aa 1-281)	33 (67.4%)
1-████████████████████-227	Frag. N4 (aa 1-227)	8 (16.3%)
14-████████████████████-347	Frag. N5 (aa 14-347)	0
46-████████████████████-648	Frag. M1 (aa 46-648)	11 (22.5%)
227-████████████████████-473	Frag. M2 (aa 227-473)	0
227-████████████████████-687	Frag. C1 (aa 227-687)	34 (69.4%)
473-████████████████████-687	Frag. C2 (aa 473-687)	34 (69.4%)
497-████████████████████-687	Frag. C3 (aa 497-687)	0
473-████████████████████-648	Frag. C4 (aa 473-648)	0

**Figure 2.19.** Antibody reactivity to different fragments of tissue transglutaminase<sup>62</sup>.

**Peptide V**, i.e. tTG(41-55) and **Peptide VI**, i.e. tTG(51-65), overlap the peptide fragment tTG(41-65) and both contain the protein fragment tTG(52-54). The tripeptide Ala-Ser-Val, i.e. tTG(52-54) is characterized by a type I  $\beta$ -turn conformation, as reported in the UNIPROT Data Base<sup>68</sup>. In particular, this type I  $\beta$ -turn was identified in the structure deposited in the PDB, by Pinkas *et al.*<sup>56</sup>, and more recently Lindemann *et al.*<sup>69</sup> of the tTG in complex with two inhibitors, in the open conformation, that is the one considered having non-self antigen properties. The position of this tripeptide is slightly different from the one found in the inactive enzyme.

<sup>68</sup> <http://www.uniprot.org/uniprot/P21980>.

<sup>69</sup> Lindemann, I.; Boettcher, J.; Oertel, K.; Weber, J.; Hils, M.; Pasternack, R.; Heine, A.; Klebe, G., To be published, **2012**, DOI:[10.2210/pdb3s3p/pdb](https://doi.org/10.2210/pdb3s3p/pdb).

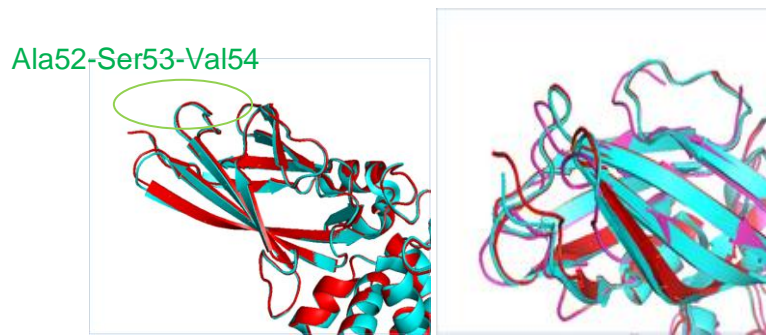


**Figure 2.20.** Right, overlap of the two structures solved in presence of an inhibitor mimicking natural substrates of tTG. Left, overlap of the two structures solved by Pinkas and Lindemann (red and light blue ribbons) in comparison with the inactive enzyme (purple ribbon)<sup>56,69</sup>.

$\beta$ -Turn structures are secondary structures frequently associated with antigenic sites, particularly when they are adjacent to  $\beta$ -sheets or  $\alpha$ -helical structures in hydrophilic regions and polypeptide chain flexibility.  $\beta$ -Turns usually occur on the exposed surface of proteins and hence likely represent antigenic sites or involve molecular recognition, as presumably occurs when tTG is in the open conformation. These considerations let us to hypothesize that the peptide tTG(41-65) is recognized as a linear epitope.

**Peptide XVI**, i.e. tTG(151-165), overlaps a very hydrophilic part of the protein and contains a minimum of hydrophobicity, [*Position: 155 Score: -3.067 (min)*], according to Kyte and Doolittle algorithm]. Highly hydrophilic sequences are likely to be on the surface of a molecular fold and thus they can be considered putative epitopes.

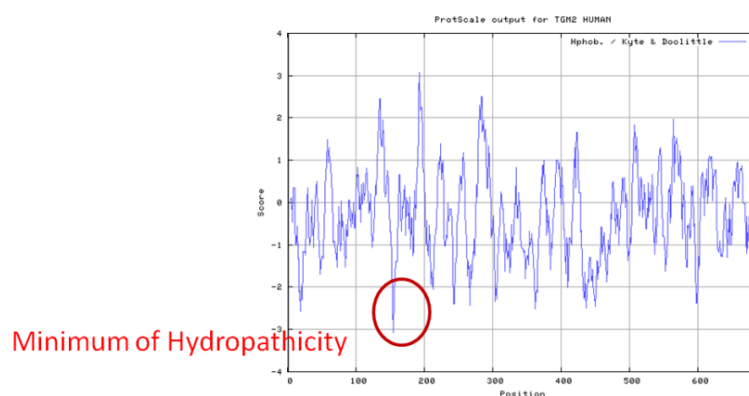


**Figure 2.21.** Profile of hydropathicity calculated according to Kyte and Doolittle algorithm<sup>70</sup>.

Moreover, the **Peptide XVI** contains a negatively charged sequence composed of Glu residues, tTG(153-155). Glu153 and Glu 154, as reported by Simon-Vecsei *et.al*, are located on the first alpha-helix of the core domain and together with Arg19 on the first alpha-helix of the N-terminal domain and Met659 constitute an important conformational epitope<sup>60</sup>.

<sup>70</sup><http://www.uniprot.org/uniprot/P21980>

## **2.4 Cross-linked peptide probes for the development of an *in vitro* diagnostics for Coeliac Disease**

Untreated CD patients have high levels of circulating IgAs and IgGs directed to different autoantigens, and in particular tTG, gliadin and endomysium (EMA) whose presence is strictly correlated with the gluten dietary intake. Moreover, they are directly involved in mucosal injury by inhibiting the differentiation of epithelial cells<sup>40,71</sup>. Clinical evaluation and diagnosis of CD may require several years because of the large variety of associated symptoms and the low specificity and sensitivity of the available serological tests, thus leading to an increasing probability to develop additional disorders. Thus, reliable assays are necessary not only for an early diagnosis but also for monitoring the disease activity by evaluating antibodies, as specific biomarkers<sup>72</sup>. Up today the gold standard for the diagnosis of CD remains the bowel biopsy even though serological tests are in rapid development both in terms of specificity and sensitivity. Nevertheless, the bowel biopsy cannot be considered anymore as a routine diagnostics, particularly for infants.

The improvement of the sensitivity of serological tests replacing extracted or recombinant antigens with synthetic peptide probes could assume a particular relevance if applied to a disease in which only the 20% of patients is thought to be diagnosed as exemplified by the model of the coeliac iceberg in

*Figure 2.22.*

---

<sup>71</sup> Halttunen, T. ; and Mäki, M., *Gastroenterology*, **1999**, 116, 566-572.

<sup>72</sup> Roland, P.; Atkinson, J.A.; and Lesko, L.J., *Clin. Pharm. Ther.*, **2003**, 73, 284-291.

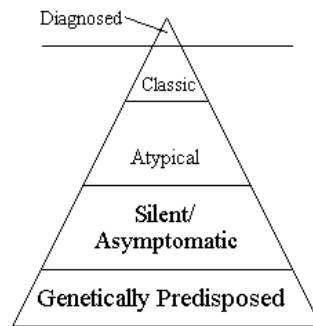


**Figure 2.22.** *The coeliac Iceberg.*

Therefore, it could be of relevant importance the design and synthesis of peptides mimicking aberrant modifications occurring in protein antigen (tTG) involved in the coeliac disease pathogenesis in order to dissect the mechanisms of the autoimmune response and developing new diagnostic tools. Recently, it has been reported the introduction in the coeliac disease diagnostics a new generation of diagnostic tools based on tissue transglutaminase-gliadin constructs formed *in vivo*<sup>73</sup>.

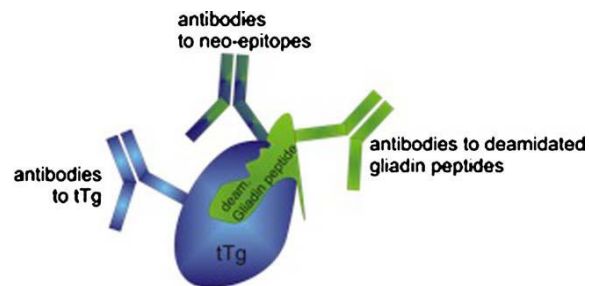


**Figure 2.23.** *tTG-gliadin constructs.*

This new generation of kit uses a unique antigen approach based on human tTG antigens crosslinked with deamidated gliadin specific peptides coated on the ELISA plate wells. The antigen used up to now for detecting CD-

<sup>73</sup> Matthias, T.; Not, T.; and Selmi, C., *Clinic Rev Allerg Immunol*, **2010**, 38, 298–301.

## PART A

associated antibodies is the purified cross-linked complex which is formed under *in vivo* physiological conditions, designed to detect IgA and IgG antibodies to tTG. Transamidation can be considered the aberrant PTM triggering autoantibodies in CD. Therefore, cross-linked peptides between Lys- and Glu- side-chains of tTG and Gliadin peptide epitopes could be innovative tools to develop peptide-based *in vitro* diagnostics for CD. Synthetic cross-linked peptide probes could replace protein extracts thus giving rise to a new class of even more sensitive and specific diagnostic tools .

### **2.4.1 Tissue Transglutaminase' fragments selection**

Digested peptides forming covalent complexes between tTG and gliadin were characterized investigating the chemical nature of the linkage. In order to trigger an autoantibody response via a hapten carrier-like model in coeliac sprue, 'neo-epitopes' as tTG–gliadin adducts should be relatively stable.

Gliadin peptides can be covalently linked to the enzyme either via thioester bond to the active site cysteine or via isopeptide bond to particular lysine residues of the enzyme. The isopeptide form dominates when more than one peptide is linked to tTG, rather than the deamidation reaction, thus presumably is the most common form in the case of patients with active and undiagnosed CD following a gluten-rich diet.

In these conditions, at high molar excess of gliadin peptides, 6 Lys residues were identified as participating residues in isopeptide bonds formation to the targeted Gln residues giving important insights on how antibodies to tTG are formed in CD. These acyl acceptor residues were univocally identified by mass spectrometry experiments applied to the proteolytic digested tTG-gliadin *in vivo* formed adducts, as reported by Fleckenstein *et al*<sup>74</sup>, and shown in *Table 2.3*.

Table 2.3. tTG-derived peptides.

Entry	tTG-derived peptides cross-linked to a representative peptide	Lys no.	Molar ratio to tTG 1:150
1	EDITHTYKYPEGSSEER	Lys-444	(+)
2	DCLTESNLIKVR	Lys-562	++
3	DLYLENPEIKIR	Lys-590	++
4	QKRK	Lys-600	+
5	TVEIPDPVEAGEEVKVR	Lys-649	+
6	AVKGFR	Lys-677	++

The signals for the tTG-derived peptides I–VI covalently linked to the representative were found with very low, (+), intermediate, +, or high intensities, ++, in the MALDI-TOF and ESI mass spectra.

Lys-590, Lys-600, Lys-649, and Lys-677 are all located in the C-terminal domain 4, Lys-444, and Lys-562 are situated in domain 2. Interestingly, Lys-677 is located at the interface of domain 2 and 4, rather buried in the interior of the protein exposed at the surface. Also, Lys-562 appears to be partly buried, whereas the other four lysine residues are clearly exposed to the surface of the protein<sup>74</sup>.

<sup>74</sup>Fleckenstein, B.; Qiao, S.-W.; Larsen, M.R.; Jung, G.; Roepstorff, P.; and Sollid, L.M., *J. Biol. Chem.*, **2004**, 279(17), 17607–17616.

PART A

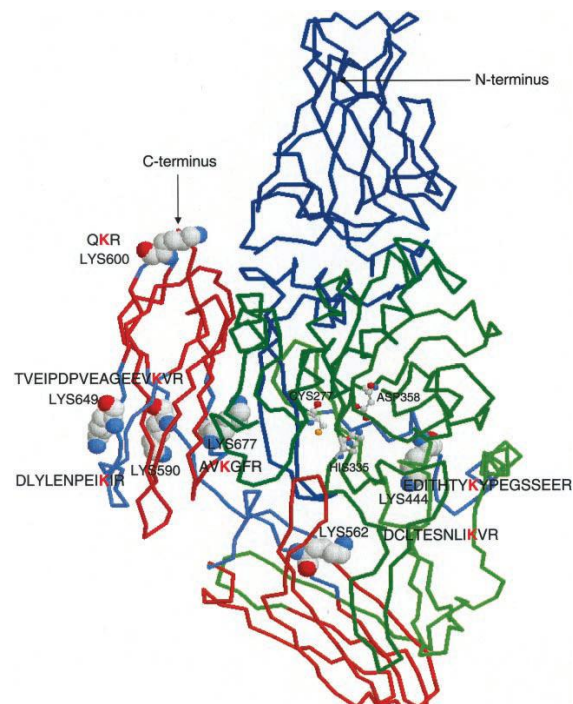


**Figure 2.24.** Data Bank file, shows the location of the identified acyl acceptor Lys residues within the three-dimensional protein structure. Only the side chains of the six Lys residues (space-fill model) participating in the isopeptide bond formation and those of the catalytic triad (ball and sticks) are illustrated. The backbone of domains 1–4 is colored in blue, green, orange, and red, respectively<sup>74</sup>.

On the basis of these experimental findings we selected the more representatives tTG fragments. From *Table 2.3* we selected, as tTG epitopes, peptide fragments. II, III and VI that showed a higher frequency in giving the isopeptide bonds in comparison to the other listed. More precisely we considered the following fragments:

- 1) **DCLTESNLIK562VR**, tTG(553-564), containing **K562** (in bold);
- 2) **DLYLENPEIK590IR**, tTG(581-592), containing **K590** (in bold);
- 3) **AVK677GFR**, tTG(675-680), containing **K677** (in bold).

#### 2.4.2 Identification of the possible antigenic gliadin epitopes

Regiospecific deamidation and transamidation of the immunogenic gliadin peptides by tTG increases their affinity for HLA, both DQ2 and DQ8, as well as the potency with which they activate patients-derived gluten-specific CD4+ T-cells<sup>75</sup>. These T-cells usually recognize gluten peptides that have been post-translationally modified by tTG<sup>76,77</sup>. Although the propensity for either of the two modifications may differ slightly for some peptide substrates, the substrate specificity for deamidation and transamidation seems to be very similar<sup>78</sup>. In addition, it has been proved that these two post-translational modifications can occur on distinct Gln residues within the same peptide. The majority of the identified transamidated peptides, whose isopeptide bonds are not susceptible to the proteolytic cleavage that hydrolyze normal peptide bonds<sup>79</sup>, contain intact known T-cells epitopes (9mer core regions) or their truncated versions<sup>80</sup>. The stability of the fragments generated by brush border enzyme degradation, associated with their remarkable resistance to proteolysis is reported as one of the driving forces in the selection of epitopes in CD for gluten T-cell response. The majority of gluten T-cell epitopes identified in celiac disease so far are derived from  $\alpha$ - and  $\gamma$ -gliadins. Epitopes derived from  $\alpha$ -gliadin have been shown to be recognized by T cells isolated from nearly all

---

<sup>75</sup> Molberg, O.; Kett, K.; Scott, H.; Thorsby, E.; Sollid, L. M.; and Lundin, K. E., *Scand. J. Immunol.* **1997**, 46, 103–109.

<sup>76</sup> Molberg, O.; McAdam, S. N.; Korner, R.; Quarsten, H.; Kristiansen, C.; Madsen, L.; Fugger, L.; Scott, H.; Noren, O.; Roepstorff, P.; Lundin, K. E.; Sjostrom, H.; and Sollid, L. M. *Nat. Med.* **1998**, 4, 713–717.

<sup>77</sup> van der Wal, Y.; Kooy, Y.; van Veelen, P. A.; Pena, S.; Mearin, L.; Papadopoulos, G.; and Koning, F. *J. Immunol.* **1998**, 161, 1585–1588.

<sup>78</sup> Stammaes, J.; Fleckenstein, B.; and Sollid, L.M., *Biochim Biophys Acta.*, **2008**, 1784(11), 1804-11.

<sup>79</sup> Miller, M.L.; and Johnson, G.W., *J Chromatogr.*, **1999**, 732, 65–72.

<sup>80</sup> Dørum, S.; Arntzen, M.Ø.; Qiao, S.-W.; Holm, A.; Koehler, C.J.; Thiede, B.; Sollid, L.M.; and Fleckenstein, S.-W., *PlosOne*, **2010**, 5(11), e14056.



epitopes. The epitope selection presumably deals with the anchoring position positively charged in HLA. In addition, it is possible to establish a deep correlation between the rate of deamidation of the different epitopes and their T-cell immunostimulatory capacity<sup>83</sup>.

The more representative CD4+T-cell epitopes identified in  $\alpha 2$ -Gliadin fraction of wheat gluten are listed below (their importance is established on the basis of the CD4+T-cell response):

- 1) PFPQPQLPY (DQ2- $\alpha 2$ -I), [ $\alpha 2$ -Glia(61-69), 9mer];
- 2) PQPQLPYPQ (DQ2- $\alpha 2$ -II), [ $\alpha 2$ -Glia(63-71), 9mer];
- 3) PYPQPQLPY (DQ2- $\alpha 2$ -III), [ $\alpha 2$ -Glia(68-76), 9mer];
- 4) LQLQPFQPQLPYPQPQLPYPQPQLPYPQPQP [  $\alpha 2$ -Glia(57-89), 33mer].

*Underlined Gln residues are those expected to be targeted by the enzyme*

Gliadin peptides 1), 2), and 3) are the identified T- cell epitopes in wheat gluten (9 mer core regions), these three peptides derive from the super antigen, sequence no. 4. It has been demonstrated that such shorter version can be as potent as the 33 mer in stimulating intestinal T-cell response<sup>84</sup>.

## 2.5 Peptide-based cross linked antigens design and synthesis

Following our “Chemical Reverse Approach”<sup>24</sup>, we selected three tTG peptide epitopes, e.g., tTG(553-564), tTG(581-592), and tTG(675-680) and three  $\alpha 2$ -Gliadin peptide epitopes, e.g.,  $\alpha 2$ -Glia(61-69),  $\alpha 2$ -Glia(63-71), and  $\alpha 2$ -Glia(68-76) to design nine peptides containing cross-links between Lys- and Glu side-chains in tTG and  $\alpha 2$ -Glia linear fragments, respectively.

---

<sup>84</sup>Camarca, A.; Anderson, R.P.; Mamone, G.; Fierro, O.; Facchiano A, et al. *J Immunol*, **2009**, 182, 4158–4166.

**Table 2.4. tTG and  $\alpha$ 2-gliadin protein fragments.**

Protein Fragment	Sequence	Target Residue
tTG (553-564)	DCLTESNLI <u>K</u> VR	Lys562
tTG (581-592)	DLYLENPEI <u>K</u> IR	Lys590
tTG (675-680)	AV <u>K</u> GFR	Lys677
$\alpha$ 2-Gliadin (61-69)	PFQP <u>Q</u> LPY	Gln66
$\alpha$ 2-Gliadin (63-71)	PQP <u>Q</u> LPYPQ	Gln66
$\alpha$ 2-Gliadin (68-76)	PYPQP <u>Q</u> LPY	Gln73

The nine cross- linked peptides were synthesized by Fmoc/tBu SPPS and the target Gln residues were replaced with Glu, for synthetic requirements to generate the new cross linked peptides. In particular the peptides were synthesized starting from a Rink-Amide Resin and were acetylated on the <sup>a</sup>N-terminus.

**Table 2.5. tTG and  $\alpha$ 2-gliadin peptides.**

Peptide	Sequence
tTGI	Ac-DCLTESNLI <u>K</u> VR-NH <sub>2</sub>
tTGII	Ac-DLYLENPEI <u>K</u> IR-NH <sub>2</sub>
tTGIII	Ac-AV <u>K</u> GFR-NH <sub>2</sub>
DQ2(I)	Ac-PFPQP <u>E</u> LPY-NH <sub>2</sub>
DQ2(II)	Ac-PQP <u>E</u> LPYPQ-NH <sub>2</sub>
DQ2(III)	Ac-PYPQP <u>E</u> LPY-NH <sub>2</sub>

Coupling reactions were performed in heterogeneous phase with the tTG fragments still anchored on the resin, and  $\alpha$ 2-gliadin peptides coupled in solution. The neo-epitopes were tested in ELISA to evaluate the IgA and IgG response to tTG- $\alpha$ 2Glia constructs in coeliac patients' sera, at the diagnosis, to develop a new ELISA based on peptides as an even more powerful diagnostic tool in terms of specificity and sensitivity.

**Table 2.6. tTG and  $\alpha$ 2-gliadin cross-linked peptides.**

Cross-linked Peptides	Cross-linked protein fragments	Sequence
tTGI-DQ2(I)	tTG (553-564)- $\alpha$ 2Gli(61-69)	Ac- DCLTESNLIKVR-NH <sub>2</sub>   Ac- PFPQPELPY-NH <sub>2</sub>
tTGI-DQ2(II)	tTG (553-564)- $\alpha$ 2Gli(63-71)	Ac- DCLTESNLIKVR-NH <sub>2</sub>   Ac- PQPELPYPQ-NH <sub>2</sub>
tTGI-DQ2(III)	tTG (553-564)- $\alpha$ 2Gli(68-76)	Ac- DCLTESNLIKVR-NH <sub>2</sub>   Ac- PYPQPELPY-NH <sub>2</sub>
tTGII-DQ2(I)	tTG (581-592)- $\alpha$ 2Gli(61-69)	Ac- DLYLENPEIKIR-NH <sub>2</sub>   Ac- PFPQPELPY-NH <sub>2</sub>
tTGII-DQ2(II)	tTG (581-592)- $\alpha$ 2Gli(63-71)	Ac- DLYLENPEIKIR-NH <sub>2</sub>   Ac- PQPELPYPQ-NH <sub>2</sub>
tTGII-DQ2(III)	tTG (581-592)- $\alpha$ 2Gli(68-76)	Ac- DLYLENPEIKIR-NH <sub>2</sub>   Ac- PYPQPELPY-NH <sub>2</sub>
tTGIII-DQ2(I)	tTG (675-680)- $\alpha$ 2Gli(61-69)	Ac- AVKGFGR-NH <sub>2</sub>   Ac- PFPQPELPY-NH <sub>2</sub>
tTGIII-DQ2(II)	tTG (675-680)- $\alpha$ 2Gli(63-71)	Ac- AVKGFGR-NH <sub>2</sub>   Ac- PQPELPYPQ-NH <sub>2</sub>
tTGIII-DQ2(III)	tTG (675-680)- $\alpha$ 2Gli(68-76)	Ac- AVKGFGR-NH <sub>2</sub>   Ac- PYPQPELPY-NH <sub>2</sub>

### 2.5.1 Automatic synthesis of linear gliadin peptides: DQ2(I), DQ2(II), and DQ2(III)

The three  $\alpha$ 2-Gliadin-derived peptides, i.e. **DQ2(I)** Ac-PFPQPELPY-NH<sub>2</sub>, **DQ2(II)** Ac-PQPELPYPQ-NH<sub>2</sub>, and **DQ2(III)** Ac-PYPQPELPY-NH<sub>2</sub>, were synthesized by Fmoc/*t*Bu SPPS using an automatic peptide synthesizer, *Apex 396* equipped with a 8-wells reaction block (0.16 scale), starting from Fmoc *Rink-Amide* resin (Iris Biotech GmbH), according to the general procedure for the SPPS described in details in the Experimental Part and using th

## PART A

commercially available Fmoc-protected amino acids and TBTU/DIPEA activation.

**Table 2.7. Synthesis of  $\alpha$ 2-gliadin-derived peptides.**

Peptide	Protein Fragment	Sequence
DQ2(I)	$\alpha$ 2-Gliadin (61-69)	Ac-PFPQPE <u>L</u> LPY-NH <sub>2</sub>
DQ2(II)	$\alpha$ 2-Gliadin (63-71)	Ac-PQPE <u>L</u> PYPQ-NH <sub>2</sub>
DQ2(III)	$\alpha$ 2-Gliadin (68-76)	Ac-PYPQPE <u>L</u> LPY-NH <sub>2</sub>

The three  $\alpha$ 2-Gliadin-deriving peptides were modified replacing Gln target residues (present in the native sequence) with Glu residues at positions 66 in  $\alpha$ 2-Gliadin (61-69) and in,  $\alpha$ 2-Gliadin (63-71), at position 72 in  $\alpha$ 2-Gliadin (68-76) to perform the cross coupling reaction with the target Lys residues on the tTG peptide-fragments. The peptides were acetylated on the <sup>o</sup>N-terminal function and cleaved from the resin as described in the general procedure reported in the Experimental Part. After cleavage of the linear peptides from the resin and deprotection of the amino-acid side chains, the crude products were purified by SLFC and characterized by RP-HPLC ESI-MS. Analytical data are reported in *Table 2.8*.

**Table 2.8. Analytical data of the peptides DQ2(I), DQ2(II) and DQ2(III).**

Peptide	Rt (min) <sup>a</sup>	ESI-MS [M+H] <sup>+</sup> (m/z) calc(found)
DQ2(I)	4.10	1128.8 (1128.6)
DQ2(II)	2.81	1109.9 (1109.6)
DQ2(III)	3.42	1144.8 (1144.7)

<sup>a</sup>Analytical HPLC gradients at 0.6 mL min<sup>-1</sup>, <sup>a</sup>20-70% B in 5 min, solvent system are A: 0.1% TFA in H<sub>2</sub>O, B: 0.1% TFA in CH<sub>3</sub>CN.

### 2.5.2 Manual synthesis of the peptide **tTGI**, a case study.

The synthesis of the **tTGI** peptide, Ac-DCLTESNLIKVR-NH<sub>2</sub>, presented difficult couplings at the level of the N-terminal tetrapeptide DCLT.

**Table 2.9 Peptide reproducing selected tTG protein fragment.**

Peptide	Sequence	Target Residue
<b>tTGI</b>	Ac-DCLTESNLI <u>K</u> VR-NH <sub>2</sub>	Lys 562

The first attempt to obtain the peptide **tTGI** was performed using the manual peptide synthesizer *PLS ChemTech* starting from the Fmoc *Rink-Amide* resin (Iris Biotech GmbH, 0.63 mmol/g loading) and *via* TBTU/NMM activation. This approach was unsuccessful. Therefore, we decided to use a lower loaded Fmoc *Rink-Amide* resin (Iris Biotech GmbH, 0.14 mmol/g loading). In order to identify the critical steps of the synthesis, each coupling reaction was monitored by the Kaiser test and a micro-cleavage (monitored by RP-HPLC ESI-MS) was performed each four residues as described in details in the Experimental Part. In particular, we found deletion sequences at the level of the four N-terminal coupling steps. To overcome these synthetic problems we performed a systematic study for the coupling reactions using different activating agents (TBTU/NMM, HATU/NMM, DIC/HOBt, and TBCR/NMM) in different reaction conditions, e.g. we performed the couplings both at room temperature, at 40 °C, and assisted by microwaves (35 Watt and 70 °C).

#### *Coupling reactions using HATU at room temperature, at 40°C, and assisted by microwave irradiation*

We used the most performing 2-(1*H*-7-azabenzotriazol-1-yl)-1,1,3,3-tetramethyl uronium hexafluorophosphate methanaminium (HATU) as a coupling reagent instead of TBTU. The HATU/NMM activation system was applied in the case of the last 4 coupling steps of the manual peptide synthesis.

## PART A

HATU is a HOAt-based reagent developed by Carpino in 1994, who demonstrated increased reactivity when the activating agent presented strongly electronegative heteroatoms (i.e., nitrogen or oxygen) as in the azabenzotriazolyl ring. In fact, the withdrawing effect of nitrogen can decrease electron density at the carbon atom of the ester group linked to the ring in the activated form of the amino acid, increasing its reactivity towards nucleophiles. The difference in activities of these coupling reagents compared to the corresponding HOBt-based reagents could be explained by the hydrogen bond formed between the additional nitrogen atom in HOAt and HATU, stabilising the activated ester intermediate *via* an anchimeric assistance effect. Moreover, the possible transition state energy is lowered thus resulting in a higher coupling rate<sup>85</sup>.

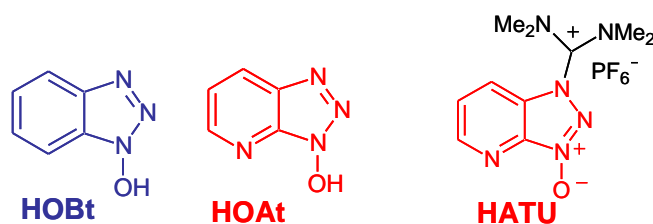


**Figure 2.25.** Commercially available HOBt (blue), HOAt, and HATU [both HOAt-based (red) coupling reagents].

Notwithstanding the use of this more potent reagent, the final yield of the crude **tTGI** resulted lower than 5% by RP-HPLC ESI-MS analysis of the crude performed after micro-cleavage.

Therefore HATU activation was coupled with the microwave irradiation (35 Watt and 70 °C) during the coupling reactions. Kinetic problems due to

<sup>85</sup> a) Carpino, L.A.; El-Faham, A.; Albericio, F. *Tetrahedron Lett.*, **1994**, 35, 2279-2282; b) L. A. Carpino, *J. Am. Chem. Soc.*, **1993**; 115: 4397; c) L. A. Carpino, *J. Am. Chem. Soc.*, **1993**, 115: 4397 –4398; d) L. A. Carpino, A. J. El-Faham, *Org. Chem.*, **1995**, 60, 3561 –3564; e) L. A. Carpino, F. J. Ferrer, *Org. Lett.*, **2001**; 3: 2793–2795.

intermolecular aggregation or steric hindrance of protecting groups can generate premature termination of the sequence (causing deletion sequences) during the different steps of the SPPS. Recently, the use of microwave energy has been proposed to fulfill the requirement to couple a high-speed technology with an efficient solid-phase synthetic strategy. In particular, microwave irradiation allows homogeneous heating of the reaction vessel. Although conventional SPPS remains the principal strategy for peptide synthesis, the use of microwave energy in SPPS represents an important breakthrough in difficult couplings of numerous peptides (hydrophobic, sterically hindered sequences, i.e. polyArg; etc.), in terms of decreasing chain aggregation and improving the coupling rates during the syntheses, as reported by Rizzolo *et al.* for microwave assisted synthesis of the antibiotic peptide gramicidin A<sup>86</sup>.

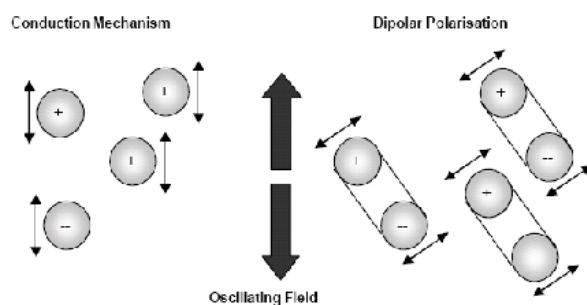


**Figure 2.26.** Advantages of heating by microwave irradiation.

The last four couplings of the synthesis of **tTGI**, Ac-DCLTESNLIKVR-NH<sub>2</sub>, were performed using the standard microwave protocol reported in *Table 2.10* using HATU/NMM activation. Unfortunately no improvement in final yield of the peptide **tTGI** was achieved.

<sup>86</sup> Rizzolo, F.; Sabatino, G.; Chelli, M.; Rovero P.; and Papini A.M., *Int. J. of Pept. Res. and Ther.*, **2007**, 13(1-2), 203-208.

**Table 2.10** Microwave-assisted coupling conditions.

Step	Temp(°C)	MW Power (W)	Time (sec)
Coupling of all aa	70	35	300
Coupling of Fmoc-Cys554(Trt)-OH	35	30	300

The synthesis of the entire sequence of the peptide **tTGI** was repeated performing the coupling reaction at 40°C, using HATU/NMM activation. We failed once again, and in particular in this case we observed Ser558 epimerization.

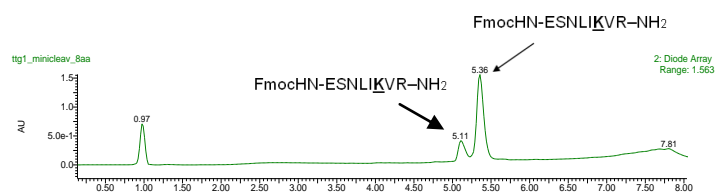


**Figure 2.27** RP-HPLC profile of Fmoc-Glu-Ser-Asn-Leu-Ile-Lys-Val-Arg-NH<sub>2</sub> after microcleavage.

In the general conditions of the SPPS (large excess of the reagents and fast coupling reactions) the racemization is usually reduced, but this can be a serious problem during the coupling of peptide fragments in the presence of Cys, His, Phe, and Ser residues as an example<sup>87</sup>.

#### *DIC/HOBt activation strategy*

**tTGI**, i.e. Ac-DCLTESNLIKVR-NH<sub>2</sub>, was therefore synthesized again using DIC/HOBt as activation system. At the end of the synthesis, the peptide was acetylated at the N-terminus following the general procedure described in the Experimental Part. Then the Dde protecting group on the side chain of Lys562 was removed as described in the general procedure using 2% v/v hydrazine in

<sup>87</sup> a) Di Fenza A.; Tancredi M.; Galoppini C.; Rovero P., *Tetr. Lett.*, **1998**, 39, 8529-8532;  
b) Di Fenza, A.; Rovero, P. *Let. Pept. Sci.*, **2002**, 9, 125-129.

DMF for 3-5 minutes. The peptide purity was checked by RP-HPLC ESI-MS after micro-cleavage as described in the Experimental Part.

**Table 2.11. RP-HPLC-ESI MS characterization of tTGI after micro-cleavage**

Peptide	Sequence	Rt (min) <sup>a</sup>	[M+2H] <sup>2+</sup> (m/z) Calc.(found)	HPLC Crude Purity
tTGI	Ac-DCLTESNLIKVR-NH <sub>2</sub>	3.7 <sup>b</sup>	716.4 (716.7)	<10%

<sup>a</sup> Analytical HPLC gradients at 0.6 mL min<sup>-1</sup>, <sup>b</sup>20-60% B in 5 min, solvent system are A: 0.1% TFA in H<sub>2</sub>O, B: 0.1% TFA in CH<sub>3</sub>CN.

We tried to synthesize tTGI using DIC/HOBt as activation system coupled to a microwave assisted protocol using the same coupling conditions described in Table 2.10 without obtaining the peptide in acceptable purity (data not shown).

#### *TBCRs-based strategy*

Because of the bad results obtained using as coupling reagents TBTU/NMM, HATU/NMM, and DIC/HOBt, we decided to switch to the Triazine Based Coupling Reagents (TBCRs) previously developed by Kaminski *et al.* and successfully applied and validated for SPPS<sup>88</sup>. TBCRs structurally derive from the commercially available and unstable 2-chloro-4,6-dimethoxy-1,3,5-triazine (CDMT) that was demonstrated not to be useful in SPPS.

<sup>88</sup>(a) Kaminski, Z.J.; Kolesinska, B.; Kolesinska, J.; Sabatino, G.; Chelli, M.; Rovero, P.; Blaszczyk, M.; Glowka, M.L.; Papini, A.M. *J. Am. Chem. Soc.* **2005**, 127, 16912. (b) "Process for the preparation of *N*-triazinylammonium salts". Filing date 07/11/2005. Applicant: Italvelluti S.p.a. Inventors: Z. Kaminski, A. M. Papini, B. Kolesinska, J. Kolesinska, K. Jastrzabek, G. Sabatino, R. Bianchini. PCT/EP2005/055793, **2005**.

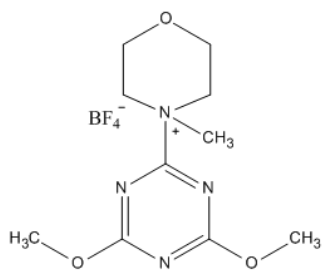


**Figure 2.28.** TBCR·BF<sub>4</sub> structure.

On the contrary acylation of amino acids in SPPS by the most stable and soluble TBCR, the tetrafluoroborate of 4-(4,6-Dimethoxy-1,3,5-triazin-2-yl)-4-methyl morpholinium (*Figure 2.28*), can take advantage of the stepwise mechanism of amide bond formation via TBCRs in which the tetrahedral intermediate is formed after the nucleophilic attack of the amino function, followed by expulsion of the leaving group (*Figure 2.29*).

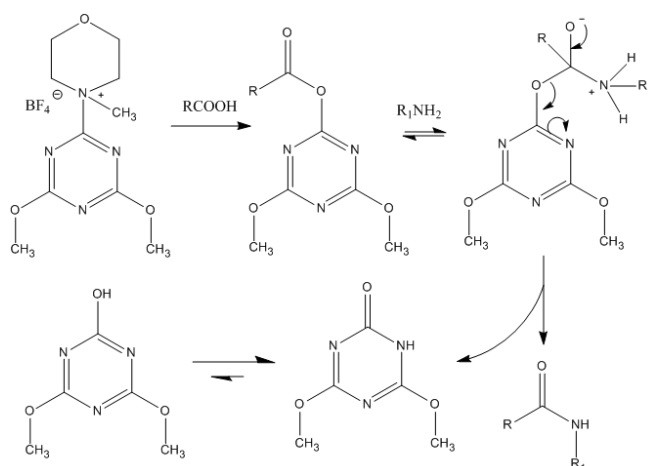


**Figure 2.29.** Mechanism of amide bond formation via TBCRs.

In fact, the concept of “superactive esters”<sup>89</sup> via TBCRs, lowering the energy of the amide formation transition state below the energy of the transition state relative to tetrahedral intermediate formation, is justified by a favoured process

<sup>89</sup>Kaminski, Z. J., *Biopolymers*, **2000**, 55, 140-165.

associated with the departure of the leaving groups releasing an additional energy (Figure 2.30).

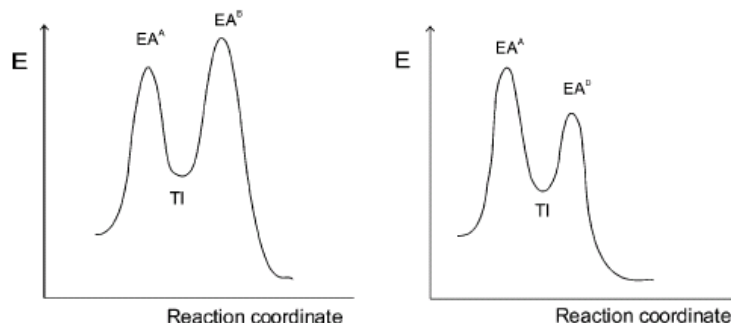


**Figure 2.30.** Energetic profile of amine acylation by active ester (left side) and “superactive ester” (right side).

The energetically favoured process by TBCRs, of prototropic rearrangement of the enol to the more stable keto form contributes with a sufficient driving force changing the energetic profile of the coupling reaction. Since their inception<sup>90</sup>, TBCRs have been considered promising coupling reagents, particularly suitable for peptide synthesis. Triazine esters have already been found more reactive than any other acylating reagent, including *N*-hydroxybenzotriazole esters. Moreover, many authors used successfully triazine reagents for the synthesis of peptides, carboxylic acid esters, amides, pholic acid antagonists,  $\alpha$ -lactames, carotenoids, fullerenes, and other compounds.

TBTU/NMM activation was replaced by TBCR·BF<sub>4</sub>/NMM to synthesize **tTGI**, i.e. Ac-DCLTESNLIKVR-NH<sub>2</sub>. A solution of TBCR·BF<sub>4</sub> in CH<sub>3</sub>CN, was added of the Fmoc-protected amino acids pre-dissolved in DMF and NMM. The reaction mixture was stirred for 30min before adding to the resin. The coupling mixture was left overnight at room temperature or, alternatively 1 min and 30’’ + 3min in the case of microwave-assisted couplings (reaction conditions summarized in Table 2.12).

<sup>90</sup>Kamiński, Z.J., *Int. J. Pept. Protein Res.*, **1994**, *43*, 312-319.

## PART A

RP-HPLC-ESI-MS of the crude product after microcleavage from the resin showed no improvement even in the case of this strategy. A particular critical step in the peptide chain elongation resulted the coupling of the penultimate residue Fmoc-Cys554(Trt)-OH.

### *Use of ChemMatrix resin and replacement of Fmoc-Ser(tBu)-OH with Fmoc-Ser(Trt)-OH*

We decided to use in the peptide synthesis Fmoc-Ser-(Trt)-OH bearing the more hindered trityl protecting group instead of the conventionally used Fmoc-Ser(tBu)-OH. This was to try to overcome some possible aggregation effects usually dramatically affecting final yield. Moreover, the synthesis of **tTGI**, Ac-Asp-Cys-Leu-Thr-Glu-Ser-Asn-Leu-Ile-Lys-Val-Arg-NH<sub>2</sub>, was performed starting from a Fmoc-Rink-Amide Chem Matrix<sup>®</sup> resin according to the General Procedure for the SPPS described in details in the Experimental Part and using the commercially available Fmoc-protected amino acids and TBTU/NMM activation. Chem Matrix<sup>®</sup> resins (*Figure 2.31*) are polyethyleneglycol-based resins and the solid support is exclusively composed of primary ether bonds and, therefore, it is claimed to have higher chemical stability. Its usefulness has been reported in several recent papers for the synthesis of complex, long, and highly hydrophobic peptides.

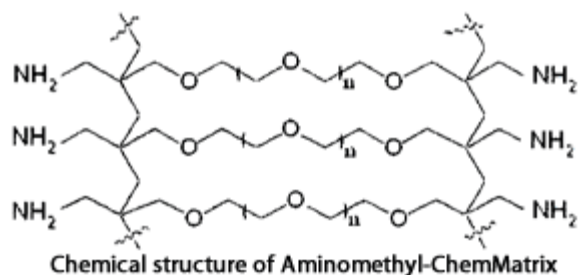


*Figure 2.31. Chemical structure of the polymeric polyethilenglycol support of ChemMatrix<sup>®</sup> resins.*

This synthetic process let us to obtain finally the **tTGI** peptide in acceptable purity(75%) as evaluated by RP-HPLC of the crude after micro-cleavage. In

Table 2.12 are summarised the different strategies performed to arrive to an optimised synthetic protocol to obtain **tTGI**.

**Table 2.12. Comparison of the different synthetic strategies performed during the optimization of the synthesis of tTGI**

Entry	Coupling reagent	Temp. °C	Time min	MW W	Yield %	Fmoc-Rink-Amide-Y Resin	Fmoc-Ser558(X)-OH
1	TBTU/NMM	20	20	-	<5%	Y=PS Resin	X=tBu
2	HATU/NMM	20	20	-	<5%	Y=PS Resin	X=tBu
3	HATU/NMM	70	5	35	<5%	Y=PS Resin	X=tBu
4	HATU/NMM	40	20	-	<5%	Y=PS Resin	X=tBu
5	DIC/HOBt	20	20	-	<10%	Y=PS Resin	X=tBu
6	DIC/HOBt	70	5	35	<5%	Y=PS Resin	X=tBu
7	TBCR/NMM	20	O.N.	-	<5%	Y=PS Resin	X=tBu
8	TBCR/NMM	70	1.5+3	100	<5%	Y=PS Resin	X=tBu
9	TBTU/NMM	20	20	-	75%	Y=Chem Matrix <sup>®</sup> Resin	X=Trt

The Peptide **tTGI** was then acetylated on the <sup>α</sup>N-terminal function as described in the general procedure reported in the Experimental Part. The target Lys side-chains in **tTGI** peptide sequence, Lys562 was protected by 1-(4,4-dimethyl-2,6-dioxacyclohexylidene)ethyl (Dde)<sup>91</sup> that was orthogonally removed to react regioselectively with the Glu side chains in α2-Gliadin peptide fragments, as reported in details in the Experimental Part. Dde is easily removed under nucleophilic conditions treating the resin with 2% v/v hydrazine in DMF for 3-5 minutes. The deprotection reaction was followed by UV detection at 290nm because of the formation of 3,6,6-trimethyl-4-oxo-

<sup>91</sup>Nash, I.A.; Bycroft, B.W.; and Chan, W.C., *Tetrahedron Letters*, **1996**, 37(15), 2625–2628.

## PART A

4,5,6,7-tetrahydro-1*H*-indazole. Dde is stable under Fmoc- and Boc-deprotection conditions. On the contrary Fmoc is readily deprotected with 2% v/v hydrazine in DMF. Therefore Dde has to be removed only at the end of the synthesis after introducing the last amino acid protected as Boc on the N-terminus or after acetylation with acetic anhydride in the presence of NMM, as in our case. The peptide purity was checked by RP-HPLC ESI-MS after micro-cleavage from the resin as described in the Experimental Part.

Analytical data are reported in *Table 2.13*.

**Table 2.13. Analytical data of the peptide tTGI.**

Peptide	Sequence	Rt (min) <sup>a</sup>	[M+2H] <sup>2+</sup> (m/z) Calc. (found)	HPLC Purity
tTGI	Ac-DCLTESNLIK <u>V</u> R-NH <sub>2</sub>	3.62 <sup>b</sup>	716.4 (716.7)	75%

<sup>a</sup> Analytical HPLC gradient at 0.6 mL min<sup>-1</sup>, <sup>b</sup>20-60% B in 5 min, solvent system are A: 0.1% TFA in H<sub>2</sub>O, B: 0.1% TFA in CH<sub>3</sub>CN.

### 2.5.3 Manual synthesis of the linear peptides tTGII and tTGIII

The peptides, tTGII, Ac-DLYLENPEIKIR-NH<sub>2</sub> and tTGIII, Ac-AVKGGFR-NH<sub>2</sub> were synthesized by Fmoc/*t*Bu SPPS using the manual peptide synthesizer *PLS ChemTech* starting from Fmoc-*Rink-Amide* resin (Iris Biotech GmbH), according to the general procedure for the SPPS described in details in the Experimental Part and using the commercially available Fmoc-protected amino acids and TBTU/NMM activation.

**Table 2.14. Peptides reproducing the selected tTG protein fragments.**

Peptide	Sequence	Target Residue
tTGII	Ac-DLYLENPEIK <u>I</u> R-NH <sub>2</sub>	Lys590
tTGIII	Ac-AVK <u>G</u> GFR-NH <sub>2</sub>	Lys677

Each coupling step was monitored by the Kaiser test in order to follow the coupling reactions. The peptides were acetylated on the <sup>a</sup>N-terminal function as described in the general procedure reported in the Experimental Part.

The target Lys side chains in the **tTGII** and **tTGIII** peptide sequences, **Lys590** e **Lys677** respectively, were protected by Dde. Therefore the Lys side chains were orthogonally deprotected with 2% v/v hydrazine in DMF at the end of the synthesis to react regioselectively with the Glu side chains in  $\alpha$ 2-Gliadin peptide fragments, as reported in details in the Experimental Part. Peptides purity was checked by RP-HPLC ESI-MS after micro-cleavage as described in the Experimental Part. Analytical data are reported in *Table 2.15*.

**Table 2.15. Analytical data for the peptides tTGII and tTGIII.**

Peptide	Sequence	Rt (min) <sup>a</sup>	ESI-MS	HPLC Purity
			[M+2H] <sup>2+</sup> (m/z) Calc(found)	
<b>tTG II</b>	Ac-DLYLENPEI <u>K</u> IR-NH <sub>2</sub>	3.9 <sup>b</sup>	772.4 (772.7)	95%
<b>tTG III</b>	Ac-AV <u>K</u> GFR-NH <sub>2</sub>	3.5 <sup>c</sup>	359.7 (359.8)	80%

<sup>a</sup> Analytical HPLC gradients at 0.6 mL min<sup>-1</sup>, <sup>b</sup>20-60% B in 5 min, <sup>c</sup>10-60% B in 5 min; solvent system are A: 0.1% TFA in H<sub>2</sub>O, B: 0.1% TFA in CH<sub>3</sub>CN.

#### 2.5.4 Synthesis of the nine cross-linked tTG-Gliadin peptides: *tTGI-DQ2(I), tTGI-DQ2(II), tTGI-DQ2(III), tTGII-DQ2(I), tTGII-DQ2(II), tTGII-DQ2(III), tTGIII-DQ2(I), tTGIII-DQ2(II), and tTGIII-DQ2(III).*

The nine cross-linked peptides were obtained starting from the linear **tTGI**, **tTGII**, and **tTGIII** and the  $\alpha$ 2-Gliadin peptides, **DQ2(I)**, **DQ2(II)**, and **DQ2(III)** obtained as described in the previous sections. Coupling reactions were performed in heterogeneous phase with the tTG peptide fragments still anchored on the resin, adding solutions of the  $\alpha$ 2-Gliadin peptides.  $\alpha$ 2-Gliadin peptides were purified up to 95% purity before the cross-linking reaction.

PART A

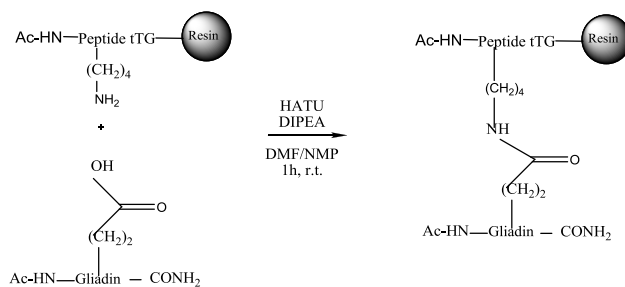


**Figure 2.32.** Cross-linking reaction in heterogeneous phase.

100mg of resin (1 eq.) bearing each tTG peptide fragment, i.e. *Rink-Amide Polystyrene Resin* for the **tTGII** and **tTGIII** peptides and *Rink-Amide Chem-Matrix Resin* for the **tTGI** peptide, were swollen in DMF before performing the cross-coupling, as reported in details in the Experimental Part.  $\alpha$ 2- Gliadin peptides (2.5 eq.), i.e., **DQ2(I)**, **DQ2(II)**, and **DQ2(III)**, were added in a solution of DMF/NMP 2:1. The coupling reactions were performed at room temperature for 1h in HATU/DIPEA activation system.

The coupling reaction was monitored by the Kaiser test and by micro-cleavage according to the general procedure reported in the Experimental Part. After cleavage of the cross-linked peptides from the resin and contemporary deprotection of amino-acids side chains of tTG peptide fragments, the crude products were purified by semipreparative RP-HPLC and characterized by RP-HPLC ESI-MS. Analytical data are reported in *Table 2.16*.

**Table 2.16. Analytical data of the cross-linked peptides.**

Cross-linked peptide	Sequence	ESI-MS [M+2H] <sup>2+</sup> (m/z) Calc (found)	HPLC (Rt,min) <sup>a</sup>
tTGI-DQ2(I)	Ac- DCLTESNLIKVR-NH <sub>2</sub>   Ac- PFPQPELPY-NH <sub>2</sub>	1271.1 (1271.02)	3.31 <sup>b</sup>
tTGI-DQ2(II)	Ac- DCLTESNLIKVR-NH <sub>2</sub>   Ac- PQPELPYPQ-NH <sub>2</sub>	1261.61 (1261.4)	3.67 <sup>d</sup>
tTGI-DQ2(III)	Ac- DCLTESNLIKVR-NH <sub>2</sub>   Ac- PYPQPELPY-NH <sub>2</sub>	1279.1 (1279.02)	2.86 <sup>b</sup>
tTGII-DQ2(I)	Ac- DLYLENPEIKIR-NH <sub>2</sub>   Ac- PFPQPELPY-NH <sub>2</sub>	1327.2 (1327.6)	3.99 <sup>b</sup>
tTGII-DQ2(II)	Ac- DLYLENPEIKIR-NH <sub>2</sub>   Ac- PQPELPYPQ-NH <sub>2</sub>	1317.71 (1318.2)	2.75 <sup>b</sup>
tTGII-DQ2(III)	Ac- DLYLENPEIKIR-NH <sub>2</sub>   Ac- PYPQPELPY-NH <sub>2</sub>	1335.21 (1335.2)	3.51 <sup>b</sup>
tTGIII-DQ2(I)	Ac- AVKGFNR-NH <sub>2</sub>   Ac- PFPQPELPY-NH <sub>2</sub>	914.50 (915.19)	3.46 <sup>b</sup>
tTGIII-DQ2(II)	Ac- AVKGFNR-NH <sub>2</sub>   Ac- PQPELPYPQ-NH <sub>2</sub>	905.01 (905.67)	3.51 <sup>c</sup>
tTGIII-DQ2(III)	Ac- AVKGFNR-NH <sub>2</sub>   Ac- PYPQPELPY-NH <sub>2</sub>	922.50 (923.22)	4.01 <sup>c</sup>

<sup>a</sup>Analytical HPLC gradients at 0.6 mL min<sup>-1</sup> solvent systems are: A (0.1% TFA in H<sub>2</sub>O MilliQ) and B (0.1 % TFA in CH<sub>3</sub>CN), <sup>b</sup>30-70% B in 5 min, <sup>c</sup>20-60% B in 5 min, <sup>d</sup>25-65% B in 5 min.

## 2.6 SP-ELISA using the nine cross-linked peptides as synthetic antigens

The nine cross-linked peptides, i.e., **tTGI-DQ2(I)**, **tTGI-DQ2(II)**, **tTGI-DQ2(III)**, **tTGII-DQ2(I)**, **tTGII-DQ2(II)**, **tTGII-DQ2(III)**, **tTGIII-DQ2(I)**, **tTGIII-DQ2(II)**, and **tTGIII-DQ2(III)** were tested in SP-ELISA to evaluate IgA and IgG antibody titre in 48 CD patients' sera at the diagnosis, and 36 normal blood donors (NBDs) as controls.

PART A

SP-ELISA experiments were performed using as secondary antibody, anti-human IgA and anti-human IgG conjugated to Alkaline Phosphatase (AP). IgA displayed only low titers. On the contrary, IgG antibodies displayed higher titers. In particular, we selected the two cross-linked peptides, ie., **tTGI-DQ2(I)** and **tTGI-DQ2(II)**, after screening 48 CD patients' sera *versus* 36 NBDs (*Figure 2.33*).

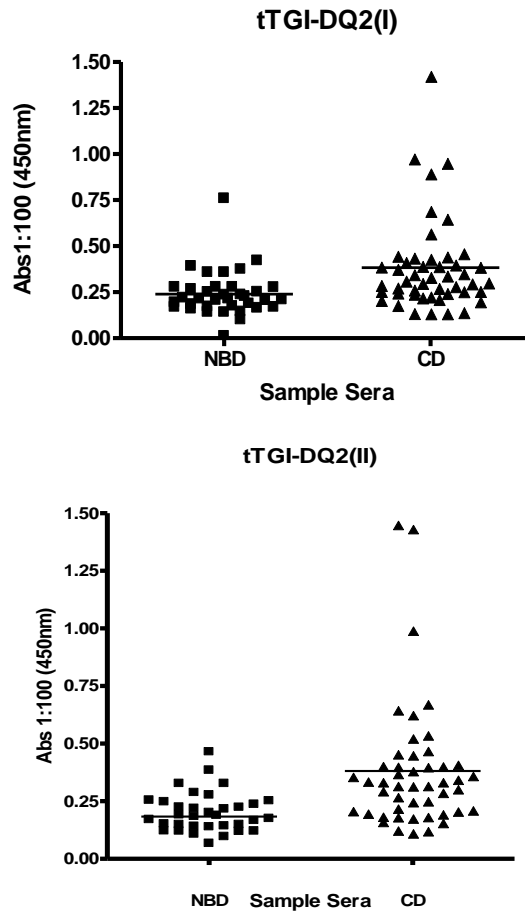


*Figure 2.33. Dispersion diagrams generated for tTGI-DQ2(I) and tTGI-DQ2(II).*

We generated the two ROC curves<sup>92</sup> reported below for the anti-cross-linked peptide **tTGI-DQ2(I)** and anti-**tTGI -DQ2(II)** IgG antibodies in 48 CD *versus* 36 NBDs.

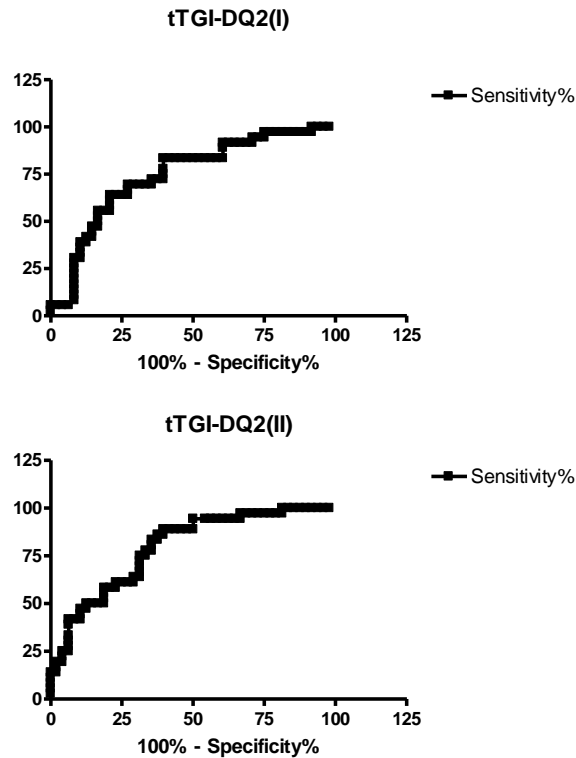


**Figure 2.34.** ROC analysis calculated for anti-**tTGI-DQ2(I)** and anti-**tTGI-DQ2(II)** IgG in 48 CD *versus* 36 NBD.

In analyzing the ROC curves there are some parameters that have to be taken into account. The parameters calculated for the two ROC curves corresponding

<sup>92</sup>Receiver Operating Characteristic (ROC) curves are often used in medicine to determine a cutoff value for a clinical test. In a Receiver Operating Characteristic (ROC) curve the true positive rate (Sensitivity, y-axis) is plotted in function of the false positive rate (100-Specificity, x-axis) for different cut-off points. Each point on the ROC curve represents a sensitivity/specificity pair corresponding to a particular decision threshold. A test with perfect discrimination (no overlap in the two distributions) has a ROC curve that passes through the upper left corner (100% sensitivity, 100% specificity). Therefore the closer the ROC curve is to the upper left corner, the higher the overall accuracy of the test. Zweig & Campbell, 1993.

PART A

to the IgG antibodies to the two selected cross-linked peptides are reported in *Table 2.17*.

**Table 2.17. ROC parameters**

<b>Parameters</b>	<b>Peptide tTGI-DQ2(I)</b>	<b>Peptide tTGI-DQ2(II)</b>
Area under the ROC curve	0.7428	0.7928
Std. error	0.05477	0.04838
95% confidence interval	0.6354- 0.8501	0.6980 - 0.8877
P value	0.0001513	< 0.0001

In particular, the area under the ROC curve (AUC) and the P value allow to measure the overall ability of the test to discriminate between CD patients and healthy controls<sup>93</sup>.

In conclusion, the peptide **tTGI -DQ2(II)** displayed the best performance in detecting autoantibodies in CD patients' sera at the diagnosis and the analysis of the ROC curve allowed us to determine the cut-off of the clinical assay (IgG Abs> 0.3 OD) using **tTGI -DQ2(II)** as a synthetic antigen in SP-ELISA.

---

<sup>93</sup>The area under the ROC curve quantifies the overall ability of the assay to discriminate between those individuals with the disease and those without the disease. ROC curve areas are typically between 0.5 and 1.0. The maximum possible AUC of an ideal test is 1.00. The software we used for data analysis calculates the P value from the z ratio, z as (Area - 0.5)/(SE Area). The P value tests the null hypothesis that the test has no skill at distinguishing patients from controls. The Significance level or P-value is the probability that the observed sample Area under the ROC curve is found when in fact, the true (population) Area under the ROC curve is 0.5 (null hypothesis: Area = 0.5). The smaller the P value is, the higher will be the ability of the assay to distinguish between the two groups, i.e. CD patients and healthy controls.

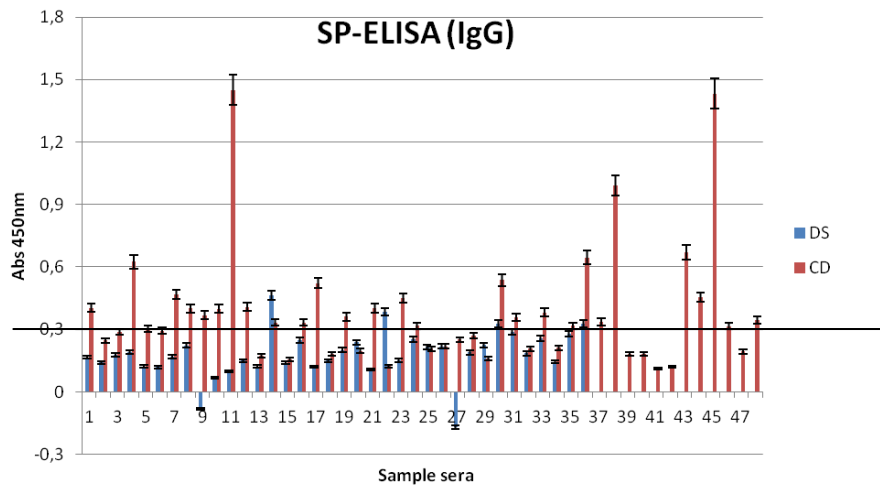


**Figure 2.35.** Results obtained from SP-ELISA using the peptide **tTGI-DQ2(II)**.

In conclusion the cross-linked peptide **tTGI-DQ2(II)** is able to recognize circulating IgG autoantibodies in coeliac patients' sera with 56% specificity and 89% sensitivity (percentage of CD patients).

### **2.6.1 Investigation of the nature of the antigen-antibody recognition by the cross-linked peptide **tTGI-DQ2(I)** in SP-ELISA**

We investigated the role of the linear peptide fragments by a comparison with the cross-linked adduct **tTGI-DQ2(II)**. To this end, we performed SP-ELISA experiments using the **tTGI** peptide, i.e. tTG(553-564), the **DQ2(II)** peptide, i.e.  $\alpha$ 2-Gliadin(63-71), a mixture of both the linear sequences **tTGI** and **DQ2(II)**, and the cross-linked peptide **tTGI-DQ2(II)** in a screening on 30 CD patients' sera and 24 NBDs, using as secondary antibody anti-human IgG conjugated to AP.

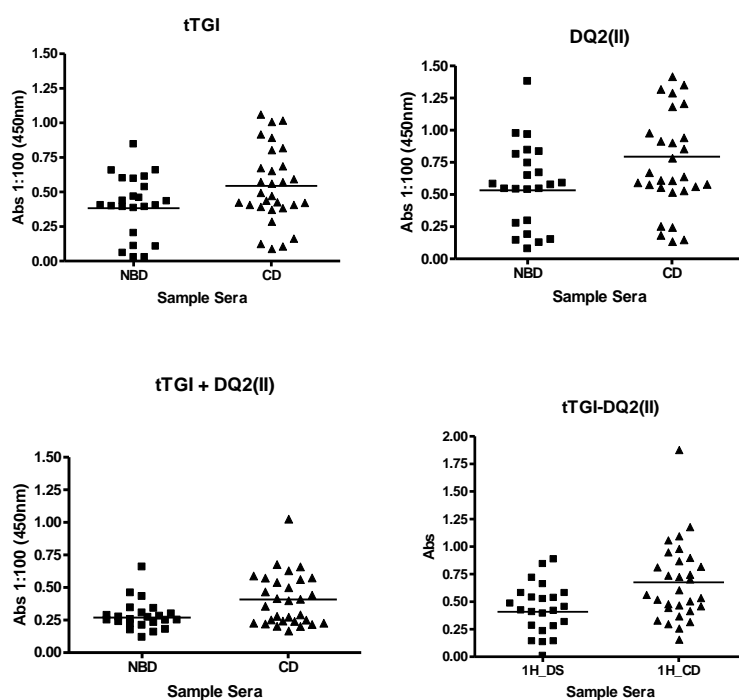


**Figure 2.36.** Dispersion diagrams generated for the linear peptides **tTGI** and **DQ2(II)**, a mixture of them, and the cross-linked adduct **tTGI-DQ2(II)**.

The results reported in *Figure 2.36* confirm the importance of the cross-link in the new peptide probe **tTGI-DQ2(II)** in recognizing IgG antibodies in CD patients' sera compared to NBDs.

### **2.6.2 Results and discussion**

Thanks to the innovative "Chemical Reverse Approach" previously developed in PeptLab of the University of Florence, we were able to select the cross-linked peptide **tTGI-DQ2(II)** as the most promising tool to recognize circulating IgG autoantibodies in sera of coeliac patients, at the diagnosis. Antibody recognition obtained using the synthetic cross-link **tTGI-DQ2(II)** confirm the previously reported results indicating protein fragments formed *in vivo*<sup>73</sup>. In particular, univocally characterised synthetic probes reproducing these fragments could mimic the *in vivo* formed antigens and can be used to set-up and validate peptide-based ELISA for CD early diagnosis. Moreover this result

underlines the importance of the criteria used to drive epitope selection since the **tTGI** peptide fragment is exposed on the surface of tTG when it is in the open conformation<sup>74,56,69</sup>. Finally we found that among the 9-mer epitopes of the 33-mer super-antigen  $\alpha 2$ -Glia(57-89), the best non-self antigen is  $\alpha 2$ -Glia(63-71), reproduced in the **DQ2(II)** synthetic peptide.

## **PART B: Glycopeptidomimetic-based immunoassays for Multiple Sclerosis**

### **3 Multiple Sclerosis: an overview**

Multiple Sclerosis was described for the first time by the french neurologist Jean Martin Charcot, in 1868. Charcot observed the accumulation of inflammatory cells in a perivascular distribution within the brain and spinal cord white matter in patients with intermittent episodes of neurologic dysfunction<sup>94</sup>. This led to the term “*sclérose en plaques disséminées*”, or Multiple Sclerosis. Later, in 1948, Elvin Kabat’s observation of increased oligoclonal immunoglobulin in the cerebrospinal fluid of patients with MS provided further evidence of an inflammatory nature of the disease<sup>95</sup>. MS twin studies demonstrated a strong genetic basis for this clinical-pathological entity<sup>96</sup>. In 1933, Thomas Rivers demonstrated that repeated injections of rabbit brain and spinal cord (CNS myelin) into primates developed a demyelinating disease (experimental autoimmune encephalomyelitis, e.g. EAE) and led to the generally accepted concept that MS is an autoimmune disease<sup>97</sup>.

MS is a chronic, inflammatory, demyelinating disease of the CNS that affects brain and spinal cord and its name comes from the numerous “sclerotic” areas observable by microscopical examination of the brain. Usually, the disease is mild, but some people lose the ability to write, speak or walk. Typical symptoms of MS are, visual disturbances, muscle weakness, trouble with

---

<sup>94</sup> a) Charcot, J.. *Gazette des Hôpitaux*. **1868**, 41, 554–566; b) Charcot, J., *The New Sydenham Society. London, United Kingdom.*, **1877**, 157–222.

<sup>95</sup> Kabat, E. A.; Glusman, M.; and Knaub, V., *Am. J. Med.*, **1948**, 4, 653-662.

<sup>96</sup> a) Mackay, R. P., *Arch. Neurol.* **1966**, 15, 449–462; b) Williams, A., Eldridge, R.; McFarland, H., *Neurology*. **1980**, 30, 1139–1147.

<sup>97</sup> Rivers, T. M. Sprunt, D.H.; and Berry, G.P., *J. Exp. Med.* **1933**, 58, 39–53.

coordination and balance, sensations such as numbness, prickling, or "pins and needles" and thinking and memory problems.

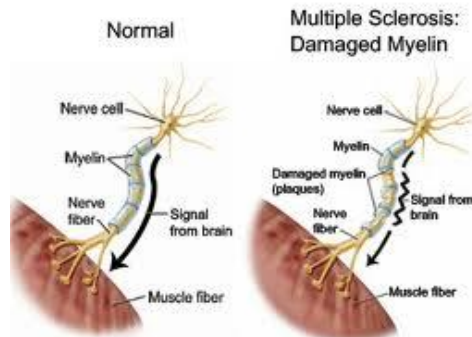


**Figure 3.1.** MS shorts out the flow of information within the brain and between the brain and body, similar to how a stripped electrical wire can short out an appliance.

MS represents the first cause of neurological disability in adult Caucasians. Today there is no cure for MS, but medicines may slow it down and help control symptoms. Physical and occupational therapy may also help.

#### *Clinical subtypes of Multiple Sclerosis*

MS onset generally occurs from the adolescence and around the age of 35. Epidemiologically, it hits women more commonly than men (2:1). The disease shows a definite relationship with latitude. The four are the clinical subtypes of MS, based on temporal profile are described below.

- 1) **Progressive relapsing MS (PR-MS)**.PR-MS is defined as progressive disease from onset, with clear acute relapses, with or without full recovery.
- 2) **Secondary progressive MS (SP-MS)**.SP-MS is defined as a disease that has an initial relapsing-remitting disease course followed by progression with or without occasional relapses, minor remissions, and plateaus.

PART B

3) **Primary progressive MS (PP-MS).**PP-MS is defined as the disease progression from the onset with occasional plateaus and temporary minor improvements.

4) **Relapsing-remitting MS (RR-MS).**RR-MS is characterized by clearly defined disease relapses with full recovery or with *sequelae* and residual deficit upon recovery. In the period between disease relapses patients are stable with lack of disease progression<sup>98</sup>.

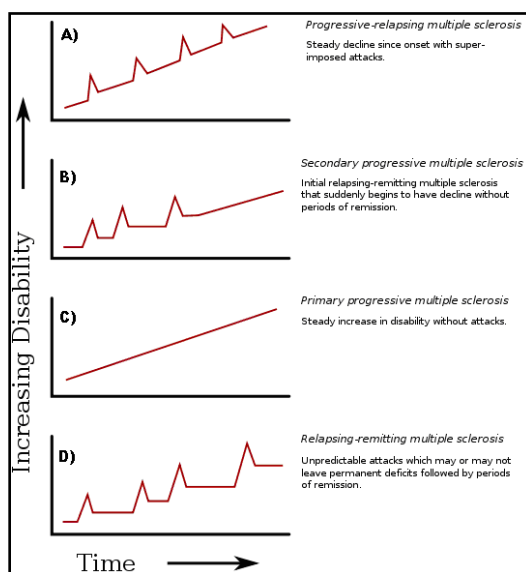


**Figure 3.2.** Clinical subtypes of MS; a) Progressive relapsing MS, b) Secondary progressive MS, c) Primary progressive MS, d) Relapsing-remitting MS.

*Pathogenesis of Multiple Sclerosis*

On the basis of myelin protein loss, the geography and extension of plaques, the patterns of oligodendrocyte destruction, and the immunopathological evidence of complement activation, Lucchinetti. *et al.* proposed four distinct patterns of MS pathology: 1) cell-mediated demyelination; 2) antibody-

<sup>98</sup> Lublin, F.D.; and Reingold, S.C., *Neurology*, **1996**, 46, 907-911.

mediated demyelination; 3) active myelin destruction; 4) oligodendroglial pathology or oligodendrocyte dystrophy<sup>99</sup>.

Two patterns (1 and 2) show close similarities to T-cell-mediated or T-cell with Ab-mediated autoimmune encephalomyelitis, respectively. The other patterns (3 and 4) are highly suggestive of a primary oligodendrocyte dystrophy, reminiscent of virus or toxin induced demyelination rather than autoimmunity. This study demonstrated that most cases share in common the T cell and macrophage dominated inflammatory reaction, lesions segregated into those with close similarities to autoimmune encephalomyelitis (i.e. patterns 1 and 2) and those with signs of oligodendrocyte dystrophy (i.e. patterns 3 and 4)<sup>100</sup>. The idea that MS is caused by an infectious agent has been controversial for almost a century. According to this hypothesis, MS is caused by primary infection of the CNS with intact or mutant virus, whereas an inadequate immune response probably contributes to disease progression. During the first phase of the disease, the virus replicates rapidly in the CNS and induces variable degrees of demyelination. After a few days, increasing mononuclear cell infiltrates targeting the virus infection are observed. Predominantly CD8<sup>+</sup> T cells, but also CD4<sup>+</sup> T cells, are crucial for controlling the virus, whereas B cells and Abs seem to be less important in the acute disease stage<sup>101</sup>.

#### *Role of the oxidative stress*

Oxidative stress refers to a state in which free radicals and their products are in excess of antioxidant defense mechanisms. Reactive Oxygen Species (ROS) and Reactive Nitrogen Species (RNS) include superoxide ions, hydrogen peroxide, nitric oxide, and peroxynitrite and are generated as part of normal cellular physiology. Overproduction of ROS can cause damage to lipids,

---

<sup>99</sup> Lucchinetti, C.; Bruck, W.; Parisi, J.; Scheithauer, B.; Rodriguez, M.; and Lassmann, H., *Ann. Neurol.*, **2000**, 47, 707-717.

<sup>100</sup> Lassmann, H.; Bruck, W.; and Lucchinetti, C., *Trends Mol. Med.*, **2001**, 7, 115-121.

<sup>101</sup> Hemmer, B.; Archelos, J.J.; and Hartung, H.P., *Nat Rev Neurosci*, **2002**, 3, 291-301.



RNS produced as part of the inflammatory response can have a potential role in tissue damage in MS.

#### *Autoimmune features*

The underlying immunological abnormalities in MS lead to various neurological and autoimmune manifestations. There is strong evidence that MS is, at least in part, an immune-mediated disease, whereas there is less evidence that MS is a classical autoimmune disease, even though many authors state this in the description of the disease<sup>107</sup>.

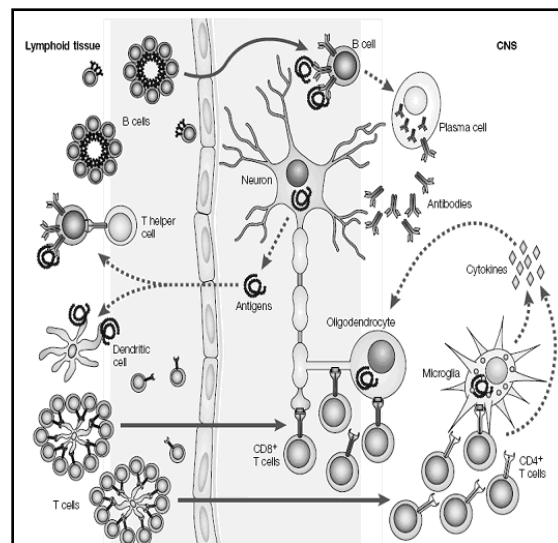


**Figure 3.4.** *Immune response in multiple sclerosis*<sup>108</sup>.

Multiple Sclerosis is thought to be an autoimmune disease in which CD4+ and CD8+ T-cells enter the CNS and initiate an inflammatory response directed against myelin and other components of CNS. Over several years, a more complex pathophysiology in which numerous cells are involved in the development of MS plaques emerged. These cells are CD8+ T lymphocytes,

<sup>107</sup>Wootla, B.; Eriguchi, M.; and Rodriguez, M., *Autoimm. Dis.*, **2012**, doi:10.1155/2012/969657.

<sup>108</sup>Hemmer, B.; Archelos, J.J.; Hartung, H-P., *Neuroscience*. **2002**, 3,291-301.

## PART B

B-cells, and Th17 cells (a population of T helper cells that secrete inflammatory cytokine IL-17). MS has classically been thought as a T-cell-dependent process associated with macrophage-mediated demyelination driven by myelin-specific auto-Ags<sup>109</sup>. In the presence of APCs, such as dendritic cells, efficient B- and T- cell responses are initiated. After priming, these cells cross the blood–brain barrier, migrate to the site of Ag exposure and develop effector functions. CNS specific autoreactive T-cells initiate an inflammatory process that results in CNS demyelination and cross the blood brain barrier by diapedesis. After entering the CNS, these T-cells re-encounter the specific Ag(s) and cause inflammation. These APCs express MHC class I and MHC class-II Ags, which increase the local inflammatory response causing the damage of saltatory conduction, which leads to MS symptoms.

The role of B-cells, plasma cells, and Abs is complex and may be involved in pathogenic, regulatory and reparative phases of MS. A possible mechanism is that the intratechal Ab response in MS patients is due to nonspecific immunodysregulation. Nevertheless autoAb production in MS patients might be driven or promoted by cross-reacting infectious Ags. To this sense molecular mimicry is an especially appealing concept with accumulating support. Abs seem to modulate the inflammatory response mediated by T cells in brain lesions. T lymphocytes disturb the blood brain barrier and start the inflammatory process by activating effector cells, such as macrophage and microglia. Although the cause of MS is still uncertain, many findings point towards the autoAb response to self antigenic proteins of the myelin family. Myelin oligodendrocyte glycoprotein (MOG), even if its role in the pathogenesis of MS has remained controversial, has been considered as one of the potential self protein Ag in MS. Studies demonstrated the serological and/or CSF presence of antibodies directed against MBP and/or MOG in MS patients. Moreover, specific Abs against MOG gain access to their target Ag on the surface of myelin sheaths and initiate myelin destruction in the model of

---

<sup>109</sup> Goverman, J.M., *J.Immunol Rev***2011**, 241, 228-240.

MOG induced autoimmune encephalomyelitis<sup>110</sup>. In a recent study, it is claimed that anti-MOG Abs are also responsible of demyelination in CNS demyelinating diseases<sup>111</sup>.

### 3.1 The N-Glucosylated peptide CSF114(Glc) for the diagnosis of MS

Different self-proteins of myelin have been investigated as potent targets for T- or B-cells in MS, e.g. MOG. In the Laboratory of Peptide & Protein Chemistry & Biology of the University of Florence, the N-glucosylated peptide [Asn<sup>31</sup>(Glc)hMOG(30-50)] was demonstrated for the first time in 1999 to be able to detect autoantibodies in MS patients' sera, in ELISA experiments<sup>112</sup>. It was then observed that the ability of the glucosylated peptide to recognize autoantibodies in MS was related not only to its conformation but to a specific *N*-linked glucosyl moiety in the autoantibody binding site on MOG glycopeptide<sup>113</sup>.

---

<sup>110</sup>Lalive, P.H.; Molnarfi, N.; Benkhoucha, M.; Weber, M.S.; and Santiago-Raber, M.L., *J. Neuroimmunol.*, **2011**, 240-241, 28-33.

<sup>111</sup>Olsson, T., *Nat Rev Neurol.*, **2011**, 7, 248-249.

<sup>112</sup>Mazzucco, S.; Mata, S.; Vergelli, M.; Fiorese, R.; Nardi, E.; Mazzanti, B.; Chelli, M.; Lolli, F.; Ginanneschi, M.; Pinto, F.; Massacesi, L.; Papini, A. M. *Bioorg. Med. Chem. Lett.*, **1999**, 9, 167-172.

<sup>113</sup>Carotenuto, A.; D'Ursi, A.M.; Nardi, E.; Papini, A.M.; Rovero, P. *J. Med. Chem.*, **2001**, 44, 2378-2381.

## PART B

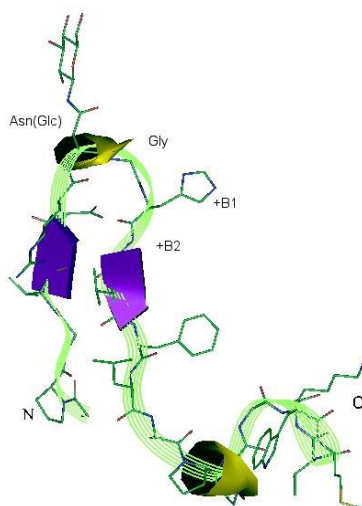


**Figure 3.5.** Calculated structures of CSF114(Glc). Ribbon diagram of the lowest energy conformer of 200 calculated structures of CSF114(Glc) derived from NMR data.

Hence, the recognition properties of the molecule were optimized through the design and screening of focused libraries of different glycopeptides by a “Chemical Reverse Approach”. A family of specific antigenic probes, termed **CSF114(Glc)** and characterized by type I'  $\beta$ -turn structures, was developed to identify autoantibodies, as biomarkers of MS, correlating with disease activity in a sub-population of MS patients. Glycopeptides based on the CSF114(Glc)structures<sup>14,114</sup>, are able to measure accurately high affinity autoantibodies in sera of a statistically significant patients' population<sup>115,116</sup> and are characterized by different types of  $\beta$ -turn structures bearing a  $\beta$ -D-glucopyranosyl moiety linked to an Asn residue. It has been demonstrated that autoantibody detection by type I'  $\beta$ -turn CSF114(Glc) glycopeptide is strictly

<sup>114</sup> Lolli, F.; Mazzanti, B.; Pazzagli, M.; Peroni, E.; Alcaro, M.C.; Sabatino, G.; Lanzillo, R.; Brescia Morra, V.; Santoro, L.; Gasperini, C.; Galgani, S.; D'Elisos, M.M.; Zipoli, V.; Sotgiu, S.; Pugliatti, M.; Rovero, P.; Chelli, M.; Papini, A.M., *J Neuroimmunol.*, **2005**, 167, 131-137

<sup>115</sup> Carotenuto, A.; D'Ursi, A. M.; Mulinacci, B.; Paolini, I.; Lolli, F.; Papini, A. M.; Novellino, E.; Rovero P., A. *J. Med. Chem.* **2006**, 49, 5072-5079.

<sup>116</sup> Carotenuto, A.; Alcaro, M.C.; Saviello, M.R.; Peroni, E.; Nuti, F.; Papini, A.M.; Novellino, E.; Rovero, P., *J. Med. Chem.*, **2008**, 51, 5304-5309.

related to the  $\beta$ -D-glucopyranosyl moiety linked to the Asn residue<sup>117</sup>, since glycopeptides lacking Asn(Glc) display a negligible activity<sup>118</sup>.

CSF114(Glc) represents an unconventional approach, since its structure is completely unrelated to MOG (or any other myelin derivative) and is not linked to any particular pathogenetic hypothesis. More than one of the myelin proteins could undergo aberrant *N*-glucosylation thus creating a family of new autoantigens and CSF114(Glc) could be a mimetic of all those *N*-glucosylated proteins. Recently, putative Ags present in rat brain, which recognize serum MS autoAbs purified through CSF114(Glc) affinity columns, termed “CSF114(Glc) Abs” were characterized. MALDI mass spectrometry analysis confirmed by ESI-MS, of the isolated Ags led to the identification of alpha actinin 1, a cytoskeletal protein abundant in CNS, as a principal MS-related Ag. Detection of cytoskeletal protein alpha actinin 1 by autoAbs from MS patients, besides signaling its involvement in the pathology, implies a derangement of the barrier shield, leading to exposure of the neurovascular niche to further degenerative injuries<sup>119</sup>. It is evident that CSF114(Glc) is a valuable tool not only for MS diagnosis but even to elucidate the inflammatory/degenerative processes of MS<sup>120</sup>.

Therefore, a further investigation of the possible molecular mechanisms involved in MS, and in particular the characterization of the native autoantigen(s) recognized by anti-CSF114(Glc) auto Abs, designing even more optimized tools may represent an important goal in the study of MS to develop simple diagnostic assays based on peptides.

---

<sup>117</sup> Nuti, F.; Paolini, I.; Cardona, F.; Chelli, M.; Lolli, F.; Brandi, A.; Goti, A.; Rovero, P.; Papini, A.M. *Bioorg. Med. Chem.* **2007**, *15*, 3965-3973.

<sup>118</sup> Nuti, F.; Peroni, E.; Real-Fernandez, F.; Bonache, M.A.; Le Chevalier-Isaad, A.; Chelli, M.; Lubin-Germain, N.; Uziel, J.; Rovero, P.; Lolli, F.; and Papini, A.M., *Biopolymers*, **2010**, *94*(6), 791-799.

<sup>119</sup> Pandey, S.; Dioni, I.; Lambardi, D.; Real-Fernandez, F.; Peroni, E.; Pacini, G.; Lolli, F.; Seraglia, R.; Papini, A.M.; and Rovero, P., *Mol. Cell. Proteom.*, **2012**, In press

<sup>120</sup> Pandey, S.; Alcaro, M.C.; Scrima, M.; Peroni, E.; Paolini, I.; Di Marino, S.; Barbetti, F.; Carotenuto, A.; Novellino, E.; Papini, A.M.; D'Ursi, A.M.; and Rovero, P., *J. Med. Chem.*, **2012**, In press.

### 3.2 Glycopeptidomimetic-based diagnostics in MS

Following the same approach that led to the generation of **CSF114(Glc)** **multiple epitope peptides** and **gluco-cyclopeptide** analogues were designed and synthesized. These synthetic probes were then tested by the use of our reverse approach to identify MS-specific autoantibodies as disease biomarkers in simple ELISA.

#### 3.2.1 *Multivalent interactions in antigen-antibody recognition system*

The nature of the antigen-antibody interaction deals with the concept of the multivalency, i.e. the interaction between multivalent receptors and/or multivalent ligands. Nature provides us with numerous examples of molecules with low-intrinsic affinity binding sites that are capable of high-avidity interactions with their targets due to multivalent binding. An antibody molecule with high affinity for a target antigen does not usually exist in the primary naive antibody library, and antibody affinity usually increases during an immune response *in vivo*, called affinity maturation. Therefore, even if the intrinsic affinity of an antibody molecule toward various invaders (e.g. virus, and/or bacterial proteins) is relatively low, high avidity can overcome the low intrinsic affinity, leading to the production of antibody molecules with high intrinsic affinity for the target antigen through affinity maturation in the immune system<sup>121</sup>. All classes of antibodies have multiple equivalent receptor sites: two (IgD, IgE, IgG, IgA), four (IgA), six (IgA), and ten (IgM). Hence, the concept of avidity in terms of antibody binding is comparable to the multivalency one<sup>122</sup>. One of the most efficient ways to increase the binding activity of an antibody to a surface (e.g. cell surface) is to make use of the

---

<sup>121</sup>Kumagai, I.; Tsumoto, K. *Encyclopedia of Life Sciences*, Nature Publishing Group, **2001**.

<sup>122</sup>Fasting, C.; Schalley, C.A.; Weber, M.; Seitz, O.; Hecht, S.; Koksche, B.; Dornedde, J.; Graf, C.; Knapp, E-W.; and Haag, R., *Angew. Chem. Int. Ed.*, **2012**, 51, 10472 – 10498

multivalency effect since multivalent interactions can be collectively much stronger than the sum of corresponding monovalent interactions<sup>123</sup>.

In 1988, Dr. James Tam<sup>124</sup> described the use of a multiple antigenic peptide (MAP) system eliciting specific antibodies in rabbits. This system represented a novel approach based on a small immunologically inert core molecule of radially branching lysine dendrites onto which a number of peptide antigens are anchored.

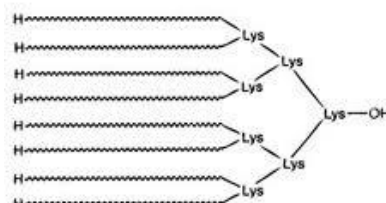


**Figure 3.6.** Branched structure of a MAP.

The result is a large macromolecule which has a high molar ratio of peptide antigen to core molecule and does not require further conjugation to a carrier protein. MAPs containing defined B-and/or T-cell epitopes of one or more antigens constitute a useful chemically unambiguous system to explore antigen-antibody interaction. Because of their shape and physical characteristics, MAPs are referred to as dendrimers and are viewed as protein mimetics and are being pursued as protein-like materials for biotechnological applications since the architecture of a multivalent ligand is a key parameter in determining its activity<sup>125</sup>. Therefore, in the context of Multiple Sclerosis it appears important the design of multivalent ligands termed Multiple Epitope peptides (MEPs), bearing multiple copies of CSF114(Glc) minimal epitopes,

<sup>123</sup> Mammen, M.; Choi, S.K.; and Whitesides, G.M., *Angew. Chem. Int. Ed.*, **1998**, *37*, 2754 -2794.

<sup>124</sup> a) Tam, J.P. *P.N.A.S.*, **1988**, *85*, 5409-5413; b) Tam, P.J. *J. of Immunol. M*, **1996**, *1*, 17-32.

<sup>125</sup> Gestwicki, J.E.; Cairo, C.W.; Strong, L.E.; Oetjen, K.A.; and Kiessling, L.L., *J.A.C.S.*, **2002**, *124*, 14922-14933.

## PART B

i.e. Asn(Glc), to characterize the immunological responses in MS patients' sera.

### 3.2.2 Synthesis of Multiple Epitope peptides

A collection of six Lys branched structures, MEps, was designed and synthesized with spacers of different length on the dendrimeric core and different peptide sequences as epitopes surrounding the sugar moiety Asn(Glc).

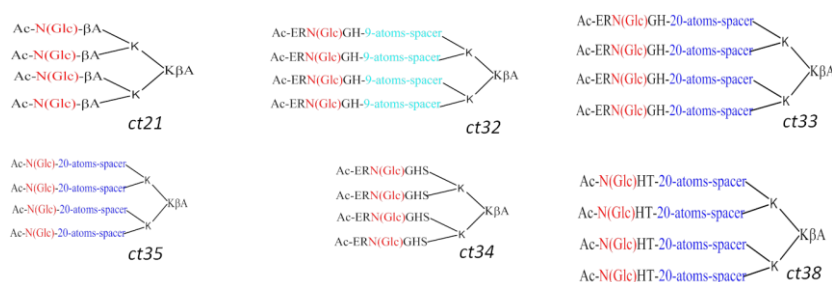
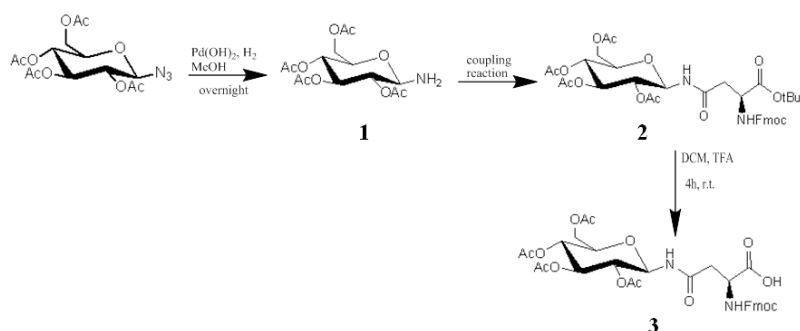


**Figure 3.7.** Collection of MEps synthesized. The 20-atoms-spacer is  $-HN-(CH_2)_3-(O-CH_2-CH_2)_3-CH_2-HN-CO-(CH_2)_2-CO-$ , the 9-atoms-spacer is  $-HN-(CH_2-CH_2-O)_2-CH_2-CO-$ .

MEps were synthesized by Fmoc/*t*Bu SPPS starting from Fmoc<sub>4</sub>-Lys<sub>2</sub>-Lys-β-Ala-Wang resin, according to the General Procedure for the SPPS described in details in the Experimental Part and using commercially available Fmoc-protected amino acids and HATU/NMM activation. The Fmoc-Asn(βGlcAc<sub>4</sub>)-OH building block was synthesized according to the method developed by Paolini *et al.*<sup>126</sup>.

<sup>126</sup> Paolini, I.; Nuti, F.; Pozo-Carrero, M.C.; Barbetti, F.; Kolesinska, B.; Kaminski, Z.J.; Chelli, M.; Papini, A.M. *Tetrahedron*, **2007**, *48*, 2901-2904.



**Scheme 1.** Synthesis of Fmoc-Asn(GlcOAc4)-OH building block according to Paolini et al.<sup>126</sup>.

We synthesized the MEps reported in *Table 3.1* based on a Lys tetrameric core bearing the different spacers,  $\beta$ -Alanine, 3,6-dioxa-octanoic acid (introducing in SPPS Fmoc-HN-(CH<sub>2</sub>-CH<sub>2</sub>-O)<sub>2</sub>-CH<sub>2</sub>-COOH, Fmoc-Ado-OH) or 1,13-diamino-4,7,10-trioxatridecan-succinamic acid (introducing in SPPS Fmoc-HN-(CH<sub>2</sub>)<sub>3</sub>-(O-CH<sub>2</sub>-CH<sub>2</sub>)<sub>3</sub>-CH<sub>2</sub>-HN-CO-(CH<sub>2</sub>)<sub>2</sub>-COOH; Fmoc-TTDS-OH), and specific peptide sequences, e.g. a N-glycosylated  $\beta$ -hairpin pentapeptide (**CT32**, **CT33**), an N-glycosylated hexapeptide (**CT34**) and an N-glycosylated consensus sequence (**CT38**), or to the simple sugar amino acid Asn(Glc) anchored to a spacer (**CT21** and **CT35**).

**Table 3.1** Sequences of the synthesized MEps

MEp	MEp sequence
<b>CT21</b>	(Ac-N(Glc)- $\beta$ A) <sub>4</sub> -K <sub>2</sub> -K- $\beta$ A
<b>CT35</b>	(Ac-N(Glc)-spacer <sub>TTDS</sub> ) <sub>4</sub> -K <sub>2</sub> -K- $\beta$ A
<b>CT32</b>	(Ac-E-R-N(Glc)-G-H-spacer <sub>Ado</sub> ) <sub>4</sub> -K <sub>2</sub> -K- $\beta$ A
<b>CT33</b>	(Ac-E-R-N(Glc)-G-H-spacer <sub>TTDS</sub> ) <sub>4</sub> -K <sub>2</sub> -K- $\beta$ A
<b>CT34</b>	(Ac-E-R-N(Glc)-G-H-S) <sub>4</sub> -K <sub>2</sub> -K- $\beta$ A
<b>CT38</b>	(Ac-N(Glc)-H-T-spacer <sub>TTDS</sub> ) <sub>4</sub> -K <sub>2</sub> -K- $\beta$ A

## PART B

Each coupling step was monitored by the Kaiser test in order to follow the synthetic process. MEps were acetylated on the <sup>a</sup>N-terminal function as described in the general procedure reported in the Experimental Part. After cleavage of the MEps from the resin and deprotection of the amino-acid side chains, deprotection of the hydroxyl functions of the sugar was performed as described in details in the Experimental Part using MeONa/MeOH. All the MEps were purified by semi-preparative RP-HPLC, and characterized by RP-HPLC ESI-MS.

Analytical data are summarized in *Table 3.2*.

**Table 3.2** Analytical data of MEps

MEPs	Rt (min) <sup>a</sup>	ESI-MS (m/z)	
		calculated	(found)
CT21	3.94 <sup>b</sup>	1017.98	1016.42 [M+2H] <sup>2+</sup>
CT35	3.96 <sup>c</sup>	1480.28	1479.35 [M+2H] <sup>2+</sup>
CT32	3.96 <sup>d</sup>	1418.12	1416.63 [M+3H] <sup>3+</sup>
CT33	4.52 <sup>e</sup>	1220.87	1219.93 [M+4H] <sup>4+</sup>
CT34	4.01 <sup>f</sup>	1339.28	1338.81 [M+3H] <sup>3+</sup>
CT38	4.01 <sup>g</sup>	1306.35	1304.38 [M+3H] <sup>3+</sup>

<sup>a</sup>Analytical RP-HPLC gradients at 0.6 mL min<sup>-1</sup> in 5 min; solvent system A: 0.1% TFA in H<sub>2</sub>O, B: 0.1% TFA in CH<sub>3</sub>CN. <sup>b</sup>02-35% B in 5 min, <sup>c</sup>07-35% B in 5 min, <sup>d</sup>05-40% B in 5 min, <sup>e</sup>07-40% B in 5 min, <sup>f</sup>03-25% B in 5 min, <sup>g</sup>10-35% B in 5 min.

### 3.3 Immunochemical assays with MEps

The antibody recognition of the six synthetic MEps synthesized was evaluated by solid-phase and competitive-ELISA on Multiple Sclerosis patients' sera. We evaluated by SP-ELISA, IgG serum antibodies to the MEps in a group of 16 MS patients positive to the original N-glycosylated type I' β-turn peptide structure CSF114(Glc) and compared to the 14 selected negative healthy blood donors. IgM and IgG responses were detected using as secondary antibody anti-human IgMs and anti-human IgGs conjugated to alkaline phosphatase

(AP). In particular, SP-ELISA absorbance values for patients and blood donors measured for the collection of MEps (data not shown) let us to select **CT35** as the most valuable tool. This result underlines the importance of the presence of Asn(Glc) as minimal epitope recognized by autoantibodies, suggesting that the surrounding amino acids, e.g. the N-glycosylated  $\beta$ -hairpin hexapeptide of CSF114(Glc) in **CT34**, the N-glycosylated  $\beta$ -hairpin pentapeptide of CSF114(Glc) in **CT32** and **CT33**, and the N-glycosylation consensus sequence (sequon) in **CT38** play a minor role. Moreover, the spacer seems to play a role in modulating the antigen-antibody interaction. In fact, in **CT35** we introduced the 1,13-diamino-4,7,10-trioxatridecan-succinamic acid as a spacer between the tetrameric Lys core and the Asn(Glc) whereas in its analogue **CT21** a  $\beta$ -alanine was employed as a spacer. This behavior could be associated to the higher flexibility of the 20 atoms spacer, compared to  $\beta$ -Ala, that could facilitate the antigen-antibody interaction.

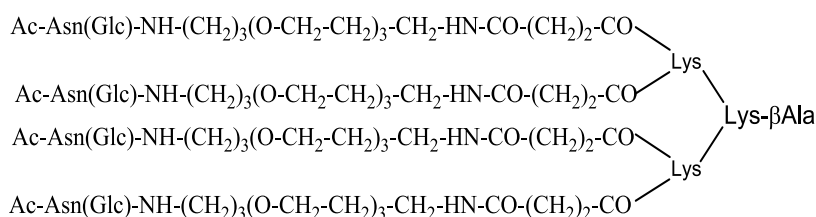


**Figure 3.8** Branched structure of **CT35**.

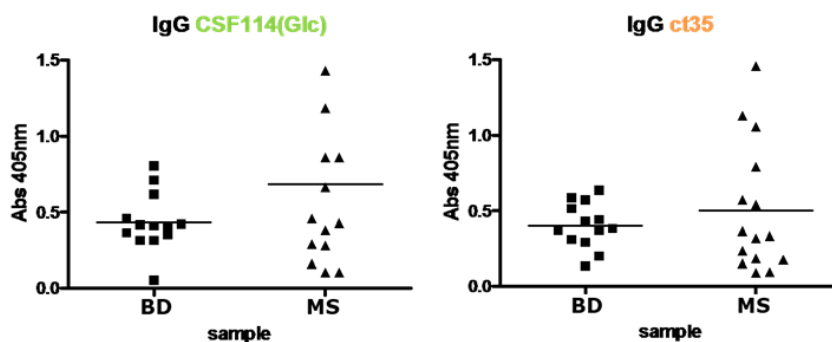


**Figure 3.9.** Dispersion diagrams obtained from data collected in SP-ELISA experiments for **CT35** in comparison with **CSF114(Glc)** for MS patients (MS) and normal blood donors (BD) at 1:100 serum dilution. Horizontal lines indicate the medium values.

## PART B

Data reported in *Figure 3.9* indicate that **CT35** is able to bind IgG autoantibodies in MS patients' sera even if the N-glycosylated peptide **CSF114(Glc)** shows the highest ability to detect disease-specific autoantibodies in the MS patients' sera tested.

Competitive ELISA was used to analyze the anti **CSF 114(Glc)** autoantibody binding affinities in solution with the newly designed MEp, **CT35**. Data shown in *Figure 3.10* indicate that **CT35** shows partial inhibition of anti-CSF114(Glc) IgGs in a significant reference MS patient's serum positive to **CSF114(Glc)**.

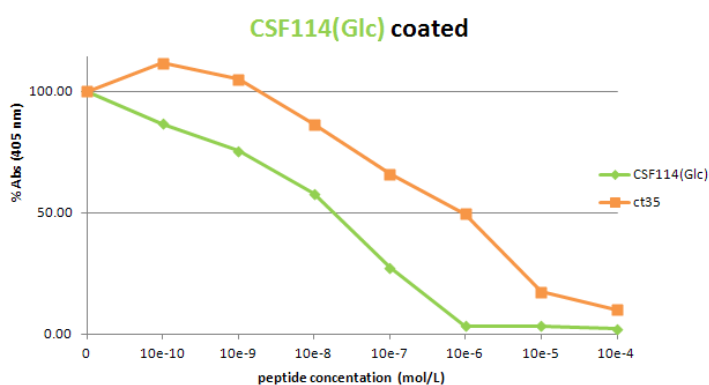


*Figure 3.10* Inhibition curves of anti-CSF114(Glc) antibodies with MEp **CT35** compared with **CSF 114(Glc)** in a competitive ELISA. The results are expressed as the percentage of inhibition of a representative MS serum (ordinate axis).

From the inhibition curves we calculated the **half maximal inhibitory concentration (IC<sub>50</sub>)** as a measure of the effectiveness of the peptide in inhibiting biological or biochemical function<sup>127</sup>.

$$IC_{50} \text{ CT35} = 8,88 \mu\text{M}.$$

$$IC_{50} \text{ CSF114(Glc)} = 0.371 \mu\text{M}.$$

<sup>127</sup> In competition binding assays, IC<sub>50</sub> is the concentration of competing antigen in fluid phase which displaces 50% of the specific binding of the antigen coated in the ELISA plate.

**CT35** shows similar, but lower, affinity to autoantibodies present in Multiple Sclerosis patients' sera compared to **CSF114(Glc)**, confirming previous findings indicating the usefulness of the synthetic peptide probe **CSF114(Glc)** to detect antibodies as biomarkers of MS.

### **3.3.1 Results and discussion**

In conclusion, this study reports for the first time that MEps, e.g. synthetic multivalent ligands, can be efficient antigenic probes to detect autoantibodies in MS. Moreover, we confirmed the importance of the N-glycosylated Asn residue as fundamental minimal epitope necessary to detect the specific antibody recognition.

### **3.4 Type I' beta turn CSF114(Glc) cyclic analogues**

Cyclic peptides have been used in medicine as active ingredients of natural extracts for thousands of years. In modern medicine, their application was rediscovered in the middle of the last century, when the cyclic decapeptide antibiotic *Gramicidin S* was isolated together with linear gramicidins from the bacterium *Bacillus brevis*. Cyclic peptides have recently acquired the status of being referred to as privileged because of their ability to bind to multiple classes of biological targets with high affinity. This led, in the past few years, to the production of combinatorial libraries of natural and synthetic cyclic peptides. Cyclic peptides, compared to linear peptides, have been considered to have greater potential as therapeutic agents due to their increased chemical and enzymatic stability, receptor selectivity, and improved pharmacodynamic properties. They have been used as synthetic immunogens, transmembrane ion channels, antigens for Herpes Simplex Virus, potential immunotherapeutic vaccines for diabetes and EAE, inhibitors against alpha-amylase and as protein stabilizers<sup>128</sup>.

---

<sup>128</sup> Katsara, M.; Tselios, T.; Deraos, S.; Deraos, G.; Matsoukas, M.T.; Lazoura, E.; Matsoukas, J.; Apostolopoulos, V.; *CurrMed Chem.*, **2006**,13(19), 2221-32.

## PART B

Cyclisation is a key step in small cyclic peptide synthesis. There are different ways to cyclise peptides, not only head-to-tail, but also side-chain-to-head, side-chain-to-tail and side-chain-to-side-chain bridges have been described. Moreover, in order to obtain cyclic peptides, sophisticated synthetic strategies have been developed. There are numerous possibilities for chemical alterations of a cyclic precursor molecule, such as insertion of a Cys residues, or modified non proteinogenic aminoacids, such as 2,3 diaminopropionic acid, amino acids bearing alkynyl or azido moieties.

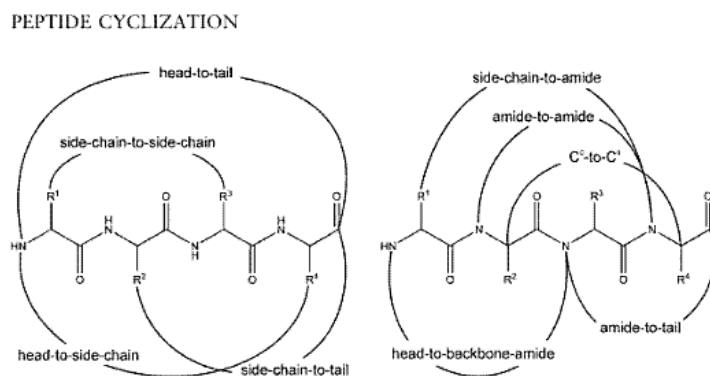


**Figure 3.11.** Different modes of cyclization for peptides<sup>129</sup>.

In light of the importance of specific sugars and conformation of epitopes involved in auto-Ab recognition in MS, we designed a synthetic cyclopeptide reproducing the antibody specific target-epitope recognized in **CSF114(Glc)**, i.e. Asn<sup>7</sup>(Glc), and the surrounding amino acids of the type I'  $\beta$ -turn and studied its capacity to recognize autoAbs in MS by ELISA. In particular, disulfide bridged containing cyclopeptides reported in *Table 3.3* were synthesized.

<sup>129</sup> Jensen, K., *Peptides and protein design for Biopharmaceutical Applications*. J.Wiley Ed., **2009**.

**Table 3.3 Glycosylated and unglycosylated cyclic peptides**

Peptide	Sequence
<b>MDP-I</b>	Ac-c[Cys-Arg-Asn-Gly-His-Cys]-NH <sub>2</sub>
<b>MDP-II</b>	Ac-c[Cys-Arg-Asn(Glc)-Gly-His-Cys]-NH <sub>2</sub>

For immunochemical application purposes, both the glucosylated cyclopeptide and the unglycosylated one as control, were synthesized.

Intra- and inter-molecular multiple disulfide bonds with the correct Cys connectivities can be generated either by simple oxidative refolding after removal of a single-type thiol protecting group from synthetic precursors or by regioselective methods based on orthogonal thiol protection schemes<sup>130,131</sup>. For the synthesis of the cyclised peptide we employed as oxidizing agent the 2,2'-dithiodipyridine (DTDP), a specific lipophilic oxidizer of thiol groups suitable even to be used with unprotected glycopeptides<sup>132</sup>.

#### **3.4.1 Synthesis of MDP-I: Ac-c[Cys-Arg-Asn-Gly-His-Cys]-NH<sub>2</sub>**

Linear precursor of **MDP-I** was synthesized by Fmoc/*t*Bu SPPS using a manual peptide synthesizer, *PLS ChemTech* starting from Fmoc *Rink-Amide* MBHA resin (Iris Biotech GmbH), according to the General Procedure for the SPPS described in details in the Experimental Part and using commercially available Fmoc-protected amino-acids and HBTU/NMM activation.

**Table 3.4 Linear unglycosylated peptide sequence**

Peptide	Sequence
<b>Lin-MDP-I</b>	Ac-Cys-Arg-Asn-Gly-His-Cys-NH <sub>2</sub>

<sup>130</sup> Andreu, D.; Albericio, F.; Solé, N.A.; Munson, M.C.; Ferrer, M.; and Barany, G., *Introd. Meth. Mol.Biol.*, **1994**, 35, 91-169

<sup>131</sup> Boulègue, C.; Musiol, H.; M.; Prasad, V.; Mododer, L., *Chemistry Today*, **2006**, 24(4), 24-36

<sup>132</sup> Hoffmann, R.; Otvos L.Jr., *Lett. Pept. Sci.*, **1996**, 3, 371-377.

PART B

Each coupling step was monitored by Kaiser test in order to optimize the synthetic process. Peptide was acetylated on the <sup>a</sup>N-terminal function as described in the general procedure reported in the Experimental Part. After cleavage of the linear peptide from the resin and concomitant deprotection of amino-acid side chains, crude product was characterized by RP-HPLC and MALDI-TOF.

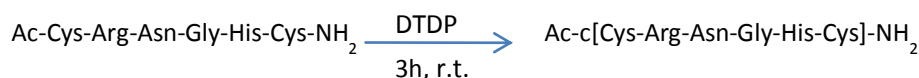
Analytical data are reported in *Table 3.5*.

**Table 3.5** Analytical data of linear peptide MDP-I

Peptide	HPLC (R <sub>t</sub> ,min) <sup>a</sup>	MALDI-TOF-MS [M+H] <sup>+</sup> Calc (found)
Lin_MDP-I	13.2	730.29 (730.44)

<sup>a</sup>Analytical HPLC gradient at 1 mL min<sup>-1</sup>, 03-15% B in 30 min, solvent system A: 0.1% TFA in H<sub>2</sub>O, B: 0.1% TFA in CH<sub>3</sub>CN.

Crude lyophilized product was solved in 0.1% of TFA in MilliQ water (1mL/mg) and then a solution of DTDP 1,2mg/mL in 0.1% of TFA in MilliQ water was added. The solution was vigorously stirred at r.t. and the formation of the intramolecular disulfide bridge was monitored by RP-HPLC. After 3 hours the reaction was quenched.



*Scheme 2.* Cyclization reaction of **MDP-I** mediated by **DTDP**.

The lyophilized cyclised peptide was then purified by semi-preparative RP-HPLC and characterized by RP-HPLC and MALDI-TOF.

Analytical data are reported in *Table 3.6*.

**Table 3.6** Analytical data of cyclic peptide MDP I

Peptide	HPLC (R <sub>t</sub> ,min) <sup>a</sup>	MALDI-TOF-MS [M+H] <sup>+</sup> Calc (found)
MDP-I	14.9	728.29 (728.18)

<sup>a</sup>Analytical HPLC gradients at 1 mL min<sup>-1</sup>, 03-15% B in 30 min, solvent system A: 0.1% TFA in H<sub>2</sub>O, B: 0.1% TFA in CH<sub>3</sub>CN.

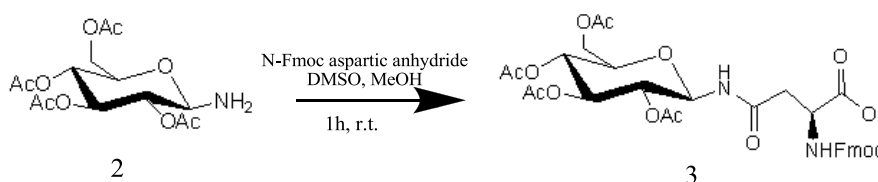
### 3.4.2 Synthesis of MDP-II: Ac-c[Cys-Arg-Asn(Glc)-Gly-His-Cys]-NH<sub>2</sub>

Linear precursor of MDP-II was synthesized by Fmoc/*t*Bu SPPS using a manual peptide synthesizer, *PLS ChemTech* starting from Fmoc Rink-Amide MBHA resin (Iris Biotech GmbH) according to the General Procedure for the SPPS described in details in the Experimental Part and using commercially available Fmoc-protected amino acids and HBTU/NMM activation.

**Table 3.7. Linear glycosylated peptide sequence of Lin MDP-II.**

Peptide	Sequence
Lin MDP-II	Ac-Cys-Arg-Asn(Glc)-Gly-His-Cys-NH <sub>2</sub>

The Fmoc-Asn( $\beta$ GlcAc<sub>4</sub>)-OH building block was prepared according to the method developed by Ibatullin *et al.*<sup>133</sup> as described in details in the experimental part and introduced during the stepwise synthesis using HATU/NMM activation.



**Scheme 3.** Synthesis of Fmoc-Asn(GlcOAc<sub>4</sub>)-OH building block according to Ibatullin *et al.*<sup>133</sup>.

Each coupling step was monitored by the Kaiser test in order to optimize the synthetic process. The peptide was acetylated on the <sup>o</sup>N-terminal function as described in the general procedure reported in the Experimental Part. Deprotection of the acetyl groups on the sugar moiety was carried with the peptide still anchored to the resin using a solution of N<sub>2</sub>H<sub>4</sub> in MeOH (4:1) as described in details in the Experimental Part. After cleavage of the linear

<sup>133</sup> Ibatullin, F.M.; Selivanov, S.I., *Tetrahedron Lett.*, **2009**, *50*, 6351–6354.

## PART B

peptide from the resin and concomitant deprotection of amino-acid side chains, the crude product was characterized by RP-HPLC ESI-MS.

Analytical data are reported in *Table 3.8*.

**Table 3.8. Analytical data of the linear peptide Lin MDP-II.**

Peptide	HPLC ( $R_t$ ,min) <sup>a</sup>	ESI-MS [M+H] <sup>+</sup> Calc (found)
<b>Lin MDP-II</b>	2.37	892.67 (892.72)

<sup>a</sup>Analytical HPLC gradients at 0.6 mL min<sup>-1</sup>, 03-15% B in 5 min, solvent system A: 0.1% TFA in H<sub>2</sub>O, B: 0.1% TFA in CH<sub>3</sub>CN.

Crude lyophilized product was solved in 0.1% of TFA in MilliQ water (1mL/mg) and then a solution of DTDP 1,2mg/mL in 0.1% of TFA in MilliQ water was added. The solution was vigorously stirred at r.t. and the formation of intramolecular disulfide bridge was monitored by RP-HPLC. After 3 hours the reaction was quenched.



**Scheme 4. Cyclization reaction of MDP-II mediated by DTDP.**

The lyophilized cyclized peptide was then purified by semi-preparative RP HPLC and characterized by RP-HPLC ESI-MS.

Analytical data are reported in *Table 3.9*.

**Table 3.9. Analytical data of the cyclic peptide MDP-II.**

Peptide	HPLC ( $R_t$ ,min) <sup>a</sup>	ESI-MS [M+H] <sup>+</sup> Calc (found)
<b>MDP-II</b>	3.16	890.67 (890.72)

<sup>a</sup>Analytical HPLC gradients at 0.6 mL min<sup>-1</sup>, 03-25% B in 5 min, solvent system A: 0.1% TFA in H<sub>2</sub>O, B: 0.1% TFA in CH<sub>3</sub>CN.

### 3.5 Immunochemical assays with cyclic glycopeptides

The antibody recognition using the type I'  $\beta$ -turnCSF114(Glc) cyclic glycopeptide analogue **MDP-II** and the unglycosylated one **MDP-I**, as

control, was evaluated by solid phase and competitive-ELISA on Multiple Sclerosis patients' sera.

We evaluated, by SP-ELISA, IgG serum antibodies to the cyclic glycopeptide **MDP-II** and the unglycosylated analogue **MDP-I** in a group of MS patients and compared the results with Normal Blood Donors' sera (NBDs). IgM (data not shown) and IgG responses were detected using as secondary antibodies anti-human IgMs and anti-human IgGs conjugated to alkaline phosphatase.

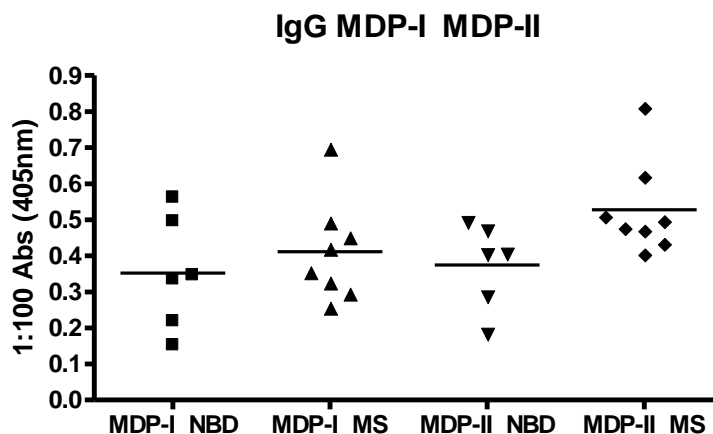


*Figure 3.12. Antibody titre in MS patients to the cyclopeptides **MDP-I** and **MDP-II**.*

The glycopeptide **MDP-II** displays higher antibody recognition if compared to the unglycosylated **MDP-I** indicating the importance of the  $\beta$ -D-glucopyranosyl moiety linked to the Asn residue and confirming the result found for MEps.

Competitive ELISA was used to analyze the anti-CSF 114(Glc) autoantibody binding affinities of the newly synthesized peptides. Data represented in *Figure 3.13* indicate that the glycosylated peptide shows partial inhibition of anti-CSF114(Glc) IgGs in a significant reference MS patient's serum, while the unglycosylated control shows no inhibition activity.

## PART B

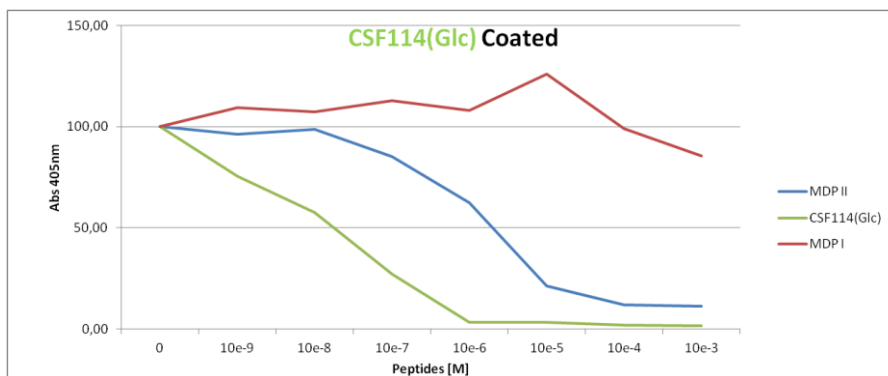


**Figure 3.13.** Inhibition curves of anti-CSF114(Glc) antibodies with peptides **MDP-I** and **MDP-II** compared with **CSF 114(Glc)** in a competitive ELISA. The results are expressed as the percentage of inhibition of a representative MS serum (ordinate axis).

From the inhibition curves we calculated the  $IC_{50}$  as a measure of the effectiveness of the peptide in inhibiting biological or biochemical function<sup>134</sup>.

$$IC_{50} \text{ MDP-II} = 3,39 \mu\text{M}$$

$$IC_{50} \text{ CSF114(Glc)} = 0.371 \mu\text{M}$$

### 3.5.1 Results and discussion

In conclusion, the cyclic glycopeptide containing the Asn(Glc) residue, i.e. **MDP-II**, shows similar, but lower, affinity to autoantibodies present in Multiple Sclerosis patients' sera, confirming previous finding indicating the usefulness of the synthetic peptide probe **CSF114(Glc)** to detect autoantibodies as biomarker of MS.

### 3.6 Side chain to side chain cyclic peptides by Glaser-coupling

In 1869, Carl Glaser observed the historic acetylenic coupling of Copper(I) phenylacetylide to diphenyldiacetylene under smooth aerobic conditions<sup>135</sup>.

<sup>134</sup>  $IC_{50}$  is the concentration of competing antigen in fluid phase which displaces 50% of the specific binding of the antigen coated in the ELISA plate.

<sup>135</sup> a) Glaser, C., *Ber.Dtsc h.Chem. Ges.* **1869**, 2, 422; b) Glaser, C., *Ann.Chem. Pharm.* **1870**, 154, 137.

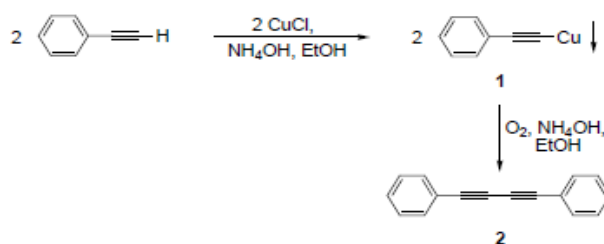


**Figure 3.14.** The first acetylenic coupling described by Glaser.

The classical Glaser type coupling is an oxidative acetylenic coupling reaction that takes place in mild conditions. Because of the high functional group tolerance of homocoupling, the Glaser reaction has been used as a key step in the modification of complex molecules as well as for the synthesis of diacetylenic macrocycles, valuable highly conjugated molecules for electronic or photonic devices. Eglinton and Galbraith improved the procedure of Glaser coupling under homogeneous conditions using a stoichiometric amount of Copper(II) acetate in pyridine<sup>136</sup>. N,N,N',N'-tetramethylethylenediamine (TMEDA) was used as the co-complexing agent in Hay's procedure for the Copper(I)-catalyzed homocoupling of terminal alkynes in the presence of oxygen as an oxidant with pyridine as a solvent<sup>137</sup>. Other methods for the synthesis of 1,4-disubstituted 1,3-diynes include the Cadiot-Chodkiewicz and the Sonogashira couplings<sup>138</sup>. More recently, it has been shown that the oxidative homocoupling of terminal alkynes can be accomplished by a combination of a Pd catalyst and a Cu(I) salt<sup>139</sup>. Oxidative alkyne-alkyne coupling is a good candidate for the synthesis of 1,3-diyne derivatives. 1,3-Diyne derivatives are very important materials in biological, polymer, and

<sup>136</sup> Eglinton, G.; Galbraith, A. R. *Chem. Ind. (London)* **1956**, 737.

<sup>137</sup> a) A. S. Hay, *J. Org. Chem.* **1960**, *25*, 1275; b) A. S. Hay, *J. Org. Chem.* **1962**, *27*, 3320.

<sup>138</sup> a) Cadiot, P.; Chodkiewicz, W. In *Chemistry of Acetylenes*; Viehe, H. G., Ed.; Marcel Dekker: New York, 1969; p 597; b) Sonogashira, K.; Tohda, Y.; Hagihara, N. *Tetrahedron Lett.* **1975**, *16*, 4467.

<sup>139</sup> Rossi, R.; Carpita, A.; Bigelli, C. *Tetrahedron Lett.* **1985**, *26*, 523.

## PART B

materials science because they can be converted into various structural entities, especially substituted heterocyclic compounds<sup>140</sup>.

### *Mechanistic investigations of the oxidative coupling*

The classical oxidative alkyne couplings have been the most extensively studied, among the alkyne couplings, yet their exact mechanism remains unknown, and the existence of several hypotheses regarding the oxidation state and structure of the postulated intermediary copper acetylides have generated considerable discussion.

The earliest mechanistic proposals postulated the formation of acetylenic radicals, which would then recombine to afford the corresponding diynes. An early kinetic investigation by Klesansky *et al.*<sup>141</sup> demonstrated that Copper(II) ions served as direct oxidizing agent. They also noted that the rate of coupling was faster in basic media for more acidic terminal alkynes. In light of these findings, the homolytic bond cleavage proposed earlier by Zalkind and Fundyler<sup>142</sup> was discarded in favor of a heterolytic cleavage followed by the transfer of a single electron to the Copper(II) salt.

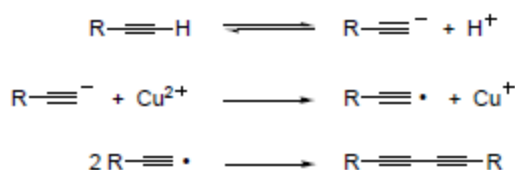


**Figure 3.15** Early proposal for the mechanism of oxidative acetylenic coupling

Clifford and Waters in 1963 proposed the formation of Copper(I) acetylides, using  $\text{Cu}(\text{OAc})_2$  in pyridine in absence of  $\text{O}_2$ , which were rapidly oxidized by the transfer of a single electron to Copper(II) through an acetate ligand bridge.

<sup>140</sup> a) F. Bohlmann, T. Burkhardt, C. Zdero, *Naturally Occurring Acetylenes*, Academic Press, London, 1973; b) L. Hansen, P. M. Boll, *Phytochem.*, **1986**, 25, 285; c) H. Matsunaga, M. Katano, H. Yamamoto, H. Fujito, M. Mori, K. Takata, *Chem. Pharm. Bull.* **1990**, 38, 3480.

<sup>141</sup> Klesansky, A.L.; Grachev, I.V.; Kuznetsova, J., *J Gen Chem USSR*, **1957**, 27, 3008-3013

<sup>142</sup> Zalkind, Y.S.; Fundyler, B.M., *J. Gen Chem USSR*, **1939**, 9, 1725-1728.

Decomposition of the resultant Copper(II) acetylide and recombination of the free radicals would give the coupled products.

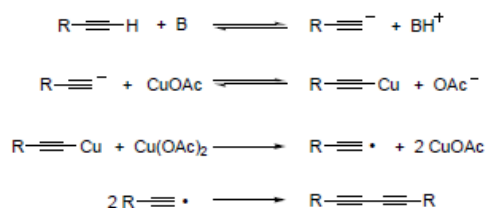


**Figure 3.16.** Mechanism proposed by Clifford and Waters, (pyridine molecules are omitted).

On the basis of the observed second-order dependence of the coupling rate on alkyne concentration, Bohlman *et al.* proposed in 1964<sup>143</sup> a mechanism in which a dinuclear Cu(II) acetylide complex is involved. This intermediate is supposed to collapse directly to the coupled product. The low experimentally determined activation energy of 21 kcalmol<sup>-1</sup> provides an argument against radical mechanism in favor of the simultaneous oxidation and the C-C bond formation formerly proposed by Bohlmann<sup>144</sup>.

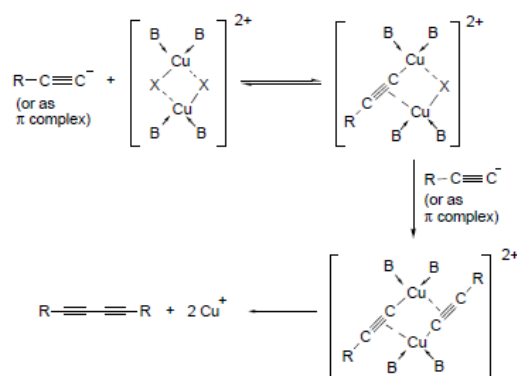


**Figure 3.17.** Mechanism proposed by Bohlmann. Dimeric copper acetylides are proposed as intermediates in the oxidative acetylenic coupling. *B* in as *N* ligand, *X* is a *Cl* or a *OAc*.

<sup>143</sup> Bohlmann, F.; Schoenowsky, H.; Inhoffen, E.; Grau, G. *Chemische Berichte*, **1964**, *97*, 794.

<sup>144</sup> Siemsen, P.; Livingstone, R.C.; Diederich, F., *Angew Chem Int. Ed.*, **2000**, *39*, 2632-2657.

## PART B

More recently a detailed mechanism of the Glaser reaction based on DFT has been proposed. The mechanism involves Cu(I)/Cu(III)/Cu(II)/Cu(I) catalytic cycle for this transformation. The key step for this reaction is the dioxygen activation occurring on the complexation of two molecules of acetylides with molecular oxygen giving Cu(III) complex<sup>145</sup>.

We can resume the most important experimental observations: (1) the presence of amines is indispensable for the reaction to occur; (2) copper acetylides produce diacetylenes when oxidized by molecular oxygen; (3) the reaction often takes place at room temperature that implies low activation energies for each step of condensation.

It can be concluded that the mechanism proposed in 1964 by Bohlmann *et al.* still provides the most reasonable and most accepted picture.

### *Naturally Occurring Diynes*

The copper-mediated acetylenic coupling is a venerable reaction that has found applications in numerous research fields spanning from total synthesis of polyene natural products<sup>146</sup>. Over the past fifty years, hundreds of di and polyene compounds have been isolated from nature. Cu-catalyzed, oxidative acetylenic homo- and hetero-coupling reactions are a very useful tool to assemble the polyene framework. Naturally occurring polyenes feature a wide range of structural diversity and display an equally broad array of biological properties<sup>147</sup>.

---

<sup>145</sup> Fomina, L.; Vazquez, B.; Tkatchouk, E.; Fomine, S., *Tetrahedron*, **2002**, *58*, 6741–6747.

<sup>146</sup> Evano, G.; Blanchard, N.; Toumi, M., *Chem. Rev.* **2008**, *108*, 3054–3131.

<sup>147</sup> a) *Angew Chem Int Ed. Engl* **2006**, *45*(7), 1034-57; b) *Nature Chemistry* **2010**;2:967–971 2; c) *Comptes Rendus Chimie* **2009**, *12*(3-4), 341–358; d) *Lipids* **2006**;41(10):883-924.

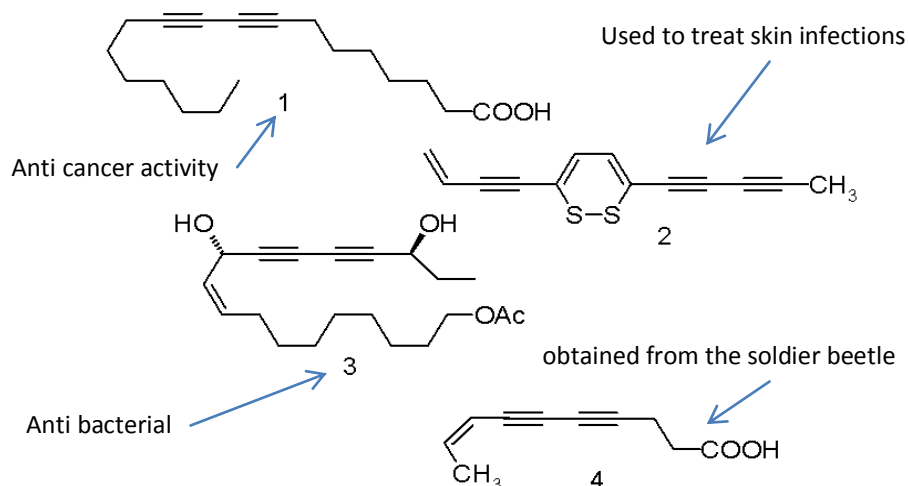


**Figure 3.18.** Examples of naturally occurring diynes.

### 3.6.1 On resin Glaser cyclization of peptides

Copper(II) salt catalyzed oxidative coupling has proved to be of great value since its discovery, but it has gained importance only in recent years. Copper(II) acetate catalyzed homo- and hetero-couplings of terminal alkynes take place under mild reaction conditions<sup>148</sup>. The outcome of the oxidative coupling critically depends on the proper choice of the base and ligand as well as reaction conditions<sup>149</sup>.

Developing a methodology for the oxidative coupling of alkynes, using inexpensive Copper(II) salts in the presence of a base with no further additives such as co-catalysts and co-oxidants, or oxygen atmosphere at room temperature, is highly desirable. This is true in particular in the case of coupling reactions performed in solution for which numerous examples of symmetrical and unsymmetrical 1,3 diynes are obtained in quantitative yields using Cu(OAc)<sub>2</sub> under aerobic conditions. Different yields are obtained performing the reaction on resin. In fact, the presence of more sterically

<sup>148</sup> Balaraman, K.; Kesavan, V., *Synthesis*, **2010**, 20, 3461-3466.

<sup>149</sup> Adimurthy, S.; Malakar, C.C.; Beifuss, U., *J.O.C.*, **2009**, 74(15), 5648-5651.

## PART B

hindered alkynyl moieties and the possible formation of intermolecular 1,3 diyne derivatives might dramatically reduce yields. Despite these possible limitations, solid-phase oxidative coupling of terminal alkynes has potential to generate numerous molecules of diverse functionalities relying on solid-phase combinatorial chemistry to generate new libraries of compounds for biological testing. The choice to perform the reaction with the peptide still attached to the resin in a more constrained environment deals with the larger applications of such an optimized method. In fact, in this approach it is possible, after the formation of the cycle, to perform the synthetic process and to avoid further steps after the cleavage of the peptide from the resin.

We developed an optimized on-resin Glaser-type reaction between the side chains of two propargyl glycine residues inserted at the beginning and at the end of the peptide sequence of two peptides Fmoc-Pra-Arg(Pbf)-Asn(Trt)-Gly-His(Trt)-Pra-*RinkAmidePSResin*, and between the side chains of two N-propargyl glycine residues in Fmoc-NPra-Arg(Pbf)-Asn(Trt)-Gly-His(Trt)-NPra-*RinkAmidePSResin* to obtain the final products **MDP-III** and **MDP-IV**. The homocoupling of terminal alkynes of the propargyl moiety to 1,3-diyne gave the cyclized compound. The cyclization reaction was performed in the presence of the Fmoc protecting group of the <sup>α</sup>N-terminal function. Our initial studies focused on the development of an optimum set of reaction conditions for the coupling of the two propargyl moieties on the Pra and NPra side chains.

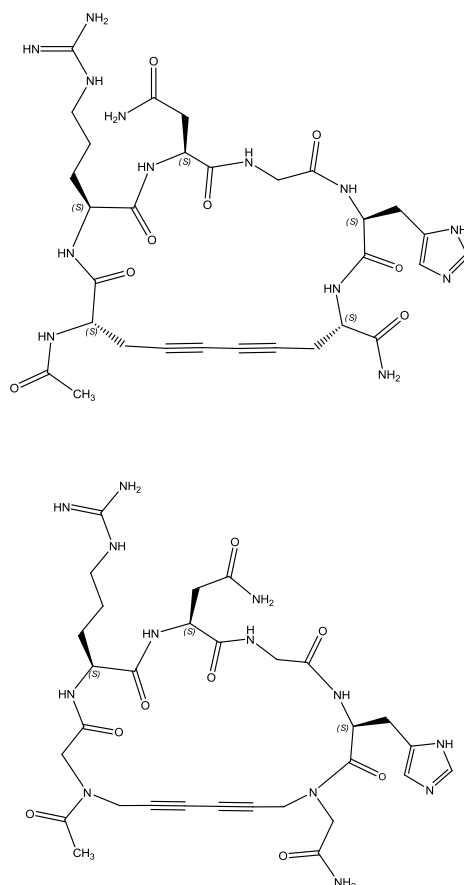


Figure 3.19. Cyclic peptides *MDP-III* and *MDP-IV*.

### 3.6.2 Optimization of the Glaser-type reaction to synthesize *Ac-c[Pra-Arg-Asn-Gly-His-Pra]-NH<sub>2</sub>*

We performed a systematic study to optimize the on-resin oxidative coupling of the propargyl moieties synthesizing a 1,3 diyne bond to give a side-chain to side-chain cyclic peptide Fmoc-c[Pra-Arg-Asn-Gly-His-Pra]-RinkAmidePSResin.



Scheme 5. On resin peptide cyclization by copper catalyzed 1,3 diyne bond formation of *MDP-III*.

## PART B

The first reaction was performed at room temperature using  $\text{Cu}(\text{OAc})_2$  as Copper complex in DCM and MeOH as solvent, and  $\text{CH}_3\text{CN}$  as a source of nitrogen atoms that are thought to be involved in the formation of the intermediate complex according to the mechanism proposed by Bohlmann. DCM was chosen because is a suitable solvent in which the polystyrene resin can be swollen. MeOH was used to solve the copper acetate.

Before adding the copper complex, the resin was swollen for 2 hours in DCM in order to facilitate the intramolecular reaction rather than the intermolecular one. RP-HPLC monitoring gave a 40:60 cyclic to linear ratio after 16h (entry 4, *Table3.10*). In order to improve the cyclization yield we decided to switch to a microwave assisted cyclization.

Today microwaves are commonly applied in several areas of the synthetic chemistry from MW-assisted SPPS to organic synthesis<sup>150</sup>. The use of microwaves irradiation allowed us not only to shorten the reaction times of several hours, from 16 h to 1h or 1h and 30' (entry 5-11, *Table3.10*), but also to obtain higher yields of cyclization. This is reported even in the case of other syntheses of carbocyclic peptides, i.e. the microwave assisted ring closing metathesis<sup>151</sup>. On the contrary, irradiation of microwave energy allows to a larger number of side reactions to overcome the activation energy barrier so that the result is a crude product with more impurities.

In the optimization process, several reaction conditions were applied. In particular, the solvent DCM was replaced with  $\text{CHCl}_3$  because the latter has an increased performance in transferring the microwave energy and has a higher boiling point than DCM. Attempts to perform the microwave-assisted Hay

---

<sup>150</sup> a) Lidstrom, P.; Tierney, J.; Wathey, B.; Wetsman, J., *Tetrahedron*, **2001**, 57, 9225; b) Kappe, C.O., *Angew. Chem. Int Ed.*, **2004**, 43, 6250.

<sup>151</sup> a) Robinson, A.; Elaridi, J.; Van Lierop, B.J.; Mujcinovic, S.; and Jackson, W.R., *J. Pept. Sci.*, **2007**, 13, 280–285; b) D'Addona, D.; Carotenuto, A.; Novellino, E.; Piccand, V.; Reubi, J.C.; Di Cianni, A.; Gori, F.; Papini, A.M.; and Ginanneschi, M., *J. Med. Chem.*, **2008**, 51(3), 512-520.

coupling and Eglington coupling using NMP and DMF as solvents, led to reagents degradation (entry 1-3, *Table3.10*), possibly because of radical reactions.

The Copper(II) complex was used in stoichiometric rather than catalytic amounts, 5 and 10 excess equivalents. Such high excess is typical of on resin synthetic strategies, i.e. SPPS. Best results were observed with the conditions reported in entry 11 of *Table3.10* (see 95:5 cyclic/linear ratio yield in the case of the small scale, e.g. the reaction performed on 20mg resin in two steps, 30'+1h, to induce a double activation of the reaction system.

**Table3.10 Comparison of the different reaction conditions**

Entry	Catalyst	Eq.	Temp. (max) °C	Time	Solvents	MW (W)	Cooling	Av. Power (W)	Cyc./Lin.
1	Cu(OAc) <sub>2</sub> ·H <sub>2</sub> O	5	100	1h	10%Py in DMF	200	yes	50	–
2	Cu(OAc) <sub>2</sub> ·H <sub>2</sub> O	5	100	1h	10%Py in NMP	200	yes	30	–
3	CuCl	5	100	30min	DMF + 10eq TMEDA	200	yes	30	–
4	Cu(OAc) <sub>2</sub> ·H <sub>2</sub> O	5	R.T	16h	DCM/MeOH(3%) / CH <sub>3</sub> CN(5%)	–	–	–	40:60
5	Cu(OAc) <sub>2</sub> ·H <sub>2</sub> O	5	70	1h	DCM/MeOH(3%) / CH <sub>3</sub> CN(5%)	25	no	15	70:30
6	Cu(OAc) <sub>2</sub> ·H <sub>2</sub> O	5	70	1h	DCM / CH <sub>3</sub> CN (20%)	200	no	25	70 :30
7	Cu(OAc) <sub>2</sub> ·H <sub>2</sub> O	5	70	1h	CHCl <sub>3</sub> / CH <sub>3</sub> CN (20%)	200	no	8	75:25
8	Cu(OAc) <sub>2</sub> ·H <sub>2</sub> O	10	70	1h	CHCl <sub>3</sub> / CH <sub>3</sub> CN (20%)	200	no	8	85:15
9	Cu(OAc) <sub>2</sub> ·H <sub>2</sub> O	5	70	1h	CHCl <sub>3</sub> / CH <sub>3</sub> CN (20%)	150	yes	110	90 :10
10	Cu(OAc) <sub>2</sub> ·H <sub>2</sub> O	10	70	1h	CHCl <sub>3</sub> / CH <sub>3</sub> CN (20%)	150	yes	110	60:40
11	Cu(OAc) <sub>2</sub> ·H <sub>2</sub> O	5	70	30min+ 1h	CHCl <sub>3</sub> / CH <sub>3</sub> CN (20%)	150	yes	110	95 :5

Formation of the 1,3 diyne bond leading to the the cyclic hexapeptide on resin was performed in absence of a base. We can hypothesize that this was possible

PART B

because of proton withdrawing by  $\text{AcO}^-$  of  $\text{Cu}(\text{OAc})_2 \cdot \text{H}_2\text{O}$ , since the bases are absolutely necessary in the process of coupling of terminal alkynes. The oxidative coupling cannot occur using weak basic copper salt catalysts such as  $\text{CuBr}$ ,  $\text{CuCl}$ , or  $\text{CuI}$  in the absence of bases or additives, such as DMSO. Very recently Niu et al. proposed a mechanism in which  $\text{AcO}^-$  of  $\text{Cu}(\text{OAc})_2 \cdot \text{H}_2\text{O}$  catalyst may take the role of the base<sup>152</sup>. According to this hypothesis, the alkynyl copper intermediate A is formed by the reaction of the terminal alkyne and  $\text{Cu}(\text{OAc})_2$ , and then it undergoes smooth oxidative dimerization with air to the  $\text{sp-sp}$  homocoupling product and water.  $\text{Cu}(\text{OAc})_2$  is then recycled.

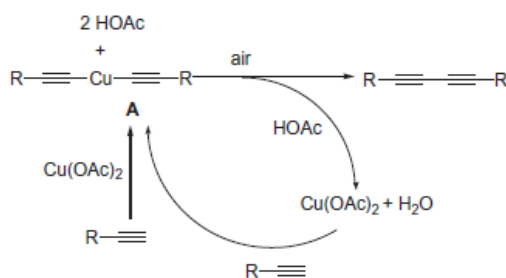


Figure 3.20 Mechanism proposed by Niu.

The optimized conditions were used to perform the synthesis of peptide **MDP-III**.

Table 3.11 Sequence of cyclic peptide **MDP-III**

Peptide	Sequence
<b>MDP-III</b>	Ac-c[Pra-Arg-Asn-Gly-His-Pra]-NH <sub>2</sub>

The inear precursor of **MDP-III**, Fmoc-Pra-Arg-Asn-Gly-His-Pra-*Rink-AmideResin* was synthesized by Fmoc/*t*Bu SPPS using a manual peptide synthesizer, *PLS ChemTech* starting from Fmoc *Rink-Amide*MBHA resin (Iris Biotech GmbH), according to the general procedure for the SPPS described in details in the Experimental Part and using the commercially

<sup>152</sup> Niu, X.; Li, C.; Li, J.; Jia, X., *Tetrahedron Lett*, **2012**, 53, 5559–5561.

available Fmoc-protected amino acids and HBTU/NMM activation. Side-chain to side-chain cyclization was achieved performing the 1,3 diyne bond formation according the reaction conditions reported in *Table 3.12*.

**Table 3.12 Large Scale cyclization peptide MDP-III**

Catalyst	Eq	T (max) °C	Time	Solvents	MW (W)	Cooling	Average (W)	Cyc /Lin	Resin (mg)
Cu(OAc) <sub>2</sub> H <sub>2</sub> O	5	70	30min+ 1h	CHCl <sub>3</sub> /CH <sub>3</sub> CN (20%)	150	yes	110	95 :5	100

To remove the copper, resin was washed with a solution of dithiodicarbamate/DIPEA in DMF. After the side-chain to side-chain on resin cyclization the Fmoc protecting group was removed from the <sup>α</sup>N terminus and the free amino function was acetylated according to the general procedure described in the Experimental Part. The crude product was lyophilized and purified by semi-preparative RP-HPLC. Analytical data are reported in *Table 3.13*.

**Table 3.13 Analytical data of peptide MDP-III**

Peptide	HPLC (R <sub>t</sub> ,min) <sup>a</sup>	ESI-MS [M+H] <sup>+</sup> Calc(found)
MDP-III	3.76	712.71 (712.66)

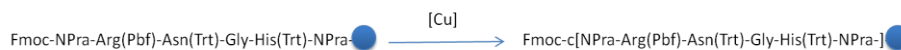
<sup>a</sup>Analytical HPLC gradient at 0.6 mL min<sup>-1</sup>, 03-15% B in 5 min, solvent system A: 0.1% TFA in H<sub>2</sub>O, B: 0.1% TFA in CH<sub>3</sub>CN.

### 3.6.3 Optimization of the Glaser-type reaction to synthesize MDP-IV

#### *Ac-c[NPra-Arg-Asn-Gly-His-NPra]-NH<sub>2</sub>*

We tested the reaction conditions optimized for the cyclization of the peptide **MDP-III**, (entry 11, *Table 3.10*), for the oxidative coupling between the two propargyl side chains in NPra.

## PART B



**Scheme 6.** On resin peptide cyclization by copper catalyzed 1,3 diyne bond formation of **MDP-IV**

We found that these conditions did not work with the NPra analogue, (entry 1, *Table 3.14*). Moreover, at 70°C we observed the reagents degradation under microwave-assisted coupling conditions indicating that this peptide is more sensitive to higher temperature. In the second experiment, (entry 2, *Table 3.14*), we decreased the maximum temperature achieved in the microwave cavity to 40°C, and we registered a low conversion from the linear to the cyclic product.

Finally, we optimized the 1,3 diyne bond formation reaction in the case of the small scale, e.g. the reaction performed on 20mg resin, up to 80:20 cyclic/linear ratio (entry 4, *Table 3.14*), adding pyridine (3%) as a base

**Table 3.14 Optimization of the reaction conditions for MDP-IV**

Entry	Catalyst	Eq. Excess	Temp. (max) °C	Time	Solvents	MW (W)	Cooling	Av. Power (W)	Cyc./Lin.
1	Cu(OAc) <sub>2</sub> ·H <sub>2</sub> O	5	70	30min+1h	CHCl <sub>3</sub> /CH <sub>3</sub> CN (20%)	150	yes	100	-
2	Cu(OAc) <sub>2</sub> ·H <sub>2</sub> O	10	40	30min+1h	CHCl <sub>3</sub> /CH <sub>3</sub> CN (20%)	100	yes	60	20:80
3	Cu(OAc) <sub>2</sub> ·H <sub>2</sub> O	10	60	1h	CHCl <sub>3</sub> /CH <sub>3</sub> CN (20%)	100	yes	50	50:50
4	Cu(OAc) <sub>2</sub> ·H <sub>2</sub> O	10	60	1h	CHCl <sub>3</sub> /CH <sub>3</sub> CN (20%)/Py(3%)	100	yes	60	80:20

Pyridine is the preferred organic base to be used in Copper(II) acetate oxidative coupling of terminal alkynes. We preferred the use of this tertiary amine rather than other secondary amines as additives since we performed the cyclization with the <sup>α</sup>N terminus still protected as Fmoc. Piperidine is reported as an excellent additive for the catalysis of homo- and hetero-couplings but it

is well known that this secondary amine readily cleaves Fmoc group, thus deprotecting the amine function.

The lower yield in cyclization achieved for the peptide **MDP-IV**, compared to the 95:5 cyclic vs. linear ratio for **MDP-III** could be due to the more constrained environment of the 1,3 diyne bond formation reaction. In fact, the propargyl moiety is linked to the same nitrogen atom bearing the Fmoc protecting group.

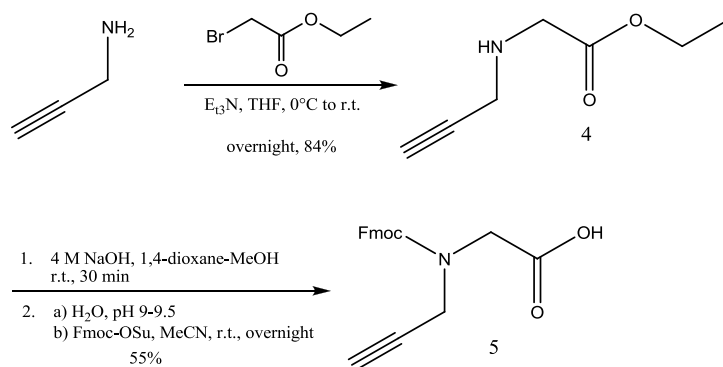
The optimized reaction conditions were used to perform the synthesis of the peptide **MDP-IV**.

**Table 3.15 Sequence of the cyclic peptide MDP-IV**

Peptide	Sequence
<b>MDP-IV</b>	Ac-c[NPra-Arg-Asn-Gly-His-NPra]-NH <sub>2</sub>

The linear precursor of **MDP-IV**, Fmoc-NPra-Arg-Asn-Gly-His-NPra-*Rink-AmideResin*, was synthesized by Fmoc/*t*Bu SPPS using a manual peptide synthesizer, *PLS ChemTech* starting from the Fmoc *Rink-Amide* MBHA resin (Iris Biotech GmbH), according to the general procedure for the SPPS described in details in the Experimental Part and using the commercially available Fmoc-protected amino acids and HBTU/NMM activation. Fmoc-N-Propargyl glycine building block was synthesized starting from propargylamine according to the procedure showed in *Scheme 7* as described in details in the experimental part and introduced during the stepwise synthesis using HATU/NMM activation.

## PART B



**Scheme 7.** Synthesis of Fmoc-N-Propargylglycine<sup>153</sup>.

The reaction conditions optimized on 20mg resin, (entry 4, *Table 3.14*), were reported to a larger scale, e.g. 100mg resin. Unexpectedly, we found only 50% yield for the cyclization reaction (entry 1, *Table 3.16*).

**Table 3.16.** Large scale cyclization of the peptide MDP IV.

Entry	Catalyst	Eq. exc.	Temp (max) °C	Time	Solvents	MW (W)	Cooling	Av. Power (W)	Cyc./ Lin.	resin (mg)
1	Cu(OAc) <sub>2</sub> ·H <sub>2</sub> O	10	60°	1h	CHCl <sub>3</sub> /CH <sub>3</sub> CN (20%)/Py(3%)	100	yes	60	50:50	100
2	Cu(OAc) <sub>2</sub> ·H <sub>2</sub> O	10	60	30min+1h	CHCl <sub>3</sub> /CH <sub>3</sub> CN (20%)/Py(3%)	100	yes	60	90:10	75

In the last experiment, (entry 2, *Table 3.16*) we increased again the reaction time and we performed the reaction in a small reaction vessel with the same amount of solvents used in the small scale reaction. These reaction conditions allowed us to obtain a 90:10 cyclic vs. linear ratio for the peptide Fmoc-NPra-Arg(Pbf)-Asn(Trt)-Gly-His(Trt)-NPra-RinkAmideResin. To remove the copper in excess, the resin was washed with a solution of dithiocarbamate/DIPEA in DMF. After the side-chain to side-chain on resin cyclization, the Fmoc protecting group was removed from the <sup>α</sup>N terminus and the free amino

<sup>153</sup>Norgren, S.A.; Budke, C.; Majer, Z.; Heggemann, C.; Koop, T.; Sewald, N., *Synthesis* **2009**, 3, 0488–0494.

function was acetylated according to the general procedure described in the Experimental Part. The crude product was lyophilized and purified by semi-preparative RP-HPLC. Analytical data are reported in *Table 3.17*.

**Table 3.17** Analytical data of the cyclic peptide MDP IV

Peptide	HPLC ( $R_t$ ,min) <sup>a</sup>	ESI-MS [M+H] <sup>+</sup> Calc.(found)
MDP IV	3.46	712.71 (712.59)

<sup>a</sup>Analytical HPLC gradient at 0.6 mL min<sup>-1</sup>, 03-15% B in 5 min, solvent system A: 0.1% TFA in H<sub>2</sub>O, B: 0.1% TFA in CH<sub>3</sub>CN;

### 3.6.4 Results and discussion

In summary, we developed a method to perform a microwave-assisted on-resin Glaser-type reaction to obtain side-chain to side-chain cyclic peptides that have Pra or NPra residues in their sequence. The Copper(II) acetate monohydrate catalysis allowed to perform coupling of terminal alkynes either in the presence or in absence of a base with very good cyclization yield (e.g. 95:5 and 90:10 cyclic vs. linear ratio for **MDP-III** and **MDP-IV**, respectively) without any other additives such as a co-catalyst or oxygen atmosphere. The on-resin approach allowed cyclisation optimisation via a simple workup procedure. Moreover, unreacted copper catalyst could be easily removed compared to the liquid-phase approach.

## CONCLUSIONS

### 4. Conclusions

Peptides are unique and versatile chemical molecules with a huge pharmaceutical potential as active drugs and diagnostics in several areas of Medicinal and Clinical Chemistry. They can be produced by efficient synthetic strategies as univocally characterised molecules controlling primary, secondary tertiary, and quaternary structures. In the context of immune-mediated diseases, the use of such synthetic peptides reproducing antigens involved *in vivo* in triggering autoantibodies can guarantee specificity and selectivity of recognition overcoming limitations demonstrated in the case of the use of recombinant proteins or protein extracts. This hypothesis has recently assumed a particular relevance for the characterisation of disease-specific biomarkers (i.e., autoantibodies) setting up specific peptide-based diagnostic immunoassays and to explore the antigen-antibody interactions by using synthetic peptide probes selected by the "*Chemical Reverse Approach*".

In this PhD research project, we demonstrated for the first time, in the case of **Coeliac Disease**, how synthetic peptides can be useful because mimicking aberrant modifications presumably involved in the disease pathogenesis. In fact, by the strategy of overlapping peptide synthesis it was possible to develop four new synthetic peptides **tTG(1-15)**, **tTG(41-55)**, **tTG(51-65)**, and **tTG(151-165)** reproducing protein fragments of the native N-terminal portion tTG(1-230), giving important insights on the nature of the Ag-Ab interaction identifying minimal linear epitopes. Moreover, studying the molecular mechanisms at the basis of the pathogenesis of CD it was possible to design and select by the use of the reverse approach a very promising diagnostic tool, i.e, the cross-linked peptide probe **tTGI-DQ2(II)** reproducing the aberrant modification occurring *in vivo*.

In the case of **Multiple Sclerosis**, we started from the observation that aberrant post-translational modifications of protein antigens, such as N-glycosylation, could play a fundamental role in triggering an autoimmune mechanism

## CONCLUSIONS

mediated by antibodies. We developed innovative peptide probes, e.g., Multiple Epitope Peptides and a new disulfide cyclopeptide bearing the previously recognised minimal epitope Asn( $\beta$ -Glc) residue. Investigation of these two different systems confirmed previous results that led to the selection of the first specific antigenic probe for MS, a family of beta-turn structures termed CSF114(Glc), indicating for the first time the utility of synthetic peptide secondary structures in detecting autoantibodies as biomarkers of MS. In the context of developing efficient peptide synthesis to obtain new scaffolds to be used to build up collections of new peptides as diagnostics, we set up a method to perform a microwave-assisted on-resin Glaser-type reaction to side-chain to side-chain cyclic peptides via 1,3-diyne bond formation. This part of the PhD research was performed during the last 4 months at the Ecole Normale Supérieure in Paris under the supervision of Prof. S. Lavielle, in the context of a cooperation with PeptLab.

## 5. Experimental Part A

### 5.1 Materials and Methods

The chemicals were purchased from Sigma-Aldrich and used without further purification. Peptide-synthesis grade N,N-dimethylformamide (DMF) was from Scharlau (Barcelona, Spain). HPLC-grade MeCN was purchased from Carlo Erba (Italy). Protected amino acids and resins were obtained from Iris Biotech AG (Germany). HATU, TBTU, HOBt and DIC were purchased from Advanced Biotech Italia (Milano, Italy). Activation product containing triazine was obtained from EspiKem (Firenze).

Microwave assisted reactions and micro-cleavages were performed with a microwave apparatus CEM EXPLORER 48® (CEM Corporation).

Spot Liquid Chromatography Flash was performed using a Li-Chroprep C-18 column on an Armen Instrument working at 20 mL/min using as solvent systems H<sub>2</sub>O (MilliQ) and CH<sub>3</sub>CN. Semi-preparative purifications via RP-HPLC were performed by a Phenomenex Jupiter C-18 (250 × 4.6 mm) column at 28 °C using an Waters instrument (Separation Module 2695, detector diode array 2996) working at 4 mL/min, with the indicated linear gradients. The solvent systems used were: A (0.1% TFA in H<sub>2</sub>O) and B (0.1 % TFA in CH<sub>3</sub>CN). Peptides were characterized by RP-HPLC ESI-MS. HPLC system is an Alliance Chromatography (Waters) with a Phenomenex Kinetex C-18 column 2.6 μm (100 × 3.0 mm) working at 0.6 mL/min, with the indicated linear gradients, coupled to a single quadrupole ESI-MS (Micromass ZQ). The solvent systems used were: A (0.1% TFA in H<sub>2</sub>O) and B (0.1 % TFA in CH<sub>3</sub>CN). Peptides were lyophilized using a Edward Modulyo lyophilizer.

All the compounds were purified by RP-HPLC (>95%) to be used for autoantibody detection.

SP-ELISA assays were performed using 96 wells plates NUNC Maxisorp (Sigma) or Enhanced Binding (EB, LabSystem, Thermo Scientific). Washings steps were done with Hydroflex microplate washer (Tecan). Anti-*h*IgG and Anti-*h*IgA–Alkaline Phosphatase used in ELISA are by Sigma, PNPP is by Fluka (System A). Anti-*h*IgG and Anti-*h*IgA–Horseradish Peroxidase used in ELISA and TMB are by Dienes Ricerche (System B). Absorbance values were measured using a Sunrise Tecan ELISA plate reader at 405nm or at 450nm. Competitive ELISA was performed using a commercial kit *Eu-tTG-IgA, Aeskulisa* (code 9105, 96 test). The Eu-tTG IgA is an *in vitro* diagnostic enzyme immunoassay for qualitative ELISA test for the semi-quantitative diagnostic detection of IgA specific antibodies directed against the recombinant enzyme tissue transglutaminase (tTG) in human serum.

## 5.2 Solid Phase Peptide Synthesis

### 5.2.1 General procedure for in batch SPPS on the manual PLS 4x4 synthesizer

Peptides are synthesized on a manual batch synthesizer (PLS 4x4, Advanced ChemTech) using a Teflon reactor (20 or 10 mL), following the Fmoc/*t*Bu SPPS procedure. The resin is placed in the Teflon reactor, equipped with a filter. Mixing is provided by vortex, while filtration is performed connecting the reactor to a *vacuum* pump. The resin is swollen for 40 min with DMF (1 mL/100 mg of resin) before use. Each amino-acid cycle is characterized by the following four steps:

- *Fmoc-deprotection*: Resin is stirred twice (1 × 5 min + 1 × 15 min) with a solution of 20% piperidine in DMF (1 mL/100 mg of resin).
- *Washings*: DMF (3 × 3 min).

## EXPERIMENTAL PART A

- *Coupling reaction:* Fmoc-protected amino acid in DMF (1 mL/100 mg resin), TBTU/NMM or HATU/NMM, or DIC/HOBt or TBCR:BF<sub>4</sub>/NMM as coupling system for 20 min.
- *Washings:* DMF (3 × 3 min) and DCM (2 × 3 min).

Deprotection of the second residue should be performed by a fast protocol to avoid DKP formation (3 × 5 min). For the coupling step a solution of the Fmoc-amino acid (5 equiv), TBTU (5 equiv), and NMM (7 equiv) in DMF (1 mL × 100 mg resin) or HATU (5 equiv), and NMM (7 equiv) in DMF (1 mL × 100 mg resin); or the Fmoc-amino acid (4 equiv) DIC (4 equiv), and HOBt (4 equiv) in DMF (1 mL × 100 mg resin) is added to the resin. After DCM washings each coupling reaction is monitored by Kaiser test<sup>154</sup>. After the last Fmoc-removal the resin is washed with DCM and dried under vacuum.

*Preparation of the peptide bond: typical procedure via TBCR:BF<sub>4</sub>*

To the vigorously stirred solution of TBCR:BF<sub>4</sub> (4 equiv.) solved in the minimal amount of CH<sub>3</sub>CN, cooled to 0°C for 30', NMM (4 equiv) and appropriate Fmoc-protected amino acid (4 equiv) solved in DMF is added. The stirring is continued for additional 60 min, at 0°C. Then the mixture is let to achieve room temperature, added to the deprotected resin and the coupling system is stirred for 1.5+3 min in the case of microwave assisted coupling or overnight at room temperature. Then the resin is then filtered, washed in DMF (3×2 min), DCM (3×2 min), and dried.

### **5.2.2 General procedure for in batch SPPS on an automatic peptide synthesizer**

All the reactions are performed in Advanced ChemTech Apex 396 synthesizer using a Fmoc/tBu protection scheme equipped with a 8-wells reaction block

---

<sup>154</sup> Kaiser, E.; Colescott, R.L.; Bossinger, C.D.; Cook, P.I., *Anal Biochem*, **1970**, 34, 595-598.

(0.16 scale), starting from Fmoc-Rink Amide AM-PS resin (0.35 g, 0.63 mmol/g). A robotic needle-like arm allows the distribution of reagents predissolved (0.5 M amino acids and coupling reagent, TBTU, in DMF) and 2M DIPEA in NMP. Fmoc-deprotection is achieved with a solution of 20% piperidine in DMF (1 mL/100 mg of resin). The resin is swollen for 40 min. Each amino-acid cycle is characterized by the following four steps:

- *Fmoc-deprotection*: Resin is stirred twice (1 × 5 min + 1 × 15 min)
- *Washings*: with DMF (3×2 min).
- *Coupling reaction*: (1 x 20 min).
- *Washings*: with DMF (3×2 min).

Deprotection of the second residue should be performed by a fast protocol to avoid DKP formation (3 × 5 min). For the coupling reaction a 0.5 M solution of the Fmoc-protected amino acid(5 equiv) in DMF, 0.5 M solution of TBTU(5 equiv) in DMF, and 2 M solution of DIPEA (7 equiv) in NMP are used. After removal of the last Fmoc-residue, the resin is washed with DCM and dried under N<sub>2</sub> flow for 30 min.

### **5.2.3 General procedure for peptides $\alpha$ N-terminal acetylation**

Acetylation of the  $\alpha$ N-terminal is carried out after Fmoc protecting group removal on the alfa amino function of the last residue anchored to the resin according the following procedure.

- Resin is swollen for 20min in DCM and filtered.
- Resin is stirred in a solution of Ac<sub>2</sub>O (20eq) and NMM (20 eq) in DCM (1mL/100mg of resin) at room temperature for 2 hours (2x1h).
- Resin is then washed with DCM (3x3min) and dried.

#### **5.2.4 General procedure for Dde protecting group removal**

Lys side chain  $\epsilon$ -amino group orthogonally protected with 1-(4,4'-dimethyl-2,6-dioxocyclohexylidene) ethyl group (Dde) is selectively deblocked with a solution of 2% hydrazine in DMF<sup>155</sup> following steps reported below:

- Resin is swollen for 20min in DMF and filtered.
- Resin is vigorously stirred with a solution of 2% N<sub>2</sub>H<sub>4</sub> in DMF (3x3min).
- Resin is then washed with DMF (3X3min) and DCM (3x3min) and dried.

#### **5.2.5 General procedure for cross-coupling reactions**

Cross-linking reactions are performed in heterogeneous phase with the tTG fragments still anchored on the resin, and  $\alpha$ 2-Glia peptides coupled in solution following the procedure reported below:

Resin is swollen for 40min in DMF and filtered.

- *Coupling reaction:* purified peptides DQ2(I), DQ2(II) and DQ2(III) (2.5 equiv) are pre-dissolved in a solution of DMF:NMP/2:1 (1 mL  $\times$  100 mg resin), then HATU (2.5 equiv), and NMM (5 equiv) are added. The mixture is added to the resin and stirred at room temperature for 1h.
- *Washings:* DMF (3  $\times$  3 min) and DCM (2  $\times$  3 min).

After DCM washings each the cross coupling is monitored by a Kaiser test and the resin is washed with DCM and dried under vacuum.

#### **5.2.6 General procedure for cleavage**

---

<sup>155</sup> Rohwedder, B.; Mutti, Y.; and Mutter, M. *Tetrahed Lett*, **1998**, *39*, 1175.

Peptides are cleaved from the resin using as cleavage mixture TFA/EDT/thioanisole/H<sub>2</sub>O/phenol (82.5:5:2.5:5:5) (reagent K) or TFA/H<sub>2</sub>O/TIS (95:2.5:2.5), as indicated for each compound. The peptide-resin is treated for 3 h with cleavage mixture (1 mL × 100 mg of resin) at room temperature. The resin is filtered off and the solution is concentrated flushing with N<sub>2</sub>. The peptide is precipitated from cold Et<sub>2</sub>O, centrifuged and lyophilized. Micro-cleavages are a useful tool to monitor stepwise syntheses. They can be performed at room temperature or alternatively microwave assisted to reduce reaction times. Microwave assisted micro-cleavages were performed using Discover<sup>TM</sup> (CEM Corporation, Matthews, NC) as reported in the *Table 5.1*.

**Table 5.1. Microwave assisted micro-cleavages.**

Reaction	Temp. (°C)	MW Power (W)	Time (min)
Micro-cleavage	50	35	10

The resin is filtered off and the solution is concentrated flushing with N<sub>2</sub>. The peptide is precipitated from cold Et<sub>2</sub>O or isopropyl ether, centrifuged and lyophilized.

### ***5.2.7 General procedure for purification by Spot Liquid Chromatography Flash***

Spot Liquid Chromatography Flash (SLCF) is performed on RP-C18 LiChroprep columns on an automatic Armen Instrument. Main steps are reported here: Column washings with MeOH (3 column volumes) and CH<sub>3</sub>CN (3 column volumes); column conditioning with H<sub>2</sub>O (3 column volumes); dissolving the peptide in H<sub>2</sub>O (1 column volume), checking the pH that should be neutral. Peptides solved in water are absorbed and eluted as reported in Table 5.2 with different H<sub>2</sub>O/ CH<sub>3</sub>CN gradients. Fractions are checked by analytical RP-HPLC ESI-MS to homogeneous ones, and then lyophilized.

**Table 5.2. Peptides purification by SLCF.**

<b>Step</b>	<b>Time(min)</b>	<b>Flow (mL/min)</b>	<b>%H<sub>2</sub>O</b>	<b>%CH<sub>3</sub>CN</b>
<b>1</b>	0	20	100	0
<b>2</b>	07	20	100	0
<b>3</b>	12	20	80	20
<b>4</b>	32	20	30	50
<b>5</b>	33	20	0	100
<b>6</b>	38	25	0	100

*Purification:* AllPeptides are further purified by semipreparative RP-HPLC using methods and solvent system reported in tables. Fractions are checked by RP-HPLCESI-MS to homogeneous ones.

### **5.2.8 Synthesis of peptides *DQ2(I)*, *DQ2(II)*, *DQ2(III)***

Peptides **DQ2(I)**, **DQ2(II)**, and **DQ2(III)**, were synthesized using a Fmoc/*t*Bu protection scheme on the multiple Apex 396 synthesizer (Advanced ChemTech) equipped with a 8-wells reaction block (0.16 scale), as reported in the general procedure, starting from Fmoc-Rink Amide AM-PS resin (350 mg, 0.63 mmol/g). The Acetylation of the <sup>α</sup>N-terminal was carried as reported in the general procedure. Peptide cleavage from the resin and contemporary deprotection of the amino acids side chains was carried out using TFA/H<sub>2</sub>O/TIS (95:2.5:2.5) as cleavage mixture, as reported in the general procedure. The crude products were purified by Spot Liquid Chromatography Flash and characterized by RP-HPLC-ESI-MS. After lyophilization and purification, compound **DQ2(I)** was obtained in 29% yield, **DQ2(II)** was obtained in 23% yield, and **DQ2(III)** was obtained in 30% yield. Analytical data are reported in Table 2.8.

### **5.2.9 Synthesis of peptide *tTGI***

Peptide **tTGI** was synthesized on a PLS 4x4 synthesizer, as described in the general procedure, starting from *Fmoc-Rink-Amide Chem-Matrix*® resin, (300mg, 0,56 mmol/g) and using TBTU(5equiv.) and NMM(7equiv.). Fomc-Ser(Trt)-OH instead of the commonly used Fomc-Ser(tBu)-OH was inserted in position 558 to overcome aggregation/formation of secondary structures thus improving the synthesis yields. Each coupling step was monitored by Kaiser test and the synthesis was monitored each 4 aminoacids by micro-cleavages as well as at the end of the peptide synthesis. The final deprotection is followed by on-resin acetylation, and orthogonal Dde-deprotection of <sup>ε</sup>NH<sub>2</sub> of Lys(562), each step was carried out, as described in the general procedure. The presence of the <sup>ε</sup>free amino function was checked by Kaiser test and the peptide was further analyzed by micro-cleavage performed at room temperature. Purity of the peptide linked to the resin was evaluated by RP-HPLC, compound **tTGI** was obtained with 75% purity. Analytical data are reported in Table 2.11.

#### **5.2.10 Synthesis of *tTGII*, *tTGIII***

Peptides **tTGII** and **tTGIII** were synthesized on a PLS 4x4 synthesizer, as described in the general procedure, starting from, starting from *Fmoc-Rink Amide AM-PS resin*(300mg,0.63 mmol/g)and using TBTU(5equiv.) and NMM(7equiv.). The final deprotection of **tTGII** and **tTGIII** is followed by on resin acetylation, and orthogonal Dde deprotection of <sup>ε</sup>NH<sub>2</sub> of Lys(590) and Lys(677) respectively, each step was carried out, as described in the general procedure. The presence of the free <sup>ε</sup>amino function was checked by Kaiser test and the peptides were further analyzed by micro-cleavage performed at room temperature. Purity of the peptide linked to the resin was evaluated by RP-HPLC, compound **tTGII** was obtained with 95% purity, and compound **tTGIII** was obtained with 80% purity. .Analytical data are reported in Table 2.15.

**5.2.11 Synthesis of cross-linked peptides**

Cross linked peptides were synthesized according to the general procedure. Peptide cleavage from the resin and contemporary deprotection of the amino acids side chains was carried out using Reagent K as cleavage mixture as reported in the general procedure. After lyophilization, purifications were performed by semipreparative RP-HPLC and obtained as indicated in Table 5.3. Analytical data are reported in *Table 2.16*.

**Table 5.3. Semi-prep RP-HPLC and yields.**

Cross-Linked peptide	Semi-prep RP-HPLC Method	Yield
tTG I-DQ2(I)	20-70% of B in 30 min	7%
tTG I-DQ2(II)	25-65% of B in 30 min	6%
tTG I-DQ2(III)	20-70% of B in 30 min	10%
tTG II-DQ2(I)	25-70% of B in 30 min	9%
tTG II-DQ2(II)	25-70% of B in 30 min	11%
tTG II-DQ2(III)	25-70% of B in 30 min	4.5%
tTG II-DQ2(I)	25-70% of B in 30 min	12%
tTG III-DQ2(II)	25-70% of B in 30 min	24%
tTG III-DQ2(III)	25-70% of B in 30 min	15%

**5.2.12 Synthesis of peptides I-XXIII**

Peptides **I-XXIII** were synthesized using a Fmoc/*t*Bu protection scheme on the multiple Apex 396 synthesizer (Advanced ChemTech) equipped with a 8-wells reaction block (0.16 scale), as reported in the general procedure, starting from Fmoc-Rink Amide AM-PS resin. Acetylation of the <sup>α</sup>N-terminal was carried as reported in the general procedure. Peptide cleavage from the resin and contemporary deprotection of the amino acids side chains was carried out using TFA/H<sub>2</sub>O/TIS (95:2.5:2.5) as cleavage mixture as reported in the general

procedure. The crude products were purified by SLCF and characterized by RP-HPLC-ESI-MS. After lyophilization and purification, compounds were obtained in yields comprised between 5 and 10%. Analytical data are reported in Table 2.2.

## 5.3 Immunoassays

### 5.3.1 *Solid-phase not competitive indirect ELISA (SP-ELISA)*

Serum was obtained for diagnostic purposes from patients and healthy blood donors who had given their informed consent, and stored at -20 °C until use. Antibody responses were determined in SP-ELISA.

System A) Ninety-six wells activated polystyrene ELISA plates (NUNC Maxisorp SIGMA) or Enhanced Binding (EB, LabSystem, Thermo Scientific) were coated with 1 µg per 100 µl of peptides per well in pure carbonate buffer 0.05 M (pH 9.6) and incubated at 4 °C overnight. After that, non specific binding sites were blocked by DILUENT2 (PBS/Brij/NewBorn/Methyl orange, DIESSE RICERCHE), 100 µl per well, at room temperature for 60 min. Sera diluted 1:50, or 1:100 or from 1:100 to 1:6400 were applied at 37°C for 45 min. After four washes, it was added 100 µl of horseradish peroxidase conjugated anti-human IgA (diluted 1:215 in DT20, PBS/Tween/BSA/Methyl orange, DIESSE RICERCHE) or IgG (diluted 1:2000 in DT20, PBS/Tween/BSA/Methyl orange, DIESSE RICERCHE) to each well. After 45 min at 37°C incubation and five washes, 100 µl of substrate solution consisting of 0.26 mg/mL 3,3',5,5'-Tetramethylbenzidine (DIESSE RICERCHE) in 0,01% H<sub>2</sub>O<sub>2</sub> in citrate buffer 0,05M at pH 3.8 (DIESSE RICERCHE) was applied. After 15 min, the reaction was stopped with 100 µl of 0.3M H<sub>2</sub>SO<sub>4</sub> (Stop solution Enzywell, DIESSE RICERCHE), and the absorbance was read in a multichannel ELISA reader (Tecan Sunrise) at 450 nm. ELISA plates, coating conditions, reagent dilutions, buffers, and incubation times were tested in preliminary

## EXPERIMENTAL PART A

experiments. The antibody levels are expressed as absorbance in arbitrary units at 450 nm.

System B) Ninety-six wells activated polystyrene ELISA plates (NUNC Maxisorp SIGMA) were coated with 0.5 µg per 50 µl of peptides per well in pure carbonate buffer 0.05 M (pH 9.6) and incubated at 4 °C overnight. After that, non specific binding sites were blocked by fetal calf serum (FCS), 10% in saline Tween 20 (50 µl per well) at room temperature for 60 min. Sera diluted 1:100 were applied at 4 °C overnight in saline/Tween 20/10% FCS. After five washes, it was added 50 µl of alkaline phosphatase conjugated anti-human IgA (diluted 1:1500 in saline/Tween 20/FCS) or IgG (diluted 1:8000 in saline/Tween 20/FCS) (Sigma) to each well. After 3 h at room temperature incubation and five washes, 50 µl of substrate solution consisting of 1 mg/ml p-nitrophenyl phosphate (Sigma) in 10% diethanolamine buffer was applied. After 30 min, the reaction was stopped with 1M NaOH (25 µl), and the absorbance was read in a multichannel ELISA reader (Tecan Sunrise) at 405 nm. ELISA plates, coating conditions, reagent dilutions, buffers, and incubation times were tested in preliminary experiments. The antibody levels are expressed as absorbance in arbitrary units at 405 nm (sample dilution 1:100).

### **5.3.2 Measurement of antibody affinity by competitive ELISA**

Antibody affinity was measured following the methods previously reported<sup>156</sup>. Sera diluted (1:1000) were preincubated with synthetic peptide antigen (0 and  $2 \times 10^{-3}$  M) for 45 min at room temperature. Unblocked Abs were revealed by ELISA at 450 nm, *Eu-tTG IgA*, *Aeskulisa*, and the antigenic probe concentration-absorbance relationship was presented graphically.

---

<sup>156</sup> Rath, S.; Stanley, C. M.; Steward, M. W., *J. Immunol. Methods*, **1988**, *106*, 245–249.

## 6. Experimental Part B

### 6.1 Materials and Methods

The chemicals were purchased from Sigma-Aldrich and used without further purification. Peptide-synthesis grade N,N-dimethylformamide (DMF) was from Scharlau (Barcelona, Spain). HPLC-grade MeCN was purchased from Carlo Erba (Italy). Protected amino acids and resins were obtained from Calbiochem-Novabiochem AG (Laufelfingen, Switzerland) or Iris Biotech GmbH (Marktredwitz, Germany). HATU, TBTU, HBTU were purchased from Advanced Biotech Italia (Milano, Italy). TBCRBF<sub>4</sub> was obtained from EspiKem (Firenze). Microwave assisted reactions were performed on a microwave apparatus CEM EXPLORER 48® (CEM Corporation).

TLC were carried out on silica gel precoated plates (Merck; 60 Å F<sub>254</sub>) and spots located with: (a) UV light (254 and 366 nm), (b) ninhydrin (solution in acetone), (c) Floram® (Fluka; fluorescamine, 4-phenyl-spyro[furan-2(3H),1'-isobenzofuran]-3,3'-dione) in acetone, (d) CH<sub>2</sub>Cl<sub>2</sub>-MeOH-AcOH, 97:2.5:0.5. Flash Column Chromatography (FCC) was performed on Merck silica gel 60 (230-400 mesh) according to Still et al<sup>157</sup>.

<sup>1</sup>H and <sup>13</sup>C NMR spectra were recorded at 400 and 100 MHz, and 200 and 50 MHz respectively, on a Varian spectrometer; or at Bruker Avance III 500 MHz spectrometer equipped with a cryogenic TCI probe in deuterated solutions and are reported in parts per million (ppm), with solvent resonance used as reference. Chemical shifts (δ) are reported in ppm relative to TMS and coupling constants (J) are reported in Hz. The multiplicity were marked as s = singlet, d = doublet, t = triplet, q = quartet, m = multiplet. Intensities of signals were estimated as vs = very strong, s = strong, m = medium, w = weak, b = broad.

---

<sup>157</sup> W.C. Still, M. Khan, A. Mitra, *J. Org. Chem.*, **1985**, *50*, 2394-2395.

## EXPERIMENTAL PART B

Semi-preparative purifications via RP-HPLC were performed by a Phenomenex Jupiter C-18 (250 × 4.6 mm) column at 28 °C using an Waters instrument (Separation Module 2695, detector diode array 2996) working at 4 mL/min. The solvent systems used were: A (0.1% TFA in H<sub>2</sub>O) and B (0.1 % TFA in CH<sub>3</sub>CN). Peptides were characterized by RP-HPLC ESI-MS. HPLC system is an Alliance Chromatography (Waters) with a Phenomenex Kinetex C-18 column 2.6µm (100 × 3.0 mm) working at 0.6 mL/min, with UV detection at 215nm, coupled to a single quadrupole ESI-MS (Micromass ZQ). The solvent systems used were: A (0.1% TFA in H<sub>2</sub>O) and B (0.1 % TFA in CH<sub>3</sub>CN).

Peptide **MDP-I** was purified by RP-HPLC on a ACE 5 C18-300" (250 × 10 mm) column (Waters, Saint Quentin en Yvelines, France) at 28°C using an Waters instrument (Separation Module 2695, detector diode array 2996) working at 4 mL/min, with the indicated linear gradients. The solvent systems used were: A (0.1% TFA in H<sub>2</sub>O) and B (0.1 % TFA in CH<sub>3</sub>CN). Peptide **MDP-I** was characterized by RP-HPLC and MALDI-TOF-MS. HPLC system is an Alliance Chromatography (Waters) with a ACE 5 C18-300" (250 × 4.6 mm) column working at 1 mL/min, with UV detection at 220 and 280 nm. The solvent systems used were: A (0.1% TFA in H<sub>2</sub>O) and B (0.1 % TFA in CH<sub>3</sub>CN). Mass spectral analysis was performed by MALDI-TOF (Voyager-DE<sup>TM</sup> PRO Workstation, Applied Biosystems).

The products were lyophilized with an Edwards apparatus, model Modulyo.

All the compounds were purified by RP-HPLC (>95%) to be used for autoantibody detection.

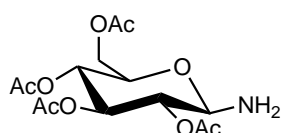
## 6.2 Synthesis of building blocks for SPPS

### 6.2.1 2,3,4,6-Tetra-O-acetyl-β-D-glucopyranosylamine(1)

To a solution of commercially available 2,3,4,6-tetra-O-acetyl-β-D-glucopyranosyl azide (10 mmol) in MeOH, we added 20% Pd(OH)<sub>2</sub>/C. The

mixture was stirred for 24 h at r.t. under H<sub>2</sub>, checked by TLC [AcOEt/hexane, 3:1; UV, fluorescamine, and vanilline], filtered over *celite*, washed with MeOH and concentrated. The desired compound **1** was re-crystallized from THF/hexane.

**2,3,4,6-tetra-O-acetyl-β-D-glucopyranosylamine (1)**, yield 98%. *R<sub>f</sub>* = 0.37.



<sup>1</sup>H NMR (200 MHz, CDCl<sub>3</sub>) δ = 2.03 (s, 3H, OAc), 2.04 (s, 6H, 2×OAc), 2.07 (s, 3H, OAc), 3.67-3.75 (m, 1H, H-5), 4.03 (d, *J* = 12.2 Hz, 1H, H-6), 4.28 (pd, *J* = 12.8 Hz, 1H, H-6'), 4.96 (t, *J* = 9.6 Hz, 1H, H-2), 5.12 (t, *J* = 10 Hz, 1H, H-4), 5.27-5.36 (m, 2H, H-1 and H-3) ppm.

### 6.2.2 Microwave assisted Synthesis of glucosylated asparagine

The Asparagine derivative was prepared according to the following procedure for microwave-assisted synthesis. Fmoc-L-Asp-OtBu (60 mg, 0.144 mmol), 2,3,4,6-tetra-*O*-acetyl-β-D-glucopyranosyl amine (**1**) (1 equiv), NMM (1 equiv), and DMT-NMM/BF<sub>4</sub><sup>158,159</sup> (1 equiv) as coupling reagent were dissolved in acetonitrile (2 ml). The vessel was charged with the reaction mixture, sealed, and placed into the microwave synthesizer CEM EXPLORER 48® applying the reaction conditions reported in Table 6.1.

**Table 6.1.MW-assisted coupling reaction.**

Reaction	Temp (°C)	Time (min)	Power (W)
Coupling reaction	70	5	100

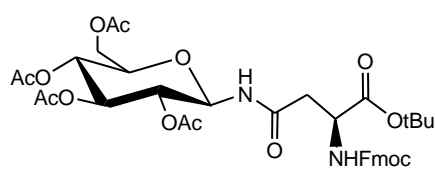
<sup>158</sup> [4-(4,6-dimethoxy-1,3,5-triazin-2-yl)-4-methylmorpholinium tetrafluoroborate], "Process for the preparation of *N*-triazinylammonium salts". Filing date 07/11/2005. Applicant: Italvelluti S.p.a. Inventors: Z. Kaminski, A. M. Papini, B. Kolesinska, J. Kolesinska, K. Jastrzabek, G. Sabatino, R. Bianchini. PCT/EP2005/055793 (2005).

<sup>159</sup> Z. J. Kamiński, B. Kolesińska, J. Kolesińska, G. Sabatino, M. Chelli, P. Rovero, M. Błaszczuk, M. L. Główska, A. M. Papini, *J. Am. Chem. Soc.*, **2005**, *127*, 16912-16920.

## EXPERIMENTAL PART B

The reaction tube was taken off after performing the coupling reaction. Then the mixture was transferred into a round bottom flask. The solvent was evaporated under reduced pressure, the residue was dissolved in  $\text{CHCl}_3$  and then washed with water, 0.5 M aqueous  $\text{KHSO}_4$ , water, 0.5 M aqueous  $\text{NaHCO}_3$ , and water again. Organic layer was dried over anhydrous  $\text{Na}_2\text{SO}_4$ , filtered off and concentrated to dryness. After purification of the residue by FCC (hexane/ $\text{AcOEt}$ , 1:1) we obtained compound **2** as a white solid. ( $R_f = 0.30$  [ $\text{AcOEt}$ :Hexane, 1:1, (fluorescamine, vanilline)];  $[\alpha]_D = 22.94$ ; ESI-MS:  $m/z$  calcd for  $\text{C}_{37}\text{H}_{44}\text{O}_{14}\text{N}_2 = 740.28$ , found  $(\text{M}+\text{H})^+ = 741.73$ ).

**Fmoc-L-Asn( $\beta\text{GlcAc}_4$ )-OtBu(2)**: yield 85%,  $^1\text{H}$  NMR (400 MHz,  $\text{CDCl}_3$ )  $\delta =$



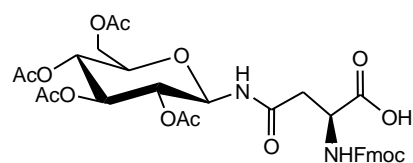
1.46 (s, 9H, *t*Bu), 1.99, 2.01 (2 s, 12H, 4 $\times$ OAc), 2.84 (system ABMX,  $J_{AB} = 16.4$  Hz,  $J_{AM} = 4.4$  Hz,  $J_{BM} = 4.0$  Hz, 2H, Asn- $\beta$ - $\text{CH}_2$ ), 3.70 (*pt*,  $J = 4.8$  Hz, 1H, H-5), 4.04 (d,  $J = 12.4$  Hz, 1H, H-6), 4.19 (t,  $J = 7.2$  Hz, 1H, Fmoc-CH), 4.23 (dd,  $J = 12.8$  Hz,  $J = 4.4$  Hz, 1H, H-6'), 4.31-4.42 (m, 2H, Fmoc- $\text{CH}_2$ ), 4.69-4.72 (m, 1H, Asn- $\alpha$ -CH), 4.98 (t,  $J = 9.6$  Hz, 1H, H-2), 5.10 (t,  $J = 10$  Hz, 1H, H-4), 5.29-5.37 (m, 2H, H-1 and H-3), 6.09 (d,  $J = 8.0$  Hz, 1H, Asn- $\alpha$ -NH), 6.87 (d,  $J = 9.2$  Hz, 1H, NH-1), 7.28 (app-t, 2H, Fmoc-Ar), 7.37 (app-t, 2H, Fmoc-Ar), 7.57 (d,  $J = 7.2$  Hz, 2H, Fmoc-Ar), 7.73 (d,  $J = 7.2$  Hz, 2H, Fmoc-Ar) ppm.  $^{13}\text{C}$  NMR (100 MHz,  $\text{CDCl}_3$ )  $\delta = 20.5, 20.5, 20.6$  (C(O) $\text{CH}_3$ ), 27.8 (C( $\text{CH}_3$ )), 37.9 (C $_{\beta}$ ), 47.1 (Fmoc CH), 50.9 (C $_{\alpha}$ ), 61.5 (C-6), 67.1 (Fmoc- $\text{CH}_2$ ), 68.0, 70.5, 72.6, 73.6 (C-2, C-3, C-4, C-5), 78.0 (C-1), 82.4 (C( $\text{CH}_3$ ) $_3$ ), 119.9, 125.1, 125.1, 127.0, 127.6, 141.2, 143.7, 143.8 (Ar-C), 156.1, 169.5, 169.7, 169.8, 170.5, 170.7, 171.0 (C=O). Results were consistent with the data previously reported<sup>160,126</sup>.

<sup>160</sup> Van Ameijde, J.; Albada, H.B.; Liskamp, R.; *J. Chem. Soc. Perkin Trans.*, **2002**, 1, 1042-1049.

### 6.2.3 *tert*-Butyl deprotection of Fmoc-protected amino acid

The pure *t*-Bu ester was dissolved in TFA in DCM (1:1). The reaction mixture was stirred for 3 hours at r.t. The solvents were evaporated and after dissolution in water and freeze drying, compound **3** was obtained.

**Fmoc-L-Asn( $\beta$ GlcAc<sub>4</sub>)-OH (3)**: yield 95%. R<sub>f</sub> = 0.19 (AcOEt/Hexane, 2:1,



UV and vanilline). <sup>1</sup>H NMR (400 MHz,

CDCl<sub>3</sub>) δ = 2.00, 2.02 (2 s, 12H, 4×OAc),

2.85 (system ABMX, J<sub>AB</sub> = 16.4 Hz, J<sub>AM</sub>

= 4.4 Hz, J<sub>BM</sub> = 4.0 Hz, 2H, Asn-β-CH<sub>2</sub>),

3.74 (pt, J = 4.8 Hz, 1H, H-5), 4.05 (d, J = 12.4 Hz, 1H, H-6), 4.19 (t, J = 7.2

Hz, 1H, Fmoc-CH), 4.27 (dd, J = 12.8 Hz, J = 4.4 Hz, 1H, H-6'), 4.31-4.40 (m,

2H, Fmoc-CH<sub>2</sub>), 4.59-4.61 (m, 1H, Asn-α-CH), 4.94 (t, J = 9.6 Hz, 1H, H-2),

5.07 (t, J = 10 Hz, 1H, H-4), 5.27-5.35 (m, 2H, H-1 and H-3), 5.59 (broad s,

1H, COOH), 6.25 (d, J = 8.0 Hz, 1H, Asn-α-NH), 7.06 (d, J = 9.2 Hz, 1H, NH-

1), 7.28 (app-t, 2H, Fmoc-Ar), 7.37 (app-t, 2H, Fmoc-Ar), 7.57 (d, J = 7.2 Hz,

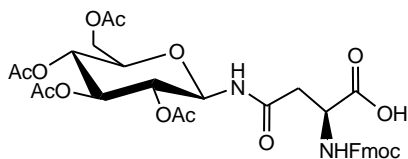
2H, Fmoc-Ar), 7.73 (d, J = 7.2 Hz, 2H, Fmoc-Ar) ppm.

### 6.2.4 One step Synthesis of glucosylated asparagine

To a stirred solution of acetylated glucosyl amine (5.0 mmol) in DMSO (3 mL), N-Fmoc-aspartic anhydride (5.0 mmol) was added. The reaction mixture was kept at ambient temperature for one hour and then diluted with methanol. The precipitate was filtered and recrystallized from methanol. In the case of disaccharide derivatives, the product was isolated by dilution of the reaction mixture with water, followed by extraction with CHCl<sub>3</sub>. Evaporation and recrystallization from methanol afforded the pure product, **3**.

## EXPERIMENTAL PART B

**Fmoc-L-Asn( $\beta$ GlcAc<sub>4</sub>)-OH(3):** yield 82%. <sup>1</sup>H NMR (DMSO-d<sub>6</sub>, 500 MHz):



d (ppm) 8.75 (d, 1H,  $J_{1NH} = 9.4$  Hz, NH-Glc), 7.88 (d, 2H,  $J = 7.5$  Hz, HAr-Fmoc), 7.70 (dd, 2H,  $J = 7.4$  Hz,  $J = 7.4$  Hz, HAr-Fmoc), 7.57 (d, 1H,  $J = 8.4$  Hz, NH-Asn),

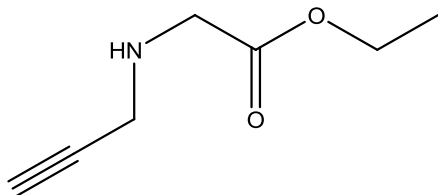
7.40 (t, 2H,  $J = 7.5$  Hz, HAr-Fmoc), 7.32 (t, 2H,  $J = 7.4$  Hz, HAr-Fmoc), 5.41 (dd, 1H,  $J_{1,2} = 9.3$  Hz, H-1), 5.33 (dd, 1H,  $J_{3,4} = 9.6$  Hz, H-3), 4.91 (dd, 1H,  $J_{4,5} = 9.7$  Hz, H-4), 4.82 (dd, 1H,  $J_{2,3} = 9.4$  Hz, H-2), 4.38 (dt, 1H,  $J_{,1} = 6.1$  Hz,  $J_{,2} = 7.4$  Hz, a-CH-Asn), 4.27 (d, 2H, a,b-CH<sub>2</sub>-Fmoc), 4.20 (dd, 1H,  $J = 6.6$  Hz, H-9 Fmoc), 4.16 (dd, 1H,  $J_{6a,6b} = 12.3$  Hz, H-6a), 4.09 (dq, 1H,  $J_{5,6a} = 4.4$  Hz,  $J_{5,6b} = 2.2$ , H-5), 3.97 (dd, 1H, H-6b), 2.64 (dd, 1H,  $J_{1,2} = 15.8$  Hz, b1-H-Asn), 2.52 (m, 1H, b2-H-Asn), 1.99, 1.98, 1.92, 1.89 (4s, each 3H, 4 -CH<sub>3</sub>CO). <sup>13</sup>C NMR (DMSO-d<sub>6</sub>, 125 MHz): d (ppm) 172.81 (COOH), 169.90 (CO-NH), 169.63, 169.39, 169.20, 169.00 (CO-Ac), 155.73 (CO-Fmoc), 143.70, 143.64, 140.59, 127.53, 126.98, 125.16, 120.00 (Ar-Fmoc), 76.70 (C-1), 72.77 (C-3), 71.99 (C-5), 70.45 (C-2), 67.69 (C-4), 65.60 (CH<sub>2</sub>-Fmoc), 61.62 (C-6), 50.12 (CH-Asn), 46.49 (CH-Fmoc), 20.41, 20.27, 20.21, 20.18 (CH<sub>3</sub>-Ac). ESI FT-ICR HRMS (m/z): 707.2066 (707.2064 calculated for C<sub>33</sub>H<sub>36</sub>N<sub>2</sub>NaO<sub>14</sub> [M+Na]<sup>+</sup>). 2,3,4,6-tetra-O-acetyl-N-[N-Fmoc-D-aspart-4-oyl]- $\beta$ -D-glucopyranosylamine. Results are consistent with previously reported data<sup>133</sup>.

### 6.2.5 Synthesis of N-(Propargyl) Glycine

Ethyl bromoacetate (100 mmol, 11.1 mL) in THF (30.0 mL) was added dropwise to a cooled (ice-bath) solution of propargylamine (100 mmol, 6.86 mL) and Et<sub>3</sub>N (200 mmol, 27.9 mL) in anhydrous THF (30.0 mL). The ice-bath was kept for 30 min before the reaction mixture was allowed to attain r.t. After stirring overnight, the mixture was filtered to remove ethylamine hydrobromide. The filtrate was washed repeatedly with Et<sub>2</sub>O and the organic

phase was removed under reduced pressure. The crude compound, **4**, did not require further purification before the next step.

**H-N-Pra-OEt(4)**: Yield 84%. <sup>1</sup>H NMR (500 MHz, CDCl<sub>3</sub>): d = 4.20 (q, J =

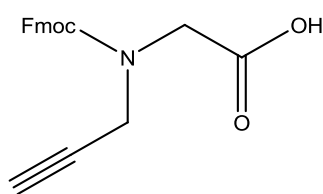


7.1 Hz, 2 H), 3.51 (s, 2 H), 3.49 (d, J = 2.4 Hz, 2 H), 2.24 (m, 1 H), 1.29 (t, J = 7.1 Hz, 3 H). <sup>13</sup>C NMR (125 MHz, CDCl<sub>3</sub>): d = 171.9, 81.2, 72.0, 60.9, 49.2, 37.7, 14.2.

**N-(9-Fluorenylmethoxycarbonyl)-N-(propargyl)glycine(5)**

Aq 4 M NaOH (20.0 mL) was added to a solution of **4** (84.0 mmol, 11.9 g) in dioxane (100 mL) and MeOH (35.0 mL). After stirring for 40 min, the reaction mixture was concentrated in vacuo. The resulting sodium salt was dissolved in H<sub>2</sub>O (80.0 mL) and the pH was adjusted to 9–9.5 with concd HCl. A solution of Fmoc-OSu (84.0 mmol, 28.3 g) in MeCN (130 mL) was subsequently added and the mixture was left to stir overnight at r.t.. The MeCN was removed under reduced pressure and the aqueous phase was acidified (pH 1–2) with concd HCl. The aqueous phase was extracted with CH<sub>2</sub>Cl<sub>2</sub> (2 × 100 mL) and the combined organic phases were washed with H<sub>2</sub>O (50 mL) and brine (50 mL), dried (Na<sub>2</sub>SO<sub>4</sub>) and concentrated under reduced pressure. Recrystallization from EtOAc–hexane gave **5** as white crystals in 55% yield (45 mmol, 15.1 g); mp 130–132 °C; R<sub>f</sub> = 0.33 (CH<sub>2</sub>Cl<sub>2</sub>–MeOH–AcOH, 97:2.5:0.5).

**Fmoc-N-Pra-OH (5)**: Yield 55%. IR (KBr): 3851 (s), 2959 (w), 2893 (w),



1736 (s), 1678 (s), 1541 (w), 1479 (m), 1460 (m), 1403 cm<sup>-1</sup> (m). <sup>1</sup>H NMR (500 MHz, DMSO-d<sub>6</sub>): d = 12.87 (s, 1 H), 7.89 (m, 2 H), 7.72 (m, 1 H), 7.60 (m, 1 H), 7.35 (m, 4 H), 4.30–4.00 (m, 7 H), 3.30 (m, 1 H). <sup>13</sup>C NMR

(125 MHz, DMSO-d<sub>6</sub>): d = 170.99/170.87, 155.48/155.45, 144.1,

## EXPERIMENTAL PART B

141.19/141.15, 128.2, 127.6, 125.75/125.56, 120.6, 79.76/79.57, 68.0 (br), 48.33/47.72, 46.98/46.89, 37.63/37.45. Results are consistent with previously reported data<sup>153</sup>.

### 6.3 Solid Phase Peptide Synthesis

#### 6.3.1 General procedure for batch SPPS on the manual PLS 4x4 synthesizer

Peptides are synthesized on a manual batch synthesizer (PLS 4x4, Advanced ChemTech) using a Teflon reactor (20 or 10mL), following the Fmoc/tBu SPPS procedure. The resin is placed in the Teflon reactor, equipped with a filter. Mixing is provided by vortex, while filtration is performed connecting the reactor to a *vacuum* pump. The resin is swollen for 40 min with DMF (1 mL/100 mg of resin) before use. Each amino-acid cycle is characterized by the following four steps:

- *Fmoc-deprotection*: Resin is stirred twice (1 × 5 min + 1 × 15 min) with a solution of 20% piperidine in DMF (1 mL/100 mg of resin).
- *Washings*: DMF (3 × 3 min).
- *Coupling reaction*: Fmoc-protected amino acids in DMF (1 mL/100 mg resin), TBTU/NMM or HBTU/NMM or HATU/NMM as coupling system for 30 min.
- *Washings*: DMF (3 × 5 min) and DCM (2 × 5 min).

Deprotection of the second residue should be performed by a fast protocol to avoid DKP formation (3 × 5 min). For the couplingstep a solution of the Fmoc-amino acid, TBTU/NMM, or HBTU/NMM or HATU/NMM in DMF (1 mL × 100 mg resin) is added to the resin. Coupling conditions, in terms of equivalents of excess and coupling reagents used are specified for each product. After DCM washings each coupling reaction is monitored by Kaiser test<sup>154</sup>. After the last Fmoc-deprotection the resin is washed with DCM and dried under vacuum.

### **6.3.2 On-Resin Glaser cyclization**

The resin aliquots were swollen for 2 h in DCM before adding the pre-dissolved copper catalyst and additives. The vessels were then transferred to the MW cavity of a manual CEM synthesizer. The cyclization reactions were performed according the conditions summarized in Table 3.12 and in Table 3.16 for each compound. The resin is washed using DMF (3 x 2 min), 0.5 % diethylthiocarbamate and 0.5% DIEA in DMF (3 x 10 min, or until brown coloration disappears), DMF (3 x 2 min) and DCM (3 x 2 min).

### **6.3.3 General procedure for peptides $\alpha$ N-terminal acetylation**

Acetylation of the  $\alpha$ N-terminal is carried out after Fmoc-protecting group removal on the alfa amino function of the last residue anchored to the resin according the following procedure.

- Resin is swollen for 20min in DCM and filtered.
- Resin is stirred in a solution of Ac<sub>2</sub>O (20eq) and NMM (20 eq) in DCM (1mL/100mg of resin) at room temperature for 2 hours (2x1h).
- Resin is then washed with DCM (3x3min) and dried.

### **6.3.4 General procedure for cleavage**

Peptides and glycopeptides are cleaved from the resin using as cleavage mixture TFA/EDT/thioanisole/H<sub>2</sub>O/phenol (82.5:5:2.5:5:5) (reagent K) or TFA/H<sub>2</sub>O/TIS (95:2.5:2.5), as indicated for each compound. The peptide-resin is treated for different times with cleavage mixture (1 mL  $\times$  100 mg of resin) at room temperature, as indicated for each compound. The resin is filtered off and the solution is concentrated flushing with N<sub>2</sub>. The peptide is precipitated from cold Et<sub>2</sub>O, centrifuged and lyophilized.

### **6.3.5 General procedures for glycopeptide deacetylation**

A) Deacetylation of the sugar linked to the MEps is accomplished by adding 0.1 M MeONa in MeOH to a solution of the raw material in dry MeOH until pH 12. After 5 h under stirring the reaction is quenched by adding conc. HCl to neutrality, the solvent is evaporated under vacuum and the residue lyophilized.

B) Deacetylation of the sugar linked to the disulfide bridge cyclopeptide is accomplished by stirring the resin in a solution of  $N_2H_4$ /MeOH 4:1 1h x2 times at room temperature. The resin is then filtered, washed with DMF (3x2min), DCM (3x2min) and dried.

*Purification:* All Peptides are purified by semipreparative RP-HPLC using methods and solvent system reported in tables. Fractions are checked by RP-HPLC ESI-MS or MALDI-TOF to homogeneous ones.

### **6.3.6 Synthesis of Multiple Epitope peptides, CT21, CT32, CT33, CT34, CT35 and CT38**

Multiple Epitope peptides were synthesized on a manual PLS 4x4 synthesizer, as described in the general procedure, starting from Fmoc4-Lys2-Lys- $\beta$ -Ala-Wang resin (100mg, 0.2 mmol/g) using HATU(5equiv.) and NMM(7equiv). Fmoc-LAsn( $\beta$ -GlcAc4)-OH (2.5 equiv), Fmoc-Ado-OH (2.5 equiv), and Fmoc-TTDS-OH (2.5 equiv) were coupled with HATU (2.5 equiv) and NMM (5 equiv) in DMF for 1 h. MEps were acetylated on the  $^n$ N-terminal as described in the general procedure. MEps were cleaved from the resin and side chains were deprotected as described in the general procedure treating the resin with a cleavage solution of TFA/ H<sub>2</sub>O/TIS (96:2:2), for 4h, at r.t.. Deprotection of the hydroxyl functions of sugars was performed as described in the general procedure, a), and the MEps were purified by semipreparative RP-HPLC with different gradients, as reported in *Table 6.2*.

**Table 6.2. Semi-prep. purification of MEps.**

MEP	RP-HPLC Method	Yield (%)
ct21	02-35% B in 30 min	1,5
ct35	07-35% B in 30 min	1,7
ct32	05-40% B in 30 min	2,1
ct33	07-40% B in 30 min	1,9
ct34	03-25% B in 30 min	2,5
ct38	10-35% B in 30 min	2,3

Characterization of the peptides was performed using analytical RP-HPLC and ESI-MS spectrometry. Analytical data are reported in Table 3.2.

### 6.3.7 Synthesis of cyclopeptide MDP-I

Linear peptide **MDP-I** was synthesized on a manual PLS 4x4 synthesizer, as described in the general procedure, starting from Fmoc-RinkAmide (MBHA) PS Resin (100mg, 0.43mmol/g) using HBTU(5equiv.) and NMM(7equiv.). Acetylation of the <sup>α</sup>N-terminal was carried out as indicated in the general procedure. **Lin-MDP-I** was cleaved from the resin and side chains were deprotected as described in the general procedure using as cleavage solution reagent K for 3h, at r.t.. After lyophilization, the intramolecular disulfide bond formation was carried out solving the crude product, in a solution of 0.1% of TFA in MilliQ water (1mg/mL). Oxidation could be performed in presence of TFA thanks to 'activation' by 2,2'-dithiodipyridine. 100 μl of a 2,2'-dithiodipyridine solution (1.2 mg/ml in distilled H<sub>2</sub>O) were added *per* milliliter of solution. The reaction progress was monitored analytical RP-HPLC. After 3 hours crude oxidation reaction mixture was concentrated by rotary evaporation, freeze-dried and lyophilized.

## EXPERIMENTAL PART B

Lyophilized cyclic peptide was purified by semi-preparative RP-HPLC 03-15% of B in 30min; HPLC gradient at 4 mL min<sup>-1</sup>, solvent system A: 0.1% TFA in H<sub>2</sub>O, B: 0.1% TFA in CH<sub>3</sub>CN. After lyophilization and purification the compound **MDP-I** was obtained in 27% yield. Analytical data are reported in Table 3.6.

### 6.3.8 Synthesis of cyclopeptide **MDP-II**

Linear peptide **MDP-II** was synthesized on a manual PLS 4x4 synthesizer, as described in the general procedure, starting from Fmoc-RinkAmide (MBHA) PS Resin (100mg, 0.43mmol/g) using HBTU(5equiv.) and NMM(7equiv.). Fmoc-L-Asn( $\beta$ GlcAc4)-OH (3 equiv) was coupled using HATU (3 equiv) and NMM (5 equiv) in DMF for 1 h. Acetylation of the <sup>o</sup>N-terminal was carried out as indicated in the general procedure. Peptide Deprotection of the hydroxyl functions of sugar was performed as described in the general procedure, b). **Lin-MDP-II** was cleaved from the resin using and side chains were deprotected as described in the general procedure as cleavage solution reagent K for 3h, at r.t.. After lyophilization, the intramolecular disulfide bond formation was carried out solving the of the crude product, in a solution of 0.1% of TFA in MilliQ water (1mg/mL). Oxidation could be performed in presence of TFA thanks to 'activation' by 2,2'-dithiodipyridine. 100  $\mu$ l of a 2,2'-dithiodipyridine solution (1.2 mg/ml in distilled H<sub>2</sub>O) were added *per* milliliter of solution. The reaction progress was monitored analytical HPLC. After 3 hours crude oxidation reaction mixture was concentrated by rotary evaporation, freeze-dried and lyophilized.

Lyophilized cyclic peptide was purified by semi-preparative RP-HPLC 03-15% of B in 30min; HPLC gradient at 4 mL min<sup>-1</sup>, solvent system A: 0.1% TFA in H<sub>2</sub>O, B: 0.1% TFA in CH<sub>3</sub>CN. After lyophilization and purification the compound **MDP-II** was obtained in 13.5% yield. Analytical data are reported in Table 3.9.

### 6.3.9 Synthesis of cyclopeptide MDP-III

Linear Fmoc-protected precursor of **MDPIII** was synthesized on a manual PLS 4x4 synthesizer, as described in the general procedure, starting from starting from Fmoc-RinkAmide (MBHA) PS Resin(100mg, 0.43mmol/g) and using Fmoc-protected amino acids (5equiv.), HBTU (5 equiv.) and NMM (7 equiv.) in DMF for 30 min. Fmoc-Pra-OH(3 equiv.) was coupled using HBTU (3 equiv). and NMM (5 equiv.) in DMF for 45 min. Side chain to side chain cyclization was achieved performing the Glaser coupling as described in the general procedure according the reaction conditions reported in Table 3.12and the cyclization yield was evaluated by RP-HPLC. Acetylation of the <sup>o</sup>N-terminal was carried out as indicated in the general procedure.**MDPIII**was cleaved from the resin and side chains were deprotected as described in the general procedure using as cleavage solution TFA/H<sub>2</sub>O/TIS (95:2.5:2.5), for 3h at r.t.. Crude lyophilized product was purified by semi-preparative RP-HPLC 03-15% of B in 30min; HPLC gradients at 4 mL min<sup>-1</sup>, solvent system A: 0.1% TFA in H<sub>2</sub>O, B: 0.1% TFA in CH<sub>3</sub>CN. After lyophilization and purification the compound **MDP-III** was obtained in 23% yield. Analytical data are reported in Table 3.13.

### 6.3.10 Synthesis of cyclopeptide MDP-IV

Linear peptide **MDP-IV** was synthesized on a manual PLS 4x4 synthesizer, as described in the general procedure, starting from Fmoc-RinkAmide (MBHA) PS Resin (100mg, 0.43mmol/g) and using Fmoc-protected amino acids (5equiv), HBTU (5 equiv) and NMM (7 equiv) in DMF for 30 min. Fmoc-N-Pra-OH(3 equiv) was coupled using HBTU (3 equiv). and NMM (5 equiv) in DMF for 45 min.Side chain to side chain cyclization was achieved performing the Glaser coupling as described in the general procedure according the reaction conditions reported in Table 3.16and the cyclization yield was evaluated by RP-HPLC. Acetylation of the <sup>o</sup>N-terminal was carried out as indicated in the general procedure.**MDPIV**was cleaved from the resin and side

## EXPERIMENTAL PART B

chains were deprotected as described in the general procedure using as cleavage solution TFA/H<sub>2</sub>O/TIS (95:2.5:2.5), for 3h, at r.t.. Crude lyophilized product was purified by semi-preparative RP-HPLC 03-15% of B in 30min; HPLC gradients at 4 mL min<sup>-1</sup>, solvent system A: 0.1% TFA in H<sub>2</sub>O, B: 0.1% TFA in CH<sub>3</sub>CN. After lyophilization and purification the compound **MDP-IV** was obtained in 8% yield. Analytical data are reported in Table 3.17.

### 6.4 Immunochemical assays

#### 6.4.1 *Solid-phase not competitive indirect ELISA (SP-ELISA)*

Serum was obtained for diagnostic purposes from patients and healthy blood donors who had given their informed consent, and stored at -20 °C until use. Antibody responses were determined in SP-ELISA. Ninety-six wells activated polystyrene ELISA plates (NUNC Maxisorp SIGMA) were coated with 1 µg per 100 µl of peptides per well or glycopeptides in pure carbonate buffer 0.05 M (pH 9.6) and incubated at 4 °C overnight. After five washes with saline containing 0.05% Tween 20, non specific binding sites were blocked by fetal calf serum (FCS), 10% in saline Tween 20 (100 µl per well) at room temperature for 60 min. Sera diluted from 1:100 to 1:100.000 were applied at 4 °C overnight in saline/Tween 20/10% FCS. After five washes, it was added 100 µl of alkaline phosphatase conjugated anti-human IgM (diluted 1:200 in saline/Tween 20/FCS) or IgG (diluted 1:8000 in saline/ Tween 20/FCS) (Sigma) to each well. After 3 h at room temperature incubation and five washes, 100 µl of substrate solution consisting of 1 mg/ml p-nitrophenyl phosphate (Sigma) in 10% diethanolamine buffer was applied. After 30 min, the reaction was stopped with 1M NaOH (50 µl), and the absorbance was read in a multichannel ELISA reader (Tecan Sunrise) at 405 nm. ELISA plates, coating conditions, reagent dilutions, buffers, and incubation times were tested in preliminary experiments. **Errore. Il segnalibro non è definito.** The antibody

levels are expressed as absorbance in arbitrary units at 405 nm (sample dilution 1:100).

#### ***6.4.2 Measurement of antibody affinity by competitive ELISA***

Antibody affinity was measured following the methods previously reported<sup>156</sup>. The semi-saturating sera dilution (1:600) was calculated from the preliminary titration curves (absorbance, 0.7). At this dilution, Abs were preincubated with increasing synthetic peptide antigen concentration (0;  $2.7 \times 10^{-11}$ ;  $2.7 \times 10^{-10}$ ;  $2.7 \times 10^{-9}$ ;  $2.7 \times 10^{-8}$ ;  $2.7 \times 10^{-7}$ ;  $2.7 \times 10^{-6}$ ;  $2.7 \times 10^{-5}$ ;  $2.7 \times 10^{-4}$ ;  $2.7 \times 10^{-3}$ ) for 1 h at room temperature. Unblocked Abs were revealed by ELISA, and the antigenic probe concentration-absorbance relationship was presented graphically.

## ABBREVIATIONS

### 7. Abbreviations

Ab: antibody;

Ac: Acetyl;

Ag: Antigen;

AGA: anti gliadin antibodies;

AP: alkaline phosphatase;

APC: Antigen presenting cell;

ATP: Adenosine triphosphate;

Boc: tert-butoxycarbonyl;

BSA: bovine serum albumine;

CD: coeliac disease

CNS: Central Nervous System

DCM: dichloromethane;

Dde: 1-(4,4-dimethyl-2,6-dioxacyclohexylidene)ethyl;

DIC: N,N'-diisopropylcarbodiimide

DIPEA: diisopropylethylamine;

DMF: N,N dimethylformamide;

EB: enhanced binding;

EDT: ethanedithiole;

ELISA: enzyme-linked immunosorbent assay;

EMA: endomysial antibodies;

ESI-MS: electrospray ionization-mass spectrometry

Fab: fragment antigen-binding;

Fc: fragment crystallizable;

FCC: flash column chromatography;

FCS: fetal calf serum;

Fmoc: 9-H-fluoren-9-ylmethoxycarbonyl;

GAD: glutamic-acid decarboxylase;

## ABBREVIATIONS

Glia: Gliadin;  
GTP: Guanosine triphosphate;  
HATU:2-(1H-7-Azabenzotriazol-1-yl)--1,1,3,3-tetramethyl uronium  
hexafluorophosphate Methanaminium  
HLA:human leukocyte antigen  
HMW: high molecular weight;  
HOBt: 1-hydroxybenzotriazole;  
HPLC: high performance liquid chromatography;  
HRP: horseradish peroxidase;  
IA 2: insulinoma antigen 2;  
Ig: immunoglobulin (IgE, IgG, etc.);  
IL: interleukin;  
IFN: interferon;  
LMW: low molecular weight;  
MALDI-TOF: matrix-assisted laser desorption ionization- time of flight;  
MAP: mutiple antigenic peptide;  
MEP: multiple epitope peptide;  
MHC: major histocompatibility complex;  
MMPs:matrix metalloproteinases;  
MOG: myelin oligodendrocyte glycoprotein;  
MS: Multiple Sclerosis;  
MW: microwaves;  
NBD's: Normal Blood Donors;  
NK: natural killer cells;  
NMM: N-methyl morpholine;  
NMR: nuclear magnetic resonance;  
NMP:N-methyl-2-pyrrolidone;  
OT: oligosaccharil transferase;  
PBS: phosphate buffered saline;  
PDB: protein data bank;

## ABBREVIATIONS

PEG: polyethylene glycol;

PNPP: para-nitrophenylphosphate;

PS: polystyrene;

RA: rheumatoid arthritis;

RIA: radioimmunoassay;

ROC: receiving operating characteristics;

RS: rett syndrome

SLCF: spot liquid chromatography flash;

SP-ELISA: solid-phase enzyme-linked immunosorbent assay;

SPPS: solid phase peptide synthesis;

TBCR: BF<sub>4</sub>: 4-(4,6-dimethoxy-1,3,5-triazin-2-yl)-4-methylmorpholinium  
tetrafluoroborate

TBCRs: Triazine Based Coupling Reagents;

TBTU: 2 - (1H-benzotriazole-1-yl) - 1,1,3,3 - tetramethyluronium;  
tetrafluoroborate;

*t*Bu: tert-butyl;

TFA: trifluoroacetic acid;

TIS: triisopropylsilane;

TJ: tight junctions;

TNF: tumor necrosis factor

Th: T-helper cell;

THF: tetrahydrofuran;

TLC: Thin layer chromatography;

TLR: toll-like receptor;

TMS: trimethylsilylamine;

TPO: Thyroid Peroxidase;

Trt: trityl;

tTG: tissue Transglutaminase.